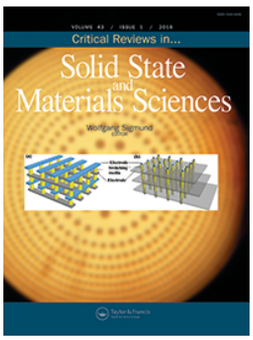

Taylor & Francis
Taylor & Francis Group

Critical Reviews in Solid State and Materials Sciences

ISSN: 1040-8436 (Print) 1547-6561 (Online) Journal homepage: http://www.tandfonline.com/loi/bsms20

Recent Progress on the Dispersion and the Strengthening Effect of Carbon Nanotubes and Graphene-Reinforced Metal Nanocomposites: A Review

Zeeshan Baig, Othman Mamat & Mazli Mustapha

To cite this article: Zeeshan Baig, Othman Mamat & Mazli Mustapha (2018) Recent Progress on the Dispersion and the Strengthening Effect of Carbon Nanotubes and Graphene-Reinforced Metal Nanocomposites: A Review, Critical Reviews in Solid State and Materials Sciences, 43:1, 1-46, DOI: 10.1080/10408436.2016.1243089

To link to this article: https://doi.org/10.1080/10408436.2016.1243089

CRITICAL REVIEWS IN SOLID STATE AND MATERIALS SCIENCES
2018, VOL. 43, NO. 1, 1–46
https://doi.org/10.1080/10408436.2016.1243089

Taylor & Francis
Taylor & Francis Group

Recent Progress on the Dispersion and the Strengthening Effect of Carbon Nanotubes and Graphene-Reinforced Metal Nanocomposites: A Review

Zeeshan Baig, Othman Mamat, and Mazli Mustapha

Department of Mechanical Engineering, Universiti Teknologi Petronas, Perak, Malaysia

ABSTRACT

This article reviews the available literature published to date on the reinforcement of metals with carbon-nanofillers (CNTs and graphene), and also offers a specific focus on issues related to the mechanical and tribological properties of nanocomposites. Carbon-nanofillers (later denoted by C-nanofillers) are known to have extraordinary mechanical properties and multifaceted characteristics and are ideal candidates for the reinforcement of metals for numerous applications. However, their incorporation for practical applications has been challenging researchers for decades. The most important issue is uniform dispersion due to sizeable surface differences between carbon-nanofillers and metals. Other concerns are structural integrity, wetting with metals, and interfacial connections. Nanocomposite applications can only be effective when these challenges are properly addressed and overcome.

Section 1 assesses the importance of C-nanofillers and expressly highlights current research efforts to optimize dispersion in different metals along with processing techniques in section 2. The authors give special attention on C-nanofillers reinforcement contribution to enhanced mechanical strength of metals presented in section 3. C-nanofillers dispersion evaluation tools are highlighted in section 4. Authors also focuses on C-nanofillers role and factors directly associated with metal nanocomposite strength, as reported in the literature. Particular consideration is also given to knowledge sharing of attendant strengthening mechanisms along with contribution reported for empirically derived models used to predict strength. Section 6 solely dedicated to the tribological aspects of C-nanofillers reinforced metallic nanocomposites. Lastly, future recommendations and works need attention is summarized.

KEYWORDS

Nanofillers; powder metallurgy (PM); dispersion; interface; strengthening

Table of Contents

1. Introduction 2
1.1. Need of carbon-nanofillers (CNTs and Graphene) and their properties 3
2. Dispersion of C-nanofillers (CNTs and Graphene) reinforced metal matrix 5
2.1. Current dispersion processing techniques and challenges 6
2.1.1. Dispersion by solid state processing 6
2.1.2. Dispersion by colloidal processing 7
2.1.3. Dispersion by colloidal & solid state hybrid processing 8
3. Previous efforts and contributions to C-nanofiller dispersion 9
3.1. CNTs dispersion in a metal matrix 9
3.2. Graphene dispersion in a metal matrix 9
4. C-nanofillers reinforced metals dispersion evaluation tools 14
5. Role and strengthening effects of C-nanofillers 15
5.1. Influential factors of C-nanofillers to Strengthen MMNCs 15
5.1.1. C-nanofillers (CNTs & graphene) dispersion effect 15
5.1.2. C-nanofiller-metal interface effect 16

CONTACT Zeeshan Baig meteng81@gmail.com

Color versions of one or more of the figures in the article can be found online at www.tandfonline.com/bsms.

5.1.2.1 C-nanofillers wetting....17
5.1.2.2. C-nanofillers structural integrity....17
5.1.2.3. C-nanofillers and metals interfacial reactions (carbide formation)....19
5.2. Strengthening mechanisms and C-nanofillers (CNTs and Graphene)....20
5.2.1. Dislocation formation by C-nanofillers in metals: A case study....25
5.3. Strengthening mechanism contribution of C-nanofillers and effect on mechanical properties....25
6. Tribological aspects of C-nanofillers (CNTs and Graphene) metal nanocomposites....30
6.1. Effectiveness of C-nanofiller addition as nanosolid lubricants (nanoSL) in metals....31
6.2. Tribological properties of MMNCs using C-nanosolid lubricants (CNTs and Graphene)....33
7. Conclusion....38
References....39

1. Introduction

There is an increasing demand from automotive and aerospace sectors to develop new advanced materials which contribute to weight savings, improve energy efficiency, withstand harsh structural loadings, and enhanced tribological performances. To attain such special attributes, the material should possess high specific strength, elastic modulus, and stiffness additional to enhanced functional characteristics. Traditionally, virgin metal and alloys were unable to fulfill these demands. Fortunately, development of metal matrix composites (MMCs), a perfect response and promising material, cater to these requirements. Tailorable characteristic and improved properties of MMCs, such as higher specific stiffness and strength, excellent wear resistance, controlled coefficient of thermal expansion, higher fatigue resistance, and better stability at elevated temperature, are now quickly replacing existing metals or their alloys.[1] They are also now employed for the design of a wide variety of structural applications, as well as for engine and other mechanical system components.

MMCs comprise of combined properties of metals (Al, Cu, Mg, Ti, Ni, and their alloys) as matrices (ductility and toughness), and ceramic or carbon-based reinforcements or micro fillers (high modulus and strength) in the form of continuous fiber, discontinuous fibers, whiskers, or particulates includes Al_2O_3, B_4C, SiC, TiC, WC, graphite, and carbon fibers.[2,3] Previous studies showed that micro-fillers, reinforced metals exhibited improved strength, increased wear resistance, and high stiffness up to acceptable levels over conventional base alloys but also accompanied poor ductility, low yield strength, poor machinability, and reduced fracture toughness.[4,5] There are some issues connected with these micro fillers such as large micron size (hundreds of micrometers and even up to few millimeters cause premature composite part failure via easy crack initiation), large volume fractions addition (cause weight increases and degrades their processability), formation of weak interface with metals due to low aspect ratios (segregation at interface led to physically small nanocracks), brittle nature, and undesired agglomeration during their processing are barriers to the implementations of MMCs in the industry. Hence, it is well recognized that crack formation liability and higher needed properties in MMCs are directly related to the reinforcement size. Therefore, it can be concluded that to minimize or avoid immature cracking and shortcomings of MMCs, it is essential to reduce the size of reinforcing fillers from micrometer to nanometer range. Recently, advances in producing particles below 100 nm size directed toward the development of high-performance composites with high strength and modulus by adding nanoparticles into metal matrix known as metal matrix nanocomposites (MMNCs).[6] Thus, the potential of nanoparticles has already been realized by the research community to reinforce metallic materials in recent years for development of novel nanocomposites. MMNCs exhibited advantages over MMCs such as extraordinarily high strength to weight ratio and enhancement in matrix-to-reinforcement load transfer efficiency due to the extremely higher surface area to volume ratio and aspect ratios (>1000) of nanofillers. Moreover, enhancement in properties can be achieved even at lower volume fractions of nano-reinforcements (<3–5%), whereas with micron scale reinforcements, higher volume fractions are required (>10%).[7]

Previous studies revealed a significant increase in mechanical and tribological properties (lower coefficient of friction and wear rate) by metal matrix nanocomposites rather than metal matrix micro composites due to a strong cohesion at atomic level between the matrix and particles[8,9]. Such a response can be attributed to the fillers nano-sized, good interface build, efficient strengthening mechanism, and effective dislocation blockade provided by nanofillers in metallic matrices. Ma et al. stated

enhancement of tensile and yield strength of pure Al by adding only 1 vol% Si_3N_4 (15 nm) nanoparticles than 15 vol% SiC (3.5 μm) microparticles.[10] Sajjadi et al. manufactured A356 aluminum alloy with micro- and nano-sized Al_2O_3 particles by stir casting. 3 wt% Al_2O_3 nanocomposite showed a significant increase in hardness and compressive strength as compared to 5 wt. % Al_2O_3 micro composites and pure Al alloy counterparts. Similarly, it has been shown that embedding 10 vol.% of 50–nm-sized Al_2O_3 particles to an Al-alloy matrix through powder metallurgy processes exhibit 15 times more yield strength than the base alloy, 6 times stronger than the same alloy containing 46 vol.% of 29 μm size Al_2O_3.[11] Kang and Chan also compare the increment in yield strength shown by Al −1 vol. % Al_2O_3 (25 nm) nanocomposite with that of the Al-10 vol. % SiC_p (13 μm) composite. Moreover, a decline in the yield and tensile strengths of Al nanocomposites has been seen up to 4 vol. % Al_2O_3 (25 nm) at the expense of tensile ductility possibly due to agglomeration.[12] Recently, a detailed study conducted by Mashhadi et al. to study the nano- and micro-sized effect of SiC particles on resulting properties of composites. They concluded that nanosized and 10 wt. % fraction of SiC particles evolved significant effect on densification and hardness of composite than 15 wt. % micron-size particles addition.[13] Other researchers also appreciate the same behavior of using nanoparticles for properties increment.[14] Similarly, besides improved mechanical performance, tribological properties of MMNCs has also outperformed MMCs. Jun et al. demonstrated that 15 vol% Al_2O_3-Al nanocomposite showed high tensile strength, low wear rate and coefficient of friction (COF) rather than micro Al_2O_3-Al nanocomposite.[15] Hosseini et al. exhibited enhanced relative density, hardness, and low wear rate of Al_2O_3 nanoparticles (30 nm) reinforced Al nanocomposites as compared to Al_2O_3 microparticles (1 μm, 60 μm).They also pointed out that low factions of nanoparticles are sufficient to attain mechanical and tribological particles than micro-sized particles.[16] But at certain volume fraction (3% V_f) of nanoparticles, a decrease in properties has been observed which can be attributed to the possible nanoparticle agglomeration.[17]

1.1. Need of carbon-nanofillers (CNTs and graphene) and their properties

Over last few decades, besides ceramics reinforcements, a considerable attention has been attracted by emerging carbonaceous reinforcements hold inherent promising attributes such as high thermal conductivity, low coefficient of thermal expansion, high damping capacity, high strength, and good self-lubricant property. These reinforcements consist of members like carbon fibers, graphite, diamond, and carbon foams were used as ideal micro fillers for some real time applications like rocket nozzles cones or nose tips, heat shields, packaging, automotive brake system, Hubble space telescope antenna, and thermal management.[18] Researchers mainly focus their research on micron-sized carbon fibers and graphite particles reinforce metal composites due to their outstanding strength, thermal, and self-lubrication characteristics.[19] As mentioned above, some major issues like high density, high reaction affinity, cost, brittle nature, and micron size of these particles along with reduce toughness (low fracture strains) of resultant metallic composites degrades properties markedly and restrict their use to some engineering applications majorly due to premature failure of parts during service. By this time, PAN-based carbon fibers and graphite microparticles have already reached their performance border. Therefore, a reinforcement with reducing size (in nanometers) with superior properties is a promising alternative to overcome the inherent issues of ceramic fillers and carbon fibers. Apparently, it seems using nanoparticle could be very effective in avoiding filler cracking, thereby improving the tensile ductility of MMNCs. It is considered that the integration low dose of nanofiller having a larger aspect ratio, higher tensile strength, and stiffness as well as better flexibility, into metals can produce MMNCs with much improved mechanical and tribological properties. Development of nanocomposites is the most pursued research area from the last few years after the groundbreaking invention of two carbonaceous nanofillers (Carbon Nanotubes and Graphene). Research in the field of carbon was modernized by the discovery of carbon nanotubes (CNTs, discovered in 1991, by Iijima et al.[20]) and graphene (2004 by Geim et al.[21]) also referred to as wonder materials. It has been very shortly realized by researcher across the globe about CNTs and graphene reinforcing capabilities amongst present nanofillers. Therefore, CNTs and graphene appeared as ideal nanofillers due to their inherent structural characteristic (high aspect ratio, planar geometry) and astonishing mechanical, physical, thermal, and electrical properties.[22] Graphene is held as the present building unit of all sp^2 hybridized graphitic structures including CNTs and fullerenes. Graphene and CNTs in the form of single or multilayer are available as the hexagonal arrangement of sp^2 hybridized carbon atoms form a honeycombed crystal lattice in two-dimensional planar sheets and rolled up graphene sheets into the seamless cylindrical manner in case of CNTs. The strong in-plane sp^2 C-C bonding but weak van der Waals interaction between the between adjacent layers having 0.34 nm inter-layer distance leading to stronger

Table 1. Properties of graphene and carbon nanotubes.[22, 228–231]

Property	CNTs	Graphene	Carbon Fiber (PAN based)
Physical Structure	Tube	Platelet ~ 1 nm	Filaments (Fibers)
Chemical Structure	Hexagonal	Hexagonal	hexagonal
Interactions	π-π bond	π-π bond	π-π bond
Available Types	Single or Multiple walls	Single or Multiple sheets	Continuous, woven, chopped (single or multiple filaments, lk~48k)
Dimensions	Single wall diameter = 1–2 nm Multi wall diameter = 4–20 nm	Single Sheets Thickness = ~1 nm Multiple sheets thickness = (Approx.) ~ no of sheets x 1 nm	Diameter = 5–10 μm Length = Up to many μm
Elastic Modulus (TPa)	01 (axial direction)	01 (in-plane)	100–500 (GPa)
Tensile Strength (GPa)	60–150	130±10	2.5–7.0
Thermal Conductivity (W/(mK))	3500	$(4.84\pm0.44)\times10^3$ to $(5.30\pm0.48)\times10^3$	21–125
Electrical Conductivity (S/m)	3000–4000	7200	—
Electrical Resistivity (Ω cm)	5×10^{-6} - 50×10^{-6}	50×10^{-6} (in-plane)	1650
Thermal Expansion (K^{-1})	Negligible in axial direction	-1×10^{-6} (in plane), 29×10^{-6} (c-axis)	—0.4 in axial direction
Density (g/cm^3)	0.8	1.8–2.2	1.75–1.93
Electron mobility ($cm^2/(V\ s)$)	$\sim10^5$	2.0×10^4	—
Theoretical specific area (m^2/g)	1300	2360	0.45–0.5
Thermal stability in air (°C)	700°C (in air); 2800°C (in vacuum)	450–650°C (in air)	350–450°C (in air)

than C-C sp^3 bonds in diamond.[23,24] The strong bonding makes graphene the strongest material ever measured, yet flexible because of unique dimensionality.

Table 1 summarizes the noteworthy properties of CNTs and graphene compared with commonly used micro-filler carbon fiber (PAN based). This table simply shows the superiority of C-nanofillers (CNTs and graphene) over carbon fiber in terms of extraordinary mechanical, thermal, electrical and physical properties. Exceptional mechanical stiffness and strength, low density, high specific area, and unique geometry make them perfect reinforcement for composites.[25] The recorded Young's modulus by various MD simulations along the CNTs axis or in the graphene plane can be as high as 1–1.8 TPa, as compared to diamond (1.2 TPa), steel (200 GPa), and copper (100 GPa). Both are half as dense as aluminum and have a tensile strength about 100–200 GPa (20 times that of high strength alloys), equaled to annealed steel (700 MPa) and annealed copper (200 MPa).[23,26–29] Likewise, extraordinary electrical properties of CNTs and graphene exhibit outstanding carrier mobility and capacity are well known which is attractive for next-generation high-speed electronics.[30] The semiconducting single-walled carbon nanotubes (SWCNTs) showed carrier mobility as high as ~80,000 $cm^2\ V^{-1}\ s^{-1}$, while exfoliated graphene varies from ~100,000 $cm^2\ V^{-1}\ s^{-1}$on insulating substrates to 230,000 $cm^2\ V^{-1}\ s^{-1}$ in suspended structures.[31–33] Also, current carrying capacity of both above 109 A cm^{-2} which is 1,000 times higher than the copper wire.[34,35] Similarly, an in-plane thermal conductivity of CNTs and graphene can be as high as 3,000–7,000 W/mK, as compared to diamond (2000 W/mK), carbon fiber (1950 W/mK) and copper (400 W/mK).[36,37] These properties of CNTs and graphene pave the way for a new generation of high-performance composites. In comparison, graphene attracted more attention than CNTs due to three distinct features: (1) 2D flat geometry (crack deflection capacity); (2) high aspect ratios (ability to interact from both sides of faces); and (3) unique surface texture (ability to mechanically interlock with matrix), less likely to rotate or impede atomic diffusion at high temperature and cost-effective production.

Researchers claim that these amazing properties make both types perfect candidates for the development of reinforced light-weight/higher-strength nanocomposites.[38] The use of C-nanofillers began with their integration in polymer matrices for engineering applications.[39,40] Almost all researchers over the last few decades have reported tremendous increment in the mechanical and thermal properties of the polymer nanocomposites (PMCs) by the addition of C-nanofillers reinforcements as compared to neat polymers.[41,42] A well-established volume of literature is available showed special attention has paid to polymer nanocomposite systems. After successful development of PMCs and their use in many practical applications has encouraged scientists to incorporate C-nanofillers in metallic matrices. Metal matrix–nanofillers have distinct advantages over polymers because of their stability at higher temperatures, greater strength, and inflexibility, as well as superior electrical and thermal conductivity. Due to nanometer dimension and low density, nanofillers possess potential to improve mechanical, physical, thermal, electrical, and magnetic properties of metal matrices and can be employed where weight savings, and higher temperature bearing ability withstand structural loadings and resistance to wear are major concerns.[43] These attributes are of great interest for various industrial sectors like automotive, aerospace, and electronics applications. Nevertheless, the challenge remains to successfully embed C-nanofillers in a metallic matrix to

produce metal-matrix-nanocomposites (MMNCs). With respect to PMCs, limited work on nanofiller metallic nanocomposites has been reported because of difficulty to uniformly disperse nanofillers within metals as well as poor wetting.[44–47] The reason for these setbacks is the greater surface area presented by nanofillers, which causes agglomerate clusters and twists secondary to strong van der Waal forces (surface tension) between carbon atoms.[48,49] This tension creates large surface energies that hinder wetting with metal and it also forces separation.[50,51]

In this context, numerous researchers accepted the challenge to better control variables and procedures to enhance dispersion and wetting outcomes[52–56] by conducting extensive studies on optimizing processing approaches.[57–59] Nonetheless, it has remained a difficult task. The authors present the efforts made to meet significant challenges by metal composite researchers over the last decade by citing associated problems reported for nanofiller-metal interactions as well as effects from different processing approaches. Furthermore, we also present a detailed review of C-nanofiller major strengthening mechanisms, their contribution and factors that determine metal matrix nanocomposite strength. Tribological (wear and friction) properties of C-nanofillers reinforced metallic nanocomposites are specially emphasized. The main purpose of this article is to provide an overview of the current state of research progress along with remaining challenges concerning graphene and CNT-reinforced metal matrix nanocomposites. The authors hope this effort will assist the research community to further enrich their investigations and developments.

2. Dispersion of C-nanofillers (CNTs and graphene) reinforced metal matrices

Introducing C-nanofillers to metal matrices presents the imposing challenge of uniformly applying a homogeneous dispersion to obtain a quality nanocomposite. For optimal dispersion of a nanofiller in the final composite, homogenous distribution early in the powder mixing process is crucial.[52] Generally, CNTs and graphene that are available in the market are agglomerations of heavily intertwined bundles and clusters. The main reason for this is the irresistible attraction of van der Waals forces and energy interaction potentials between parallel tubes is 500 eV/mm of SWCNT–SWCNT and 2 eV/nm^2 inter layer graphene sheets. For CNTs to overcome this energy of cohesion (37 kT nm^{-1} between CNT parallel tubes), 120 kT nm^{-1}is required to de-agglomerate CNT bundles.[22,60] Similarly, the order of magnitude of the force needed to overcome interaction energy of graphene sheets is 300 nN/μm^2. This robust interaction energy potential as well as the van der Waals' forces must be broken prior to nanotube dispersal, which presents a difficult task. The same behavior is shown in graphene sheets via clustering due to energy cohesion (Figure 1).

Another feature of clustering and agglomeration is their large surface areas and higher surface energies that readily allow agglomeration and clustering during the process of mixing in a metal matrix. Hence, nanofiller agglomeration and clustering are major complications that hinder uniform dispersion. The major drawback of clusters and agglomerates presence in nanocomposites is the formation of cracks, pores, and pin holes that cause premature failure of a nanocomposite and distinctly effect on final properties. Many researchers have attempted to increase the hardness of metals with the uniform mixing of CNTs. In most cases, CNT agglomerates adversely reduce hardness due to improper dispersion by impeding the sintering process, which results in defects (micro voids). On the other hand, uniformly dispersed and distributed CNTs in a metal matrix can fill gaps between metal particles during sintering; hence, no porosity is noted. Similarly, graphene sheets have presented as aggregates and also behaved like CNT agglomerations in metallic nanocomposites.

Therefore, a reasonable precondition that CNTs and graphene nanofillers are made available as single tubes or sheets, respectively, to better optimize uniform dispersion during nanocomposite processing. It is also worth noting that potentially optimized properties attending nanofillers are largely related to individual nanofillers compared to bulk CNTs and graphene sheets.

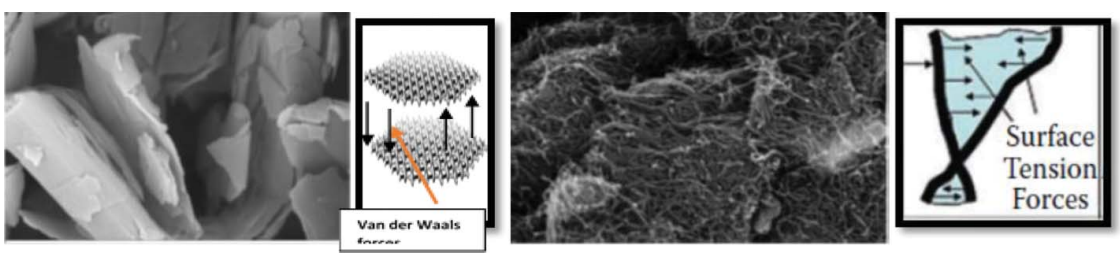

Figure 1. Agglomerations and clustering in graphene and CNTs due to attractive forces.

Realistically, metal nanocomposites can have better properties under the cited conditions, that being the uniform dispersion of individual nanofillers to optimize a composite's properties. All factors such as type, functionality, nanofiller content, matrix materials, and processing conditions considerably affect the dispersion of nanofillers in a metal matrix.

2.1. Current dispersion processing techniques and challenges

Although substantial research has been carried on the development of C-nanofiller-metal nanocomposites over the last two decades. However, due to the lack of suitable processing techniques enable uniform dispersion and issues regarding the nanofiller/metal interface are the major prevention in the attainment of desired improved properties of final nanocomposites. Further challenges such as structural damage to nanofillers from applied stress during consolidation and reactions with the matrix at elevated temperatures during sintering also hindered research advances. Noteworthy, C-nanofillers exhibited exceptional chemical stability due to the presence of sp^2 bonded carbon atoms equivalent to the (0001) plane of graphite.[18] Interaction of metal and C-nanofillers can be taken place via side contact and end contact results in metal carbides formation. End contacts are more prone to interact with metals than side contacts also known as basal planes. It has been shown thermodynamically that metal carbide formation depends on Gibbs-free energy of metallic carbides. Metals like Mg and Ni showed positive free energy indicating their carbides will not form or will not stable at certain temperatures as compared to Ti and Zr which are strong carbide former having negative free energy.[18] Similarly, metals like Al, Si, and Cr also carbide former on reacting with C-nanofillers. Nonetheless, it turned out that formation of structural defects in nanofillers (i.e., conversion of sp^2 to sp^3 bonded carbon atoms) during various processing stages serve as favorable sites for reactions with the matrix, might cause loss of C-nanofiller structure which leads to carbide formations.[61] These carbides may be in favor or adversely affect the final nanocomposite properties.[18] Thus, the selection of a suitable processing method became crucial, because all of these factors should be considered before proceeding with a metal nanocomposite fabrication.[62] Presently, three classes of researchers use different approaches to optimize dispersion and quality interface by carefully considering all such issues. As a result, efforts were/are expended to select more suitable processing techniques or a combination of procedures to obtain homogeneous C-nanofiller integration in different metals and alloys (e.g., Al, Cu, Mg, Ti, Fe, and Ni). Among these, aluminum and copper are extensively used for research, more so than others, because both are ductile and have excellent thermal and electrical properties. Hence, they apply well to structural aerospace and heat sink applications and are abundantly available as well as cost effective, although both have poor mechanical strength.

2.1.1. Dispersion by solid state processing

Processing techniques have pronounced effects on the dispersion of C-nanofillers in metals. As expected, poor dispersion results from simple mixing due to high surface energy difference between them. Hence, high energy mixing is required to achieve uniform dispersion. Powder metallurgy (P/M) emerged as superior and efficient

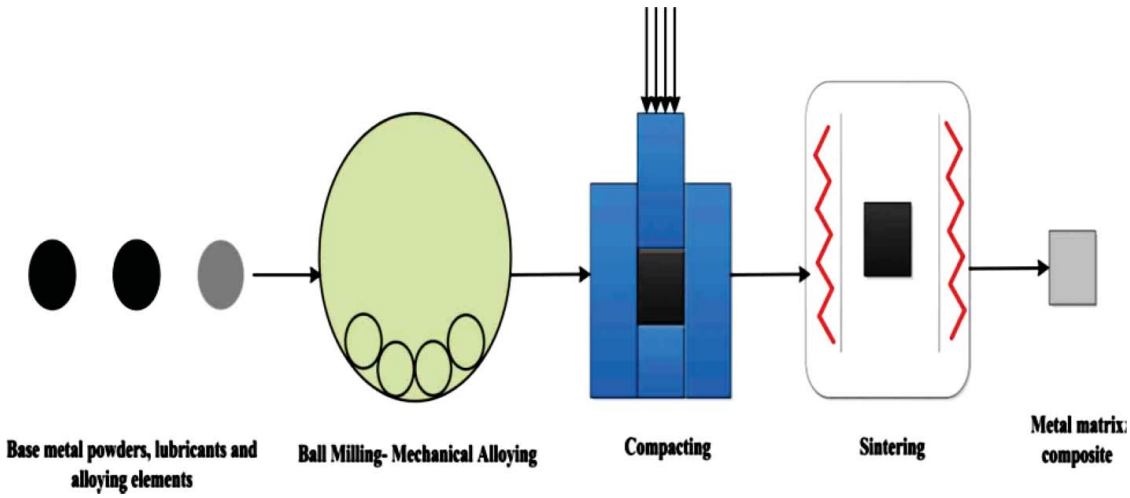

Figure 2. Schematic process of P/M technology. (© Taylor & Francis. Reprinted with permission from Munir et al.[66] Permission to reuse must be obtained from the rightsholder.)

technique with the ability to produce uniform distribution of C-nanofillers within powders.[63,64] In powder metallurgy (P/M), mechanical alloying is commonly employed to disperse C-nanofillers in a metal powders. Figure 2 depicts the conventional powder metallurgy process for the fabrication of a C-nanofiller-metal nanocomposite. This technique is well known due to simplicity, flexibility, near net shape capability, and any composition created because of less involvement of thermodynamics and the phase diagram as in the case of ingot metallurgy. The conventional P/M process start with the mixing of nanofillers with metal powders either in dry or wet conditions carried out by mechanical alloying processes, e.g., high- or low-energy ball milling experience high-energy impact forces (collisions) from grinding balls (steel or ceramic), followed by compaction consolidation and then conventional sintering or specialized consolidation processes such as hot extrusion, hot forging, hot/cold isostatic pressing, equally channel angular processing, microwave, or spark plasma sintering.[7] Powder mixing is crucial to P/M because it is the only processing step that produces homogeneous dispersion; afterwards, compaction, sintering and other processes do not effect dispersion.

A lot of researchers has taken benefit using mechanical alloying (MA) to effectively reduce the problem of agglomerations of C-nanofillers in metal matrices. However, harsh milling conditions found detrimental to C-nanofillers causing sp^3structural defects and length shortening necessary for effective load transfer, due to high impact forces from grinding media which may also led to structure integrity loss.[65] As earlier mentioned, these sp^3defects also act as potential sites trigger unfavorable chemical reactions with the matrix thus favoring carbide presence. During milling processing, metal powders also experience deformation, fracturing, cold welding, and fragmentation simultaneously which caused C-nanofillers to fully embed, breaks agglomerations and formed mechanical bonding within metal powders.[66] Nevertheless, it is acknowledged that co-milling of C-nanofillers with metals powders does have the ability to produce composites with desirable microstructure and homogeneous dispersion by controlled-optimized processing variables. Ball milling parameters have a marked effect on the C-nanofiller dispersion within metals from mill type, milling time, rotation speed, milling bead diameter and type, milling atmosphere, ingredients type, and size.[67,68] Under proper ball milling conditions, milling processing limitations can be minimized.[69]

Several researchers adopted ball milling to achieve homogeneous dispersion. Kuzumaki et al. were the first to produce CNT/Al composites by powder metallurgy using hot pressing and hot extrusion processing.[70] They expected their nanocomposite to have increased tensile strength but found no such result after using 5 and 10 vol% CNTs. In fact, the fabricated nanocomposite had the same tensile strength as unreinforced aluminum. This was likely due to improper dispersion or the lack of nanotube interactions with the matrix and consequently, no load transfer. On the other hand, Esawi et al. successfully incorporated CNTs in aluminum using P/M. They reported not only a uniform CNT dispersal but also enhanced tensile strength (by 21%) along with CNT alignment in the direction of extrusion.[71] Ostovan et al. went on to suggest that mechanical properties were mainly dependent on uniform CNT dispersion in Al after increasing milling time at a certain content level.[72] After the specified content, agglomerations began to form, these findings were also confirmed by Carvalho et al.[73]

2.1.2. Dispersion by colloidal processing

Researchers soon realized that MA was more suitable for C-nanofillers uniform dispersion in metals, although results failed to meet desired expectations. Even so, MA remains employed by many, but problems associated and origin in C-nanofiller nanocomposite require new approaches. Colloidal processing is an improved wet mixing process that modifies the surface chemistry with stable suspensions of C-nanofillers that facilitate homogeneous dispersion.[74] It is now the simplest and most widely used method for C-nanofiller dispersion, de-agglomeration, and mixing with metal powders. The process involves two steps: (1) nanofiller dispersion in a suitable solvent (DI water, ethanol, NMP, DMF, etc.) by ultrasonic energy (>20 kHz) to de-agglomerate and exfoliate C-nanofillers bundles (CNTs or Graphene); and (2) mixing with metal powders. Ultra-sonication is a physical technique adopted to disintegrate large agglomerates, produced homogeneous dispersion of C-nanofillers, and helped to improve the wettability between the matrix and the particles.[75] De-agglomeration usually governed by the interaction of the C-nanofillers with suitable solvents in the presence of shock waves provided by Sonicator.[76] Effective ultrasonic dispersion and de-bundling is achieved when optimizing variables like the level of sonication energy, type of nanofiller, sonication time and interval, type of solvent, degree of bundling, and the dispersant's (C-nanofiller) concentration ratio. Dispersion via this route also accompanied formation of defects in the form of vacancies, open edges as well as length shortening of C-nanofillers due to high shock wave energy.[75] These defects ultimately transformed to undesirable carbides which downgrades MMNCs properties. Therefore, ultrasonic exposure should be optimally limited; otherwise, extended exposure causes

structural damage to the C-nanofiller and severely effects their unique properties.[77] Recently, Simoes et al. reported that a 15-min dispersion/mixture time was suitable for effective dispersion. Less time causes non-uniform dispersion while more time increases the defect rate, which weakens mechanical properties of the final nanocomposite.[78] Consequently, any greater efficiency in C-nanofiller dispersion and de-agglomerations in solvents with sonication aid can also be achieved through surface modifications(functionalization). This step involves cationic, anionic, and/or nonionic surfactants to untangle (stabilize) CNTs and graphene clusters.[79] Although the approach proved successful, intense ultrasonic energy, chemical, and thermal treatments might cause structure of nanofillers more prone to defects that were unsuitable for quality nanocomposites. However, a number of other studies suggested this problem could be solved by a more careful selection of processing conditions.

Using this approach escorted a following problem arises after the mixing of both constituents, i.e., dispersed C-nanofillers in solution are difficult to be absorbed on metal powder surface formed weak bonding because of weak attractive forces between them due to mismatched zeta potential.[80] Therefore, C-nanofillers were just available on the surface but not fully intact. Moreover, this weak bonding might result in re-aggregation of C-nanofillers during dispersing, solvent drying, or even at consolidation stages.[61] Similarly, the size of the metal powders commonly used is in microns, i.e., 1–200 μm having small specific surface area presents difficulty for nanosized dimensions C-nanofillers to absorb on the metal powder surface.[81] It was well established by this time that uniform C-nanofiller dispersion and a strong interface with the metal matrix is essential to improve nanocomposite properties. Colloidal processing certainly appeared to have this potential. Hence, over time, several methods were devised that used ultra-sonication—covalent and non-covalent functionalization, i.e., with or without surfactants, and simultaneous mixing are mechanical agitation, magnetic stirring, nanoparticle decoration, sol gel, molecular level mixing (MLM), and semi-powder metallurgy. Of these latter, MLM emerged as the most novel approach to effectively control for the dispersion of CNT bundles and graphene agglomerates in addition to solving bonding issues.[82] Microstructural studies confirmed the presence of homogeneously dispersed nanotubes within powder particles; i.e., nanotubes were successfully embedded within the matrix rather than just on the surface. But C-nanofillers distribution is random in the as-fabricated composites, and the fabrication process is relatively complicated, time consuming and difficult to be scaled-up. Recently, Rael et al. concluded that the use of "functionalized & surfactant assisted" nanofillers exhibited excellent dispersion within metal powders processed by sonication and stirring.[83] Although use of surfactant seems to be effective but difficulty in removal even after thermal treatment and their presence cause decline of MMNCs properties. Similarly, covalent functionalization of C-nanofillers also accompanied no of processing steps, chemicals involved, and most importantly defective structure after subsequent processing markedly effect on C-nanofillers properties. Therefore, processing parameters, conditions, and materials should be carefully selected to ensure quality dispersion with maintained C-nanofillers structure for effective improvement in MMNCs properties.

2.1.3. Dispersion by colloidal & solid state hybrid processing

Momentum of present research increasingly focuses on employing combining the colloidal and solid state processes (MA technique). Efforts have thus far produced reliable quality outcomes in terms of enhance mechanical properties as compared to above mentioned processes by reducing their deficiencies. This process combines uniform dispersion, de-bundling and exfoliation at a one-time step via ultra-sonication of C-nanofillers and then dry or wet ball milling with metal powders offer increase surface area simultaneously.[84] This approach allowing for getting better incorporation of C-nanofillers between the powder particles and maximum adsorption on the surface with quality interface development to make best use of reinforcement effects. Therefore, this approach seems quite appreciable to produce with much improved results than other strategies because it has tendency to address major issues facing C-nanofillers in metal matrices. Most recently, this strategy has adopted by Chen et al.[81] by introducing solution ball milling (SBM), shown in Figure 3. As can be seen that after subsequent ultra-sonication of CNTs, wet ball milling with Al powder allow for improved dispersion, de-agglomeration, absorption of CNTs on the flat Al powder with high surface area created by milling and importantly strongly intact interface development between them. Notably, they reported good dispersion of CNTs and low structural damage due to processing in solvent medium because solution milling reduces the impact forces of the balls on the structure of the CNTs. Similarly, as a consequence of effective de-agglomeration of CNTs bundles transformed to single tubes allowed a stronger interface between CNTs and the Al matrix. Consequently, tensile strength remarkably improved due to a more competent and uniform dispersion that permitted efficient load transfer within the CNT-Al interface.[81] Similar effort conducted by Munir et al. by employing sonication-assisted ball milling to effectively disperse CNTs in a Ti matrix while retaining

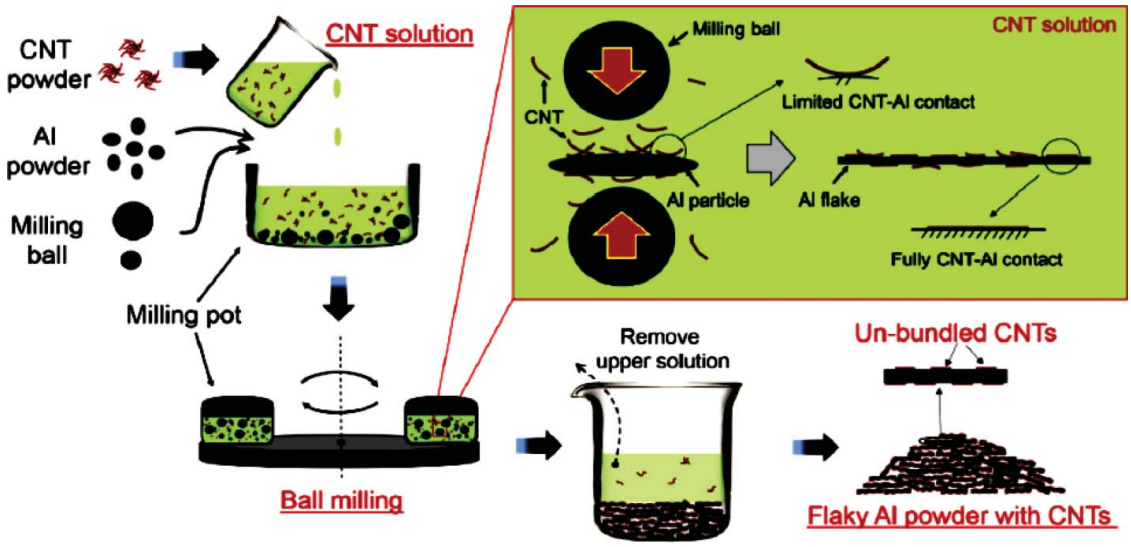

Figure 3. Diagram of Solution Ball Milling (SBM) for the uniform dispersion of CNTs. (© Elsevier Limited. Reprinted with permission from Chen et al.[81] Permission to reuse must be obtained from the rightsholder.)

CNT structure.[61] Another group, Shin et al., used the same approach with solvent-sonicated, dried-and-milled exfoliated graphene in an Al alloy via ball and attrition milling, respectively. As result of the effective graphene liquid exfoliation and high shear impact forces from milling, graphene was properly embedded and dispersed in the Al alloy, which then enhanced tensile properties.[85]

3. Previous efforts and contributions to C-nanofiller dispersion

3.1. CNT dispersion in a metal matrix

A number of researchers tried to disperse CNTs in metal matrices using various processing approaches. It has been reported that CNTs are very difficult to disperse in metals due to tubular tangles, surface energy and re-agglomeration tendency. Realizing the importance and worth place of dispersion in nanocomposites processing, we have gathered data in the form of Table 2 to highlight the current efforts of researchers to tackle this problem to date. This table allows us to know about the use and important techniques adopted and suitable for effective dispersion, parameters and conditions used so far, range of optimal content, dispersion quality, structural stability, and interface formation of the CNTs with metals after processing. As can be seen, MA is the most widely used processing component of the P/M technique which validates its importance. But issues connected with this method must be controlled by optimization to receive much better results. A best solution is to use ultra-sonication with MA to break agglomeration and uniform dispersion as presented freshly reported by mentioned above researchers. Moreover, Al and Cu were the predominate matrices owing to practical applicability. Although better dispersion processes have been established, there remains room to improve structural stability and CNT defect evolution, as well as other characteristics that have been compromised and require attention.

Choi et al. prepared aluminum nanocomposites by incorporating single-, double-, and multi-walled CNTs by mechanical milling that showed better dispersion. Although CNTs presented as agglomerates with less milling time, they gradually became embedded in Al powder particles with increased milling time.[86] More recently, Rikhtegar et al. employed flake powder metallurgy (200, 250, and 300 rpm at 1 and 2 h) assisted by sonication and ball milling using a semi-wet based route (200 rpm for 2 and 4 h) to disperse long and short functionalized CNTs in <45 and <20 μm Al powders at 1.5wt%. They discovered that (i) 2 h of ball milling was insufficient to unbundle CNTs in 45 μm Al powder but (ii) improved dispersion occurred at 2 h in 20 μm Al powder due to greater surface area, and (iii) more damage was introduced with increased milling at 4 h. Furthermore, flakes from both Al powder sizes had greater surface areas at 2 h of milling and were more compatible due to CNT bonding with Al powder particles, which also indicated enhanced dispersion.[87] Aqeeli et al. reported that sonication reduced agglomeration with sufficient milling to attain uniform CNT dispersion in an Al alloy.[88] Figure 4 demonstrates the extent of CNT dispersion for various content ratios and milling times with no sign of agglomeration.

3.2. Graphene dispersion in a metal matrix

Graphene sheets have great tendency to form clusters or wrinkles due to strong attraction of van der Waal's forces

Table 2. Effects of processing technique on dispersion quality and CNT characteristics in metal matrices.

Researchers	Matrix System	CNTs Content	Dispersion Strategy	Secondary processing treatment	Dispersion Quality	Structural integrity	Interfacial Bonding	Merits/Demerits and Mechanical Properties
Bradbury et al.[232]	Pure Al	1, 3, 6, and 9 wt.%	Planetary ball mill (BPR of 10:1 at 360 rpm, total milling time: 20 h)	Hot pressing + Hot extrusion	Effectively up to 9 wt.%	Preserved Structure	Strong	No large CNT agglomerates Hardness at HV_{20} = 151 for 6 wt% MW-CNTs.
Bustamante et al.[69, 233]	2024 Al alloy	0.5, 1.0, 2.0, 3.0, 4.0, and 5.0 wt. %	High energy mill Spex 8000 (milling times: 5, 10, 20, and 30 h)	Compaction + Pressure less sintering	Homogeneous dispersion	Damage caused during milling	Good mechanical bonds	Presence of the aluminum carbide due to defects produced with increased milling time. Increased hardness by 285% - milled for 20 h with CNT concentration of 5.0 wt. %.
Singhal et al.[234]	Pure Al	0.5–3.0 wt.%	Planetary ball milling (at 323 rpm, 5–15 h)	Uni axial pressing + Vacuum sintering	Uniform dispersion with increased milling time	Defects quantity increased but no significant structural change	Strong interfacial bonding provided by carbide layer	Prevented fCNT agglomeration. Formation of Al4C3 interfacial transition layer.
Sahraei et al.[52]	Pure Cu	0.5 and 1 wt.%	Ultrasonication + planetary ball mill (3 h at 250 rpm)	Compaction + Hot press sintering	Homogenous distribution	Increased defect density	Strong due to chemically bonded functional groups on CNTs	Micro hardness at 1 wt. % fCNT 1.7 to 2.1 times higher with increased electrical resistivity.
Koppad et al.[235]	Pure Cu	1, 2, 3 and 4wt-%	Planetary ball mill(350 rpm for 120 min)	Compaction + Vacuum sintering + hot forging	Fully embedded	Not reported	Not reported	Clusters of MWCNTs observed. Micro hardness increased.
Mindivan et al.[236]	Mg–6 wt.% Al	0.5, 1, 2 and 4 wt.%	HEBM (300 rpm for 3 h)	Cold pressing + Hot extrusion	Uniform distribution	Not reported	Weak bonding	Improved hardness and corrosion resistance at 0.5 wt. %.
Borkar et al.[237]	Pure Ni	5 vol %	HEBM (24 h at 400 rpm)	SPS	Uniform but bundles of CNTs seen	Well maintained with some defects	Good	Increased micro-hardness and tensile yield strength with higher ductility.
Basariya et al.[238]	EN AW6082 Al alloy	2 wt.%	High energy eccentric ball milling (0 to 50 h at 300 rpm, (BPR) of 10:1)	Not reported	Uniform distributed and fully embedded	No structural damage/ change seen	Fully intact	No reaction products detected. Increased micro-hardness and nano-hardness (up to 436 + 52 HV after 50 h of milling.
Chu et al.[53]	Cu +0.76 wt.% Cr	5,10 and 15 vol %	HEBM (SPEX mixer) at 1200 rpm for 120 min, (BPR) of 10:1	Hot pressing + Pressure sintering	Homogeneous at 10 vol.% CNTs	Evolution of defects	Strong interfacial bonding provided by Cr carbide layer	No CNT agglomerates found. Increased hardness and yield strength of 128% and 135%. Defects facilitate formation of Cr carbide.
Yoo et al.[239]	Pure Al	1 and 3 vol.%	HEBM (attrition mill at 400 rpm for 6 h, (BPR) of 15:1	Hot Rolling	Well embedded	Increased defect density	Good	3 vol% CNT–Al composite exhibited yield stress (YS) of 456 MPa and an ultimate tensile stress (UTS) of 571 MPa.
Liao et al.[240,241]	Pure Al	0.5 wt.%	LEBM (horizontal rolling machine) and HEBM (200 rpm.4 hr, 5:1) polyester binder-assisting (PBA) mixing	SPS + Hot extrusion	Good dispersion achieved with HEBM	CNTs structure and morphology maintained by PBA	Strong interfacial bonding seen in PBA	Enhanced strength and hardness shown by HEBM & PBA.
Simões et al.[242]	Pure Al	0.25–2.0 wt.%	Ultrasonication (15 min) + Turbula mixing (60 min)	Uni-axial pressing + Vacuum sintering	Highly improved dispersion at 0.75 wt.%	Minimal damage	Strong adhesion provided by Al4C3 layer	High CNT content (1.0 and 2.0 wt. %) promoted agglomeration and clusters. Al_4C_3 formation occurred. 200% and 50% increase in tensile strength and hardness at 0.75 wt. %.
Li et al.[103]	Pure Mg	2,4, wt. % CNTs-Al_2O_3	Planet–Ball–Grinding machine for 24 h at 400 rpm, BPR of 10:1	Pressing + Hot Extrusion	Homogeneous dispersion due to Al_2O_3	No structure destruction	Highly intact interface	Enhanced, hardness, yield strength and Elastic Modus obtained at 4 wt. % CNTs-Al_2O_3.

Mani et al.[243]	Fe-Co	upto10 vol %	Ultra-sonication + Dry Ball milling	SPS	Efficient Dispersion	Minimum defects produced at lower CNT vol. fractions	Not reported	1.5 vol% of CNTs showed increased saturation induction, mechanical hardness and mean flexural strength with a reduction in coercivity.
Suh et al.[244]	Pure Fe	2 and 4 vol %	Attrition milling at 500 rpm for 4 and 9 h, BPR of 15:1	Hot pressing +Conventional Sintering	Good dispersion and embed at 9 h milling	Defects produced	Very strong bonds by hot pressing	Formation of Fe_3C phase. Compressive yield stress increased.
Nai et al.[113]	Pure Mg	0.3 wt.% Ni coated CNTs	Planetary ball mill at 200 rpm for 1 h	Cold compaction + Microwave sintering	More uniform dispersion	Not reported	Better interface interaction by intermetallic compound	Ni coating on CNT prevents clustering of Ni–CNTs.
Kim et al.[245]	Pure Cu	5 and 10 vol%	Molecular-level mixing	SPS	Homogeneously dispersed	Not reported	Chemically bonded oxygen atoms at CNT cause strong interface	Increased yield strength of 455 MPa and elastic modulus of 138 GPa with 10 vol% CNT in Cu compared to unreinforced Cu.
Xue et al.[246]	Pure Cu	5 vol%	Molecular-level mixing	SPS + Hot Rolling	High degree of dispersion	Not Reported	Strong Adhesion	Appearance of composite powders = cluster-like. Remarkable increase in tensile and yield strength compared to ball milled composites.
Lal et al.[247]	Pure Cu	0.5 to 1.5 wt.%	Molecular-level mixing + Dry Ball milling (5 h at 250 rpm, BPR of 10:1)	Cold pressing + Vacuum Sintering	Highly dispersed CNTs	No Damage seen	Durable interfacial Bonding due to functionalized CNTs	Increased compressive strength, micro-hardness, and flexural strength seen with increase vol% content of CNTs.

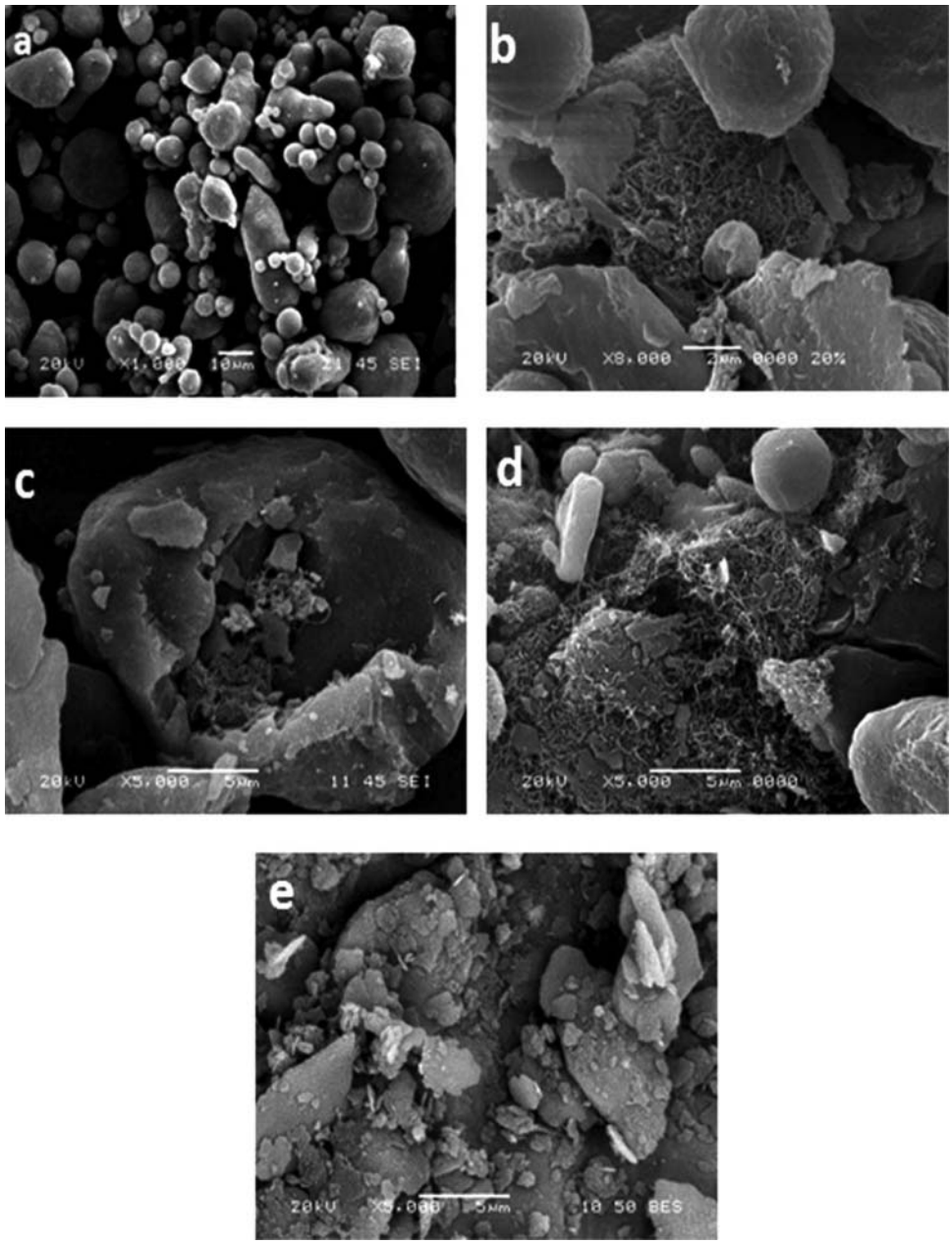

Figure 4. SEM images of Al Alloy with different CNT content ratios and process conditions: (a) raw powder; (b) 0.5 wt% CNT–milled for 1 h; (c) 0.5 wt% CNT–milled for 3 h; (d) 2.0 wt% CNT–milled for 1 h; (e) 2.0 wt% CNT–milled for 3 h. (© Elsevier Limited. Reprinted with permission from Aqeeli et al.[88] Permission to reuse must be obtained from the rightsholder.)

existence and 2D planar nature poses more difficulty to disperse than CNTs. These cluster or wrinkles were the source of cracks, pores, and pin holes which could lead to premature failure of composite. 2D form of ultrahigh surface area graphene sheets may also be lost by these clusters formation which is also a major drawback. Depending on required purity and precision, graphene is available commercially as multi-nanosheets aggregates or in other forms such as single sheets or a few layers, as nano-platelets or flakes, or graphene oxide and functionalized sheets. The properties of a single sheet, as reported in the literature, are ultra-high tensile and modulus strengths that far exceed that of multilayer samples.[89] Hence, an appropriate approach not only to disperse and exfoliate as well these 2D sheets homogeneously within a metal matrix is needed. Despite the fact, a bulk research literature is now available regarding successful synthesis of graphene polymer nanocomposite,[39,90] however, graphene metal nanocomposite research is present in its early stages and dispersion remains key concern. Table 3 shows data produced by struggling researchers to disperse graphene in different metal matrices using several processing techniques. They realized early that graphene is only dispersed effectively after exfoliation by liquid

Table 3. Effects of processing techniques on dispersion quality and graphene characteristics within metal matrices.

Researchers	Matrix System	GNPs Content	Dispersion Strategy	Secondary processing treatment	Dispersion Quality	Structural integrity	Interfacial Bonding	Merits/Demerits and Mechanical Properties
Bustamante et al.[162]	Pure Al	(0.25, 0.50, and 1.0 wt.%)	High energy ball mill Spex 8000 M (milling times: 1, 3, and 5 h, BPR of 5:1)	Compaction + Ar Sintering	Excellent dispersion	Defect density increased with milling time and structural preservation	Good mechanical bonding	Lack of GNP clusters. Presence of aluminum carbide observed. Higher hardness values were obtained at 2 h of sintering in composites milled for 5 h.
Cui et al.[93]	Pure Cu		Ball milling at 100, 200, or 300 r/min for 4 or 8 h	Compaction + pressure less sintering	Intermediate dispersion	Higher defect concentration	Intermediate bonding	Higher yield values & compressive strengths obtained at 100 r/min for 4 h milling
Bastwros et al.[92]	Aluminum alloy 6061	1.0 wt.%	SPEX 8000x ball milling at 10, 30, 60 &90 min, BPR of 2:6	Hot pressing	Fully embedded & dispersed with increased time	Disorder increased with milling	Intermediate interface formation	Strength increase for composites:47 and 34% for 60-min & 90-min
Li et al.[248]	Pure Al	0.5, 1.0, 1.5 and 2.0 wt.%	V-Blender at 17 rpm for 24 h + attritor at180 rpm for 2 h, BPR of 40:1	Hot Extrusion	Good distribution	Not reported	Strong, clean interface development	Increase in ultimate yield& strength at 1 wt.% graphene content
Yan et al.[104]	Al alloy	0.15 and 0.5 wt.%	Ball milling at 75 r/min for 12 h, BPR of 10:1	Hot isostatic pressed (HIP) + Hot Extrusion	Full surface a dsorption	No significant damage	Good interface created	Yield strength increased from 214 to 319 MPa at 0.5 wt.%
Chu et al.[110]	Pure Cu	3,5,8 and 12 vol%	Ball milling (SPEX mixer, at 1200 rpm for 3 h, BPR of 10:1)	hot pressing + sintering	Homogeneous dispersion & embedded at 8 vol%	Defects density increased with milling	Insufficient bonding	114 and 37% increases in yield strength and Young's modulus with 8 vol% GNP content.
Kim et al. [163]	Pure Cu	0.5 and 1 vol%	Ultrasonication + Dry Ball milling at 400 rpm for 4 h, BPR of 15:1	High ratio differential speed rolling	Random dispersion	Introduction of some defects and disorder	Significant interactions at interface	Considerable increase in UTS and YS at 1 vol% GNPs.
Li et al.[117]	Pure Cu	0.6 wt.%	Ultrasonication for 1 h	SPS	Good dispersion	Defects produced but decreased with annealing	Good interfacial adhesion	Yield strength and tensile strength with 0.6 wt. % RGO increased noticeably by 47.7 and 75.8%.
Hwang et al.[118]	Pure Cu	2.5 vol%	Molecular Level Mixing (MLM)	SPS	Homogeneous dispersion	Low defect density after reduction	Strong interactions between Cu and graphene facilitated by bonded oxygen	Elastic modulus and yield strength values increased up to 131 GPa and 284 MPa, respectively, ≈ 30 and 80% higher at 2.5 vol%.
Chao Zhao[249]	Pure Ni	0.9, 1.5, 2, and 4 wt.%	Molecular Level Mixing (MLM)	SPS	Uniformly distributed on Ni surface	Low defect intensity	Enhanced oxygen-mediated bonding at interface	No evidence of carbide formation. Tensile strength and yield strength enhanced by 52.8, 95.2, and 165.3% (327.6%), respectively, at 1.5 wt. % rGO.
Rashad et al.[250]	Mg–1%Al–1% Sn alloy	0.18 wt.%	Semi-Powder Metallurgy Ultrasonication for 1 h + mechanical agitation for 1 h	Compaction+ Sintering + Hot Extrusion	Homogeneous dispersion	Not reported	Highly intact interface	Improvement 29.2 and 14% in yield strength and ultimate tensile strength obtained
Dutkiewicz et al.[251]	Pure Cu	1 and 2 wt. %	Planetary ball milling for 5 h, BPR of 10:1	Hot pressing	Effective dispersion at 1 wt.%	Increased defect density	Not reported	50% increase in hardness seen with the addition of 2 wt.% GNPs.

processing and then mechanically dispersed. Some suggested that sonication-assisted-ball milling and colloidal processing are more commonly used to fabricate graphene metal nanocomposites. These developments have been attributed to the amenability of the graphene 2D planar structure to disperse in solvents..[81] An important point to realize that MA either in dry or wet is still be considered as promising choice for graphene dispersion in metals as well among other methods. But it should be kept in mind that graphene is also more prone to defect due to 2D dimension and availability of both faces to be affected during processing. So, graphene metal processing still demands greater attention to various concerns such as effects from graphene size, type, exfoliation and processing parameters.

Latief et al. first used powder metallurgy to incorporate various degrees of graphene nanoplatelets in aluminum powder. They reported increased mechanical behavior with increasing filler content.[91] Bastwros et al. conducted a study on graphene dispersion at different ball milling times and reported that 60 min of milling at 1 wt% enhanced dispersion and increased mechanical responses.[92] Cui et al. observed increased graphene dispersion affiliated with no reduction of sheets but with increased rpms and milling time.[93] Boostani et al. manufactured aluminum-SiC, which encapsulated graphene nanosheets via non-contact ultra-sonication to prevent agglomeration. This approach successfully prevented the agglomeration of nanoparticles and produced a better dispersion of the graphene sheets.[94] Das et al. reported a decline in micro-hardness with a 2% graphene load due to agglomeration.[95] Rashad et al. developed Mg alloy graphene nanoplatelets nanocomposite using sonication and stirring. They claimed superior dispersion and adhesion of graphene in the Mg matrix compared to ball milling.[96–98] They also used sonication and ball milling to study graphene dispersion in Mg powders. Figures 5a,b show SEM images of CNT graphene clusters on the surface of Mg particles before milling. Figures 5c,d are post-milling images that demonstrate the clusters were broken

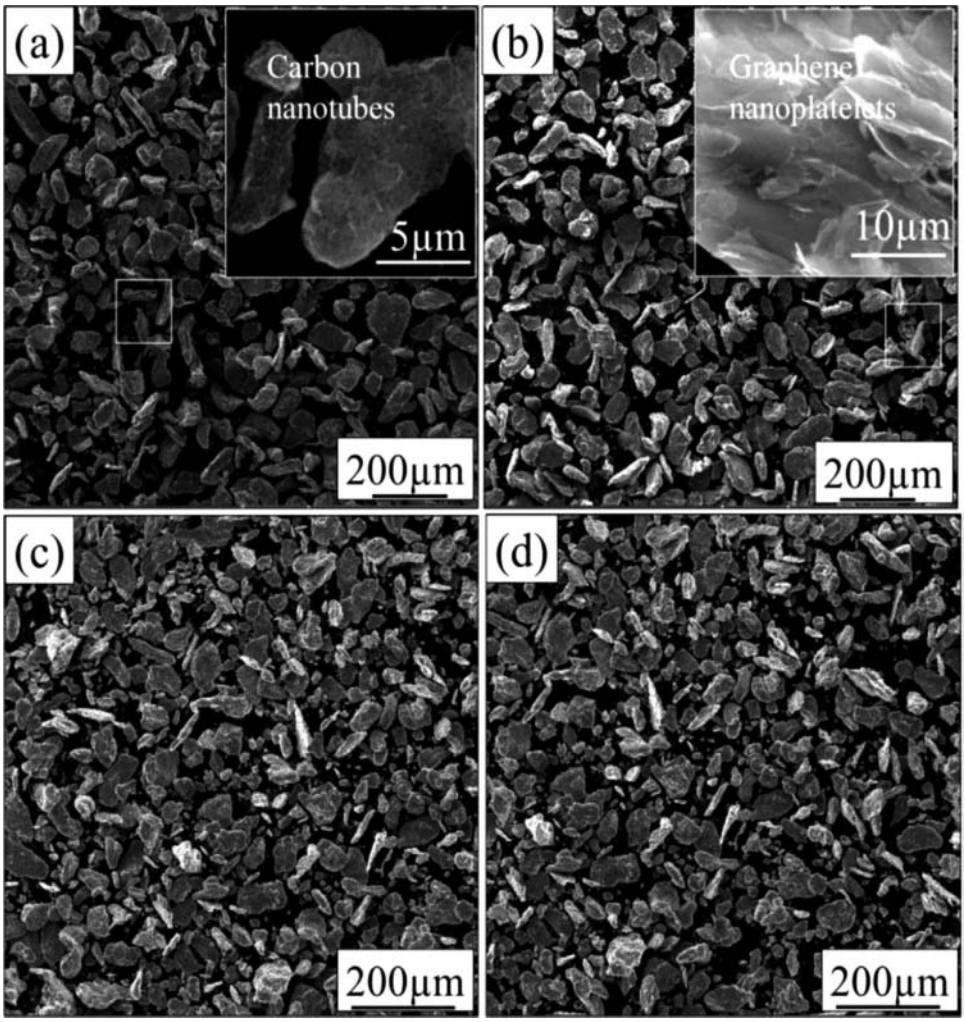

Figure 5. Before milling (a and b) and post milling (c and d) SEM images of ball milled CNTs (graphene-reinforced AZ31). (© Elsevier Limited. Reprinted with permission from Rashad et al.[99] Permission to reuse must be obtained from the rightsholder.)

and fully embedded within the Mg powder along with uniform dispersion.[99]

4. Carbon-nanofillers reinforced metals dispersion evaluation tools

So far we have discussed the importance of C-nanofiller dispersion in metals along with recent research contributions. Tools used to measure and evaluate the degree and quality of C-nanofiller dispersion reflect the multifunctional properties of a final nanocomposite. As discussed, C-nanofillers are generally dispersed in metal powders by solid or liquid processes depending on compatibility and application. For both processes modalities, microscopy and spectroscopy are normally used for quantitative and qualitative analyses. Conventional microscopy methods include optical, atomic force, field emission scanning electron microscopy (FESEM) and high-resolution transmission electron microscopy (HRTEM) cross-sectional areas, C-nanofillers dispersed metal powders, or fractured surfaces. These methods are commonly employed to assess the degree of dispersion and C-nanofiller quality by scanning very limited regions of a given nanofiller composite sample. The question then arises as to "how limited region assessments accurately reflect C-nanofiller dispersion for an entire nanocomposite." Furthermore, other than FESEM and TEM, the scanning resolution capability of some instruments is limited, which presents another drawback. Similarly, C-nanofillers that are readily dispersed in solvents can be measured by some spectroscopic techniques to assess the dispersion state. These latter include ultraviolet–visible spectroscopy (UV/Vis absorption spectroscopy or photoluminescence excitation (PLE) spectroscopy. However, they cannot all be employed for comparison purposes for different C-nanofiller types or surfactants because of differences in spectral absorbance. Additionally, the zeta potential measurement (ZPM) is a useful tool that monitors both dispersion and stability by measuring the surface potential of nanofillers as electrostatic charges on the surface. However, it is not frequently used due to unavailability of quantitative tools. Although several instruments are commonly in use, they are not entirely reliable. Hence, applicable tools or methods are also needed to better assess degrees of nanofiller dispersion. To improve the quality of dispersion evaluation, researchers have tried to measure dispersion both quantitatively and qualitatively with a combination of existing tools but with little success. Hence, there remains a need to identify better techniques to measure both dispersion and stability in solid and liquid states to improve the quality of assessing nanocomposite properties.

5. Role and strengthening effects of C-nanofillers (CNTs & graphene)

The ultimate objective of researchers is to incorporate C-nanofillers within different metal matrices and use their ultrahigh reinforcement strength to enhance the mechanical properties of final composites for potential engineering applications. As discussed earlier, the size of the reinforcement has a pronounced effect on strength and ductility of metal composites and can usually be studied through fracture analysis. Microstructural analyses of fractured surfaces confirm that micro sized particles, compared to nanosized particles, more often lead to cracks in the composite that cause premature failures.[79] Therefore, it is commonly believed that nanosized reinforcement produces superior properties and that C-nanofillers (CNTs & graphene) can greatly contribute towards increasing the mechanical properties of metals. Previous results proved C-nanofiller potential as reinforcing agents due to their exceptional load bearing ability when compared to traditional fibrous fillers such as carbon or glass fibers.[100]

Over the last few last years, C-nanofillers were extensively used to reinforce polymers.[101,102] Their results increased both the confidence and determination of researchers to apply C-nanofillers as potential strength enhancers in metals. However, problems associated with C-nanofillers in polymers such as distribution, interface reactions, etc., did not affirm their aspirations; thus, doubt arose as to the effectiveness of C-nanofiller as reinforcement in metals. Generally, C-nanofillers are thought to effectively transfer a load through the interface and take a higher share of the total load on the composite. To execute such operation there are some factors related to C-nanofillers involved which significantly contribute in strengthening are: homogeneous dispersion, strong interfacial bonding, and the chemical stability of nanofillers.

5.1. Influential factors of C-nanofillers to Strengthen MMNCs

5.1.1. C-nanofillers (CNTs & graphene) dispersion effect

As mentioned above, uniform dispersion of C-nanofillers in composites is a great challenge because it has prominent effects on a composite's strength. To the contrary, non-uniform dispersion adversely affects the strength of the composite. Therefore, homogeneous dispersion in metals is the prerequisites in order to obtain desire enhancement in properties. Recent techniques employed to cater C-nanofillers dispersion but various routes have been discussed in detail given in detail above (Tables 2

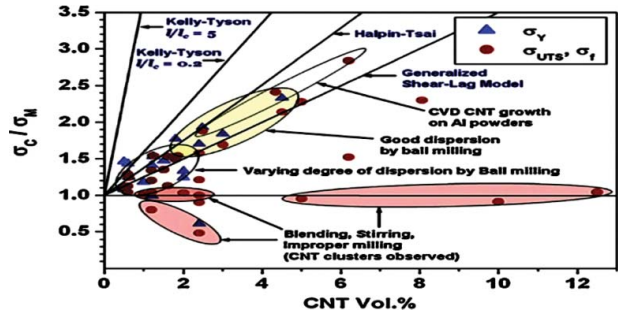

Figure 6. Prediction of tensile (σf) and yield (σy) strengths of Al-CNT composites for different CNT contents compared to micro-mechanic models. (©Elsevier Limited. Reprinted with permission from Bakshi et al.[140] Permission to reuse must be obtained from the rightsholder.)

and 3). This section typically discusses research evaluations and results that have linked metal nanocomposite strength to C-nanofiller dispersion.

Figure 6 shows the relation of dispersion quality to tensile and yield strength at various CNT fractions using different dispersion techniques and also clearly validates the importance of homogeneous dispersion of CNTs produces desirable outcomes in nanocomposites. It can be seen that the ball milling method is the most influential to obtain good dispersion. We can appreciate that good dispersion and mechanical properties are best obtained with lower CNT content due to its higher specific surface area, which facilitates dispersion. To solve agglomeration concerns at higher content and better dispersion facilitation for both CNTs and graphene nanofillers, researchers adopted different strategies that included modifications of the processing route, optimizing process parameters, wet or dry processing, particle assisted processing (Al_2O_3 or precursors), C-nanofiller surface modification (covalent, with functional groups (O_2 or carboxylic, etc.), or non-covalent, surfactant, dispersing agents), as well as metal decoration and surface covering (Cu, Ni, Ti). All researchers generally operated from the same premise that uniform dispersion and distribution were the sole requirements for significant improvements of nanocomposite mechanical properties and tribological aspects.

Recently, Munir et al. achieved both increased hardness (192%) and elastic modulus (89%) over pure Ti as the result of uniform dispersion via sonication-assisted ball milling.[61] Similarly, Li et al. fabricated a CNT/Mg nanocomposite by in situ growth of CNTs over Al_2O_3 particles via CVD followed by the PM process and hot-extrusion. Aided by the alumina particle, CNTs were uniformly dispersed in the Mg matrix with moderate ball milling. Yield strengths and elastic moduli for the 4 wt% CNT-Al_2O_3-Mg nanocomposite increased by 28.22 and 28.57%, respectively, compared to pure Mg in result of good homogenous mixing and interfacial bonding.[103] Yan et al.[104] reinforced an Al alloy with 0.15 and 0.5 wt% graphene using simple ball milling and hot isostatic pressing at 480°C and 110 MPa for 2 h. Significant increases in tensile strength, from 373 MPa to 400 and 467 MPa were observed, accompanied by yield-strengths of 214, 262, and 319 MPa. These findings can most likely be attributed to better dispersion provided by the ball milling process. Adding Al particles Rashad et al.[105] tried to disperse graphene and avoid agglomeration in a Mg matrix using semi-powder metallurgy. He compared UTS and YS results with those reported by others and found the strengths attained by his Mg/Al-GNP nanocomposites clearly surpassed formerly reported outcomes. Li et al. enhanced the mechanical properties of a graphene/Cu nanocomposite with Ni particles decorated graphene surface by chemical reduction of Ni ions followed by ultra-sonication dispersal in Cu powders and consolidation but SPS technique.[106] The 0.8 vol% Ni-Graphene/Cu composites improved 42% tensile strength at the expense of elongation vs. either a neat Cu or 0.8 vol% graphene/Cu nanocomposite, as shown in Figure 7.

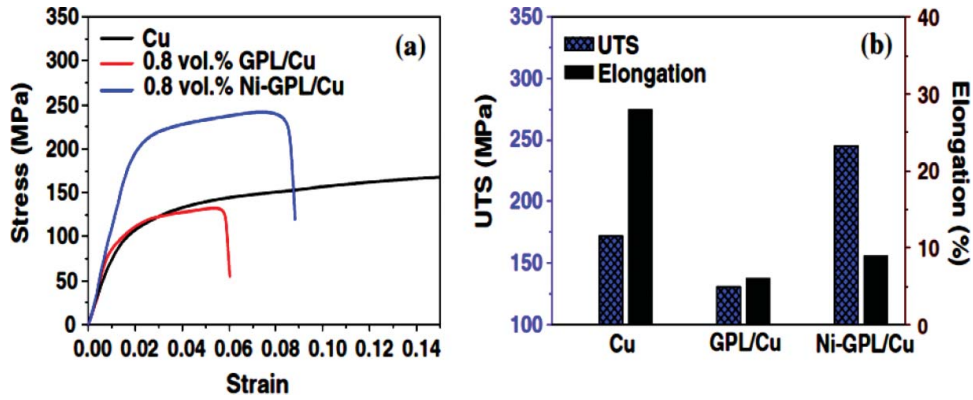

Figure 7. (a, b) Stress–strain curves and values for Cu & Ni–GPL/Cu composites. (© Springer Link. Reproduced with permission from Li et al.[106] Permission to reuse must be obtained from the rightsholder.)

Ni-decorated graphene exhibited well dispersion and strong covalent Ni–Cu powder interactions as compared to undecorated graphene which tend to aggregate and reduction in strength observed.

5.1.2. C-nanofiller-metal interface effect

Fabricating composite materials by incorporating nanofillers is challenging due to severe processing conditions, which include high temperatures and pressures. The mechanical properties of the final nanocomposite are very much dependent on the quality of the interface formation achieved. In turn, interface quality depends on a nanofillers (i) wetting ability, (ii) structural integrity, (iii) interface reactions, and (iv) carbide formation. These features are strongly influenced by the nature and type of processing to handle nanofillers in metals such as the powder metallurgy method where materials face high plastic deformation, stress and temperatures, as seen in high energy ball milling, hot extrusion and hot press consolidation.

5.1.2.1 C-nanofillers wetting. Nanocomposite strength depends on the effective transmission of applied stress through the metal matrix to the reinforcement and a nanofillers stress bearing ability. These are only achievable though strong interface bonding between the nanofiller and the matrix.[107–109] Strong bonding assures proper load transfer; otherwise, a weak interface leads to porosity and failure due to insufficient load transfer; thus, it inhibits any improvements of composite properties. Accordingly, optimizing nanofiller wettability within a metal matrix is essential to avoiding interfacial delamination and void formations. Hence, the fiber-matrix interfacial quality and strength is crucial for composite strength and high performance outcomes. It is well established that poor interfacial bonding is the result of non-wettable nanofillers that cause difficulty when mixing them with metals.[110] The large free surface energy difference, for example, of Aluminum (955 mN m^{-1}), holds 20 times more surface tension than CNTs (45.3 mN m^{-1}).[12,13] Efforts to improve wetting by increasing surface compatibility include coating and surface functionalization via electro less or electro deposition of metals (Ni, Cu, and Fe), precursor aid, and polymeric attachment to metal powders. He et al. synthesized a 5 wt% CNT/Al composite by the direct growth of CNTs on Al powder with a 1.0 wt% Ni particle coating.[68,111] Hardness and tensile strength of the CNT(Ni)–Al matrix composites were increased to 4.3 and 2.8 times that of neat Al. Maqbool et al.[112] improved interfacial bonding via electro less Cu-coated CNTs reinforced aluminum. They reported increased mechanical properties like hardness, yield strength, and tensile strength by 79%, 121%, and 107%, respectively with increasing CNTs wt % fractions due to strong binding provided by Cu-coated CNTs than uncoated CNTs as depicted in Table 4. Nai et al.[113] enhanced surface interaction by Ni-coated CNTs Mg composite synthesis. They reported greatly improved interface quality due to the formation of Mg_2Ni at the interface, which guaranteed excellent adhesion between Mg/Ni–CNT particulates with good CNT wetting. As a result, there was an increase in hardness, tensile strength, and 0.2% yield strength by 41%, 39%, and 64% respectively, for the Mg/Ni–CNT composites as compared to monolithic Mg were obtained.

Table 4. Mechanical properties of Uncoated vs. Cu-Coated CNT/Al.

Sample	CNT wt.%	Hardness Hv	Yield Strength(MPa)	Ultimate Tensile Strength (MPa)	Elongation (%)
Pure Al	0	39	86	140	31.5
Uncoated	0.25	44	96	170	21.5
CNT/Al	0.50	46	101	189	14.8
	0.75	51	134	214	10.5
	1.0	56 ↑ 44%	136 ↑ 58%	227 ↑ 62%	7.2 ↓77%
Cu-Coated	0.25	61	143	237	31.5
CNT/Al	0.50	68	148	249	18.2
	0.75	71	156	261	9.7
	1.0	103 ↑ 79%	190 ↑121%	290 ↑ 107%	5.0 ↓ 84%

Using graphene oxide (GO) is another strategy implemented by many researchers to improve bonding of graphene with metal matrix. Chao Zhao,[114] Lin et al.,[115] and Peng et al.[116] used graphene oxide instead of graphene nanoplatelets to investigate increase strength in Ni, Fe, and Cu matrices. They reported well-bonded interfaces, likely due to the presence of oxygen residue from reduced graphene functional groups that covalently bonded with metal atoms, which considerably increased the strength of the MMNCs. Similar results were reported as a result of clean interface formation between Cu and graphene oxide residue owing to covalent C–O–Cu bonding after reduction and successful SPS consolidation.[117] Hwang et al. used a combination of molecular-level mixing and SPS processing to successfully fabricated reduced graphene oxide (RGO)/copper nanocomposite containing a healthy, tearless graphene structure, and well-bonded interface.[118] They believed that oxygen residue from the reduction of both graphene flakes and CuO allowed for the formation of strong covalent bonds that significantly enhanced the nanocomposites strength. They measured the adhesion energy between sintered graphene and Cu at 164.47 ± 28.47 J m^{-2} — far higher than the adhesion energy of 0.72 ± 0.07 J m^{-2} gained by a Cu substrate grown graphene layer. They also reported an increased elastic modulus and increased yield strength for the 2.5 vol% RGO/Cu composite by ≈30 and 80%, respectively, which were higher when compared to pure Cu.

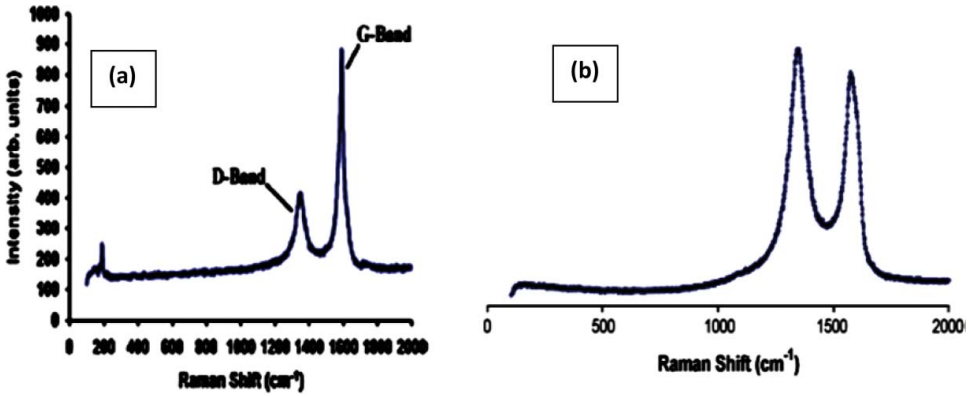

Figure 8. Raman spectral images of (a) SWCNT and (b) reduced Graphene samples. (© Elsevier Limited. Reprinted with permission from Liu et al.[120] Permission to reuse must be obtained from the rightsholder.).

5.1.2.2. C-nanofillers structural integrity. Investigators take structural damage and the amorphization of nanofillers very seriously during mixing and consolidation with metal powders. It is much necessary to maintain the C-nanofillers structure during process because all the superior characteristics of these nanofillers are due to their unique structure. Any damage caused to their structure would definitely effect their performance as reinforcing agents. Otherwise, structural impairments cause the formation of defective sites that trigger carbide reactions and lead to loss of graphitic structure[119] which, in turn, lead to failure of reinforcement purpose. Researchers tried to reduce defects by proper selection of a processing method as well as optimizing the processing parameters.

Raman spectroscopy is well known as a famously benign tool used to study C-nanofiller structure, especially as it records structural evolution data following respective processing steps. Figures 8a and 8b present the typical Raman spectra's of C-nanofillers. A spectrum data allows us to assess the reliability of a C-nanofillers structural efficiency using intensity ratios where 'D' = the number of lattice defects and finite crystal sizes due to severe 2D geometry damage and 'G' = hexagonal graphitic lattice arrangements measured as peak ratios, I_D/I_G. This means that a lower ratio indicates a better protected structure so that superior results can be expected in terms of enhanced mechanical properties.[120]

Rashad et al. fabricated a magnesium alloy (AZ31) reinforced with either 0.3 wt% CNT or grapheme using a semi-PM method with high-energy ball milling at 250 rpm for 4 h, employing a BPR of 10:1. Figure 9 shows Raman spectral images for CNT and graphene powders before and after milling vs. "as-received" CNTs and graphene nanoparticles,[99] which allow us to appreciate that ball milling clearly produced defects in both powders. The D-band of "as-received" nanomaterials depicts structural defects, whereas the G-band indicates the presence of protected hexagonal structures in both. This suggests that ball milling damages nanomaterials to some extent and creates defects that can negatively affect the strength of final composites.

According to Li et al., the structure of graphene can also be well maintained after composite processing via a

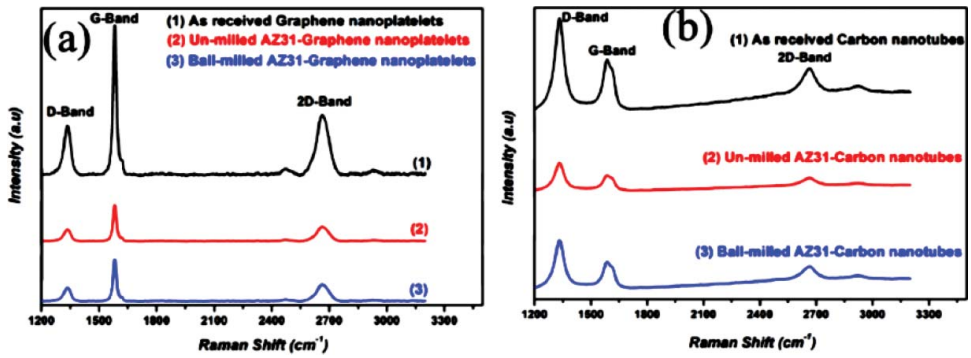

Figure 9. Raman spectroscopy: (a) "as received" graphene nanoplatelets and AZ31–graphene nanoplatelets composite powders before and after ball milling; and (b) "as received" carbon nanotubes and AZ31–Carbon nanotubes composite powders before and after ball milling. (©Elsevier Limited. Reprinted with permission from Rashad et al.[99] Permission to reuse must be obtained from the rightsholder.)

one-step thermal reaction and SPS processing. Defects were produced by subsequent processing but interestingly a decrease in I_D/I_G values were observed which can be attributed to the healing of those graphene defects by SPS consolidation.[117] Yan et al. also observed increased mechanical properties of a graphene nanosheets-Al composite due to the maintenance of graphene features without the typical interface reactions produced by ball milling.[104] Borkar et al. did not observe significant changes in D/G peaks, as their I_D/I_G ratios remained intact, indicating the survival of graphene's structure after milling.[121] Bastwros et al. and Das et al. demonstrated the increased intensity of defects that accompanies the protracted milling of graphene nanoplatelets and Al powder.[92,95,122] Although defects were induced in the grapheme structure, carbide was also produced by reactions but was not discussed in detail due to minimal formations and undetectable XRD levels. The concern is that prolonged milling fully embeds graphene nanosheets within the Al powder, which, in turn, buffers further impact forces from milling balls and therefore, delays the evolution of defect sites. Any increased level of defects in the graphene structure possibly reduces load bearing capability and seriously effects the composite's mechanical strength according to Cui et al.[93]

5.1.2.3. C-nanofillers and metals interfacial reactions (carbide formation). Another concern is that of interfacial reactions between C-nanofillers and the matrix that can be either favorable or harmful to the composite's strength. Interestingly, some researchers favor interfacial reactions that assist interfacial bonding,[123–125] while others have serious concerns about nanofillers because of transformations to carbides that can depreciate the final mechanical properties of a composite.[126–128] Apparently, much depends on the thickness of carbide formations on the nanofiller surface. A thick carbide layer is considered harmful whereas a thin (5–20 nm) layer enhances interfacial bonding.[18] Due to the nature of strong sp^2 bonded carbon atoms and the π-π bond interaction, nanofillers do exhibit chemically stable characteristics. Some researchers have reported the formation of carbides[129,130] but others have not observed their formation.[125,131] It appears that under favorable conditions, C-nanofillers easily react with a metal matrix and form reaction products such as carbides, as reported by many researchers.[132] The equation that governs reactions between nanofiller carbon and metals to form carbides is:

$$\frac{x}{y}\,M + C = \frac{1}{y}M_xC_y \tag{1}$$

where x and y are stoichiometric molar fractions; M and C represent metal and carbon based powders, respectively.

Hence, different interfacial carbides can form and settle on the C-nanofillers surface. These carbides have a shear strength that determines the amount of stress transmitted to the nanofiller. In the absence of an interfacial layer, stress is transferred through weak attractive forces between CNTs and the matrix. Figure 10 shows that the formation of carbides attached to the surface of a CNT can transfer loads in different directions.

Some researchers suggest that a thin transition layer of carbide provides a strong interfacial bond (e.g., Al_4C_3) that is produced by CNT/Al metal matrix reactions that improve wettability as well as interfacial strength.[21,22] The formation of an Al_4C_3 layer at the interface might also lower the wetting angle, as in the case of metal-graphite (from 135–140° to ~55°), and thus, lead to stronger adhesion such as covalent bonding.[133] Recently, Khorasani et al.[119] and Lara et al.[134] reported that the formation of Al_4C_3 through reactions at the interface of a CNT/Al nanocomposite possibly increased strength by establishing strong adhesion while also helpful in impeding dislocation. Zhou et al.

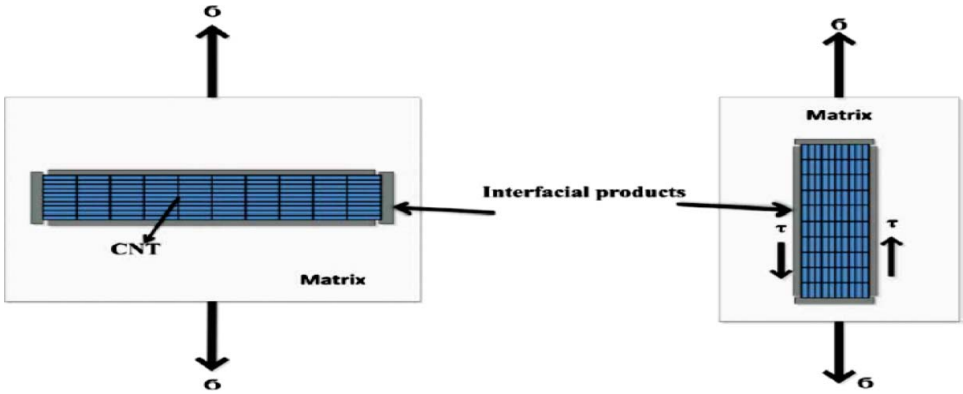

Figure 10. Carbide formation on the surface and different modes of load transfer to CNT. (© Taylor & Francis. Reprinted with permission from Munir et al.[66] Permission to reuse must be obtained from the rightsholder.)

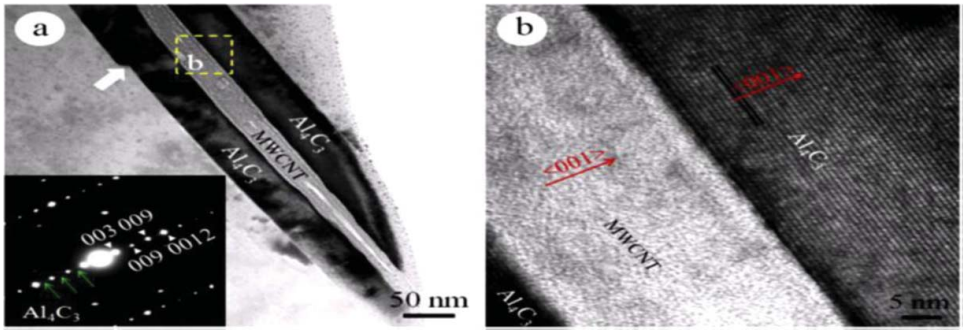

Figure 11. (a) Formation of Al_4C_3 is low along with the SAED pattern of Al_4C_3; and (b) high magnification HRTEM images of 5 vol% MWCNT-Al composite. (© Elsevier Limited. Reprinted with permission from Zhou et al.[135] Permission to reuse must be obtained from the rightsholder.)

concluded that interfacial reactions between CNTs and Al metal more favorably occurred on the edges of the active prism plane found at open ends and defect sites leading to Al_4C_3formation, as seen in Figure 11. This group also noted that a small amount of carbide formation could be helpful by providing shear resistance and also act as CNT anchors within Al as well as a cover that protects CNT structure from further damage, thus increasing load bearing capability.[135]

Some researchers intentionally used carbide-forming elements like Cr in a Cu matrix to encourage carbide formation to provide the necessary interface for wetting and bonding. Cho et al. prepared a CNTs/Cu Cr alloy nanocomposite via ultra-sonication followed by SPS and extrusion.[136] Figure 12 shows TEM images of Cr carbide at the CNTs/Cu interface, which facilitated load transfer and significantly enhanced tensile strength.

To the contrary, Bartolucci et al. did not support the formation of carbide phases for graphene reinforcement. They reported that carbide did not enhance strength and behaved rather in-elastically resulting in a decline of mechanical properties.[137,138] According to their observations, graphene was more prone to carbide formation than CNTs, likely because of its higher surface area and 2D geometry—i.e., upper and lower surfaces are easily available for defects produced during milling. In addition, excessive prismatic planes or edges of graphene platelets developed, either during graphene production or composite processing. These sites allow more defects and possible reactions with the matrix. Recently, Boostani et al. briefly described the demerits of carbide formation by fabricating encapsulated SiC graphene sheets and "as received" SiC particles (AR-SiC) to reinforce Al composites via ball milling.[94] They reported more Al_4C_3 formation in (AR-SiC) compared to SiC covered with graphene because carbide formation can only take place at impaired regions of GNSs (shown as white arrows), as confirmed by the SAD pattern, shown in Figure 13. In conclusion, AR-SiC is less able to transfer a load from the matrix to SiC particles than a graphene composite.

5.2. Strengthening mechanisms and carbon-nanofillers (CNTs and Graphene)

A large volume of research is underway to enhance the mechanical properties of metals by nanofiller reinforcement. Hence, it is important to know how nanofillers reinforce metals and which mechanisms actually enhance a composite's strength. The purpose of nanofiller-metal composites is generally defined as (i) major stress bearing enhancement of the matrix and (ii) plastic deformation intervention (dislocations) in the matrix.[85,139] Although acceptable results have been achieved thus far, at the same time, variables degrees of strengthening have been reported.[18,140] Hence, it appears that many factors contribute to strength enhancement,

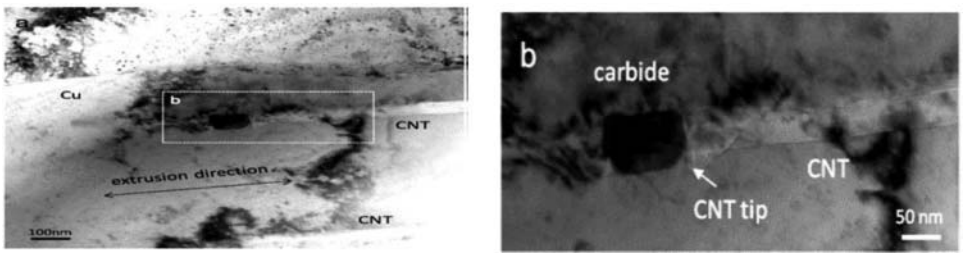

Figure 12. TEM images at low (a) and high (b) magnifications of an extruded CNT/Cu Cr composite. (© IOP Science. Reproduced with permission from Cho et al.[136] Permission to reuse must be obtained from the rightsholder.)

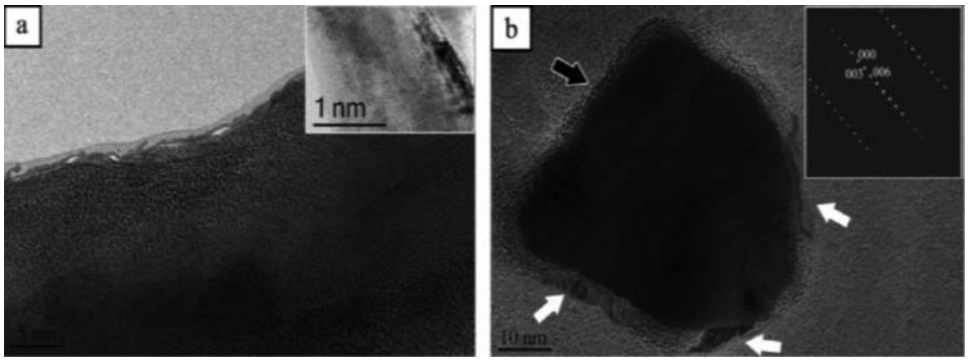

Figure 13. TEM images of microstructures showing rod-like structures and SAD pattern of Al_4C_3 at the SiC/matrix interface. (©Elsevier Limited. Reprinted with permission from Boostani et al.[94] Permission to reuse must be obtained from the rightsholder.)

some of which are directly due to nanofiller type and others due to processing conditions.[141]

As far as processing effects are concerned, different variables (temperature, pressure) and parameters generally affect the performance of C-nanofiller and results in nanocomposite with different level of strengths, as seen in most results of research previously reported. A major reason for this is that C-nanofillers respond differently in typical circumstances like during ball milling, milling time, BPR parameters, etc., define the magnitude of reinforcement role. Moreover, numerous researchers have explored C-nanofiller contributions to composite strength enhancement in terms of size, shape, concentration, aspect ratio and surface area, the number of walls or sheets, and surface morphology, etc., to evaluate strengthening effects.

Generally, C-nanofillers manage microstructural development by various strengthening mechanisms that affect the composite.[142] For this reason, metallurgists must fully understand the microstructure and mechanical properties of composite interactions. Although enhanced strengthening data is openly shared by well-documented research, the actual strengthening mechanisms of C-nanofillers remain unclear. It is also crucial to understand a nanofillers degree of strengthening efficiency and effect(s) before designing a nanocomposite. As an assessment tool of a C-nanofillers reinforcement effects in a metal matrix, "strengthening efficiency" has emerged to calculate these effects.[143] The Strengthening Efficiency (R) of reinforcement is expressed as the ratio of a composite's yield strength increase to the actual matrix yield strength, written as follows[144]:

$$\boldsymbol{R} = (\boldsymbol{\sigma_c} - \boldsymbol{\sigma_m})/\boldsymbol{V_r}\boldsymbol{\sigma_m}, \tag{2}$$

where σ_c& σ_m represent yield strength of the composite and matrix and V_r is the volume fraction of the reinforcement.

A higher R-value is directly proportional to strengthening efficiency. Recently, Xiong et al. calculated the strengthening efficiency of graphene in graphene/Cu nacres produced by the preform impregnation process.[145] The R-value calculated for graphene ranged from 100–210, which is far superior to ceramic particles and CNT-Cu matrix nanocomposites. They attributed this high R-value to (i) graphene's intrinsic properties (higher 2D structure and specific surface area vs. other reinforcements) and (ii) to the structural stability and the strategic unidirectional distribution of graphene. Carbon nanosheets in a Cu matrix exhibited a strengthening efficiency of 30.5, which was 1.5 times higher than CNTs in a 10 vol% CNT-Cu composite, per Wang et al.[144] Hence, we can conclude that the R-value not only determines strengthening efficiency but also reflects the reinforcement contribution to an applied metallic system.

Presently, few scientists follow a specific micromechanical model to forecast a composite's strength when reinforced with high aspect ratio nanofillers. However, the question remains as to whether or not such models truly represent the actual strength attained after processing. The ambiguity arises due to issues attending nanofillers and metals during processing as already discussed in details that are problematic. Some researchers put a great deal of effort into achieving results that were projected by respective models. Table 5 summarizes frequently used micromechanical models for graphene and CNTs that follow the strengthening mechanism and equations currently in use. CNT or graphene reinforcements within metals show different contributions to strengthening mechanisms than do particles due to major difference in geometry and properties. Specific types of strengthening mechanisms attributable to the nano-reinforcement of metals remain an open issue and require more detailed study. To date, numerous researchers have attempted to identify the strengthening mechanism of nanofillers both experimentally and by computer simulation. Their results indicate several assumptions that likely play key

Table 5. Different strengthening mechanisms and equations used to predict composite strength.

Strengthening Mechanisms	Model/Equation Used	Equation Expression	
		Graphene	CNTs
Load transfer (LT)	Shear Lag Model[105,151,252–254]	$\sigma_c = \sigma_m\left[\frac{V_f(s+4)}{4} + (1 - V_f)\right]$	$\sigma_c(T.S) = \sigma_{CNT}V_{CNT}\left(\frac{l}{l_c}\right) + \sigma_M(1 - V_{CNT})\ for\ l < l_c$
		(Generalized Shear-Lag)	$\sigma_c(T.S) = \sigma_{CNT}V_{CNT}\left(1 - \frac{l_c}{2l}\right) + \sigma_M(1 - V_{CNT})\ for\ l > l_c$
		$\Delta\sigma_{LT} = \frac{f_v\sigma_m}{2}$	$l_c = \frac{d\,\sigma_f}{2\tau_y}$
		(Load transfer yield strength)	$(l_c = Critical\ Length)$
		$\sigma_c = \sigma_m(1 + pV)$	$\sigma_{Y.C} = \sigma_{Y.M}\left[V_{CNT}\frac{(S_{eff}+2)}{2} + V_M\right] - 1$
		(Modified Shear-Lag)	
Grain refinement (GR)	Hall-Petch Equation[104,255,256]	$\sigma_y = \sigma_o + Kd^{-1/2}$	
		$(d = Grain\ size)$	
Dislocation Looping Strengthening (DL)	Orowan Effect[18,105,153,257]	$\Delta\sigma_{Orowan} = \frac{0.81MGbln(d_p/b)}{2\pi\sqrt{(1-\nu)}(\lambda - d_p)}$	$\Delta\tau = \frac{A}{rln(^2r/_{r_o})}\ Gbf^{1/2}$
Strengthening participant carbide (SC)	Coleman Equation[140,258]	$\sigma_c = (1 + {}^2b/_D)\left[\sigma_{Shear}\,{}^l/_D - (1 + {}^2b/_D)\sigma_m\right]V_f + \sigma_m$	
		$\Delta\sigma_{CTE} = \alpha Gb\sqrt{\frac{12\Delta T\Delta C f_v}{bd_p}}$	
Thermal & Elastic mismatch strengthening (TM &EM)	Taylor Equation[1,18,250,259–262]	$\Delta\sigma_{CTE+EM} = \sqrt{3}\ \beta Gb\left(\sqrt{\rho^{CTE}} + \sqrt{\rho^{EM}}\right)$	$\sigma = \sigma_O + \alpha M^T Gb\rho^{1/2}$
		$(Combined\ Effects\ of\ thermal\ \&Elastic\ Modulus\ mismatch)$	$\rho_{th} = \frac{10V_f\varepsilon}{bt(1-V_f)}$
		$\rho^{EM} = \frac{6v_p}{\pi d_p^3}\varepsilon$	$(\rho_{th} = Disloaction\ Density\ )$
		$(Disloaction\ Density\ by\ Elastic\ Modulus\ mismatch)$	
		$\rho^{CTE} = \frac{A\Delta\alpha\Delta T v_p}{bd_p(1-v_p)}$	
		$(Disloaction\ Density\ by\ Thermal\ Modulus\ mismatch)$	
Geometric Mismatch (GM)	[105,263]	$\Delta\sigma_{geo} = \alpha Gb\sqrt{\frac{f_v 8\gamma}{bd_p}}$	–

*Details of respective equation symbols and constants for designated references.

roles related to the reinforcement mechanisms of nanofillers in metal nanocomposites, and which go far in explaining an increase in nanocomposite strength. Possible strengthening mechanism for nanofillers (CNTs and graphene) in metals as reported in the literature include the following:

(1) load transfer strengthening;
(2) strengthening by dislocation interference (Orowan strengthening);
(3) strengthening due to thermal, elastic moduli, or geometric mismatch between nanofiller and metal matrix;
(4) grain improvement strengthening;
(5) nanofiller dispersion strengthening;
(6) solution strengthening of carbon atoms;
(7) reaction carbide transition layer strengthening;
(8) nanofiller clustering strengthening; and
(9) precipitation hardening strengthening.

In some cases, mechanisms play an individual role but at times the composite's strength results from synergistic effects.[65,105,146,147] We can express the combined effects of strengthening mechanisms by determining the yield strength of a nanocomposite using the following equation [148]:

$$\sigma_{yc\ (Predicted)} = \sigma_{ym} + \Delta\sigma_{Load} + \Delta\sigma_{Orowan} + \Delta\sigma_{Thermal\ \&\ Modulus\ CTE} + \Delta\sigma_{GEO\ CTE}, \quad (3)$$

where σ_{yc} & σ_{ym} represent yield strengths of both nanocomposite and matrix.

In most reported cases, nanofillers have followed the first four strengthening mechanisms listed above. These are most likely the predominantly effective, major strength contributors; even so, they are not so obvious. Firstly, load transfer or bearing is defined as the transfer of load from the metal matrix to nanofillers via interfacial shear stresses produced as the matrix strains when the composite is loaded. George et al. was the first to thoroughly explain the strengthening mechanism of Al -MWCNT composites via experimental results, which indicated that "load bearing" and "shear lag" models played major.[131] This mechanism has thus far received the most attention, as the nanofiller would bear the total load and properly consume its mechanical properties in the composite. Competency of a stress transfer from matrix to nanofillers can only be made ideal by reducing interfacial reaction activity while enhancing structural stability and interfacial bonding. The shear-lag model, presented by the Kelly-Tyson equation, is used to estimate the load transfer mechanism (Table 5). This model is mainly used to assess the effective strength of a composite (σ_c) metal matrix with a short fiber load-mechanism,[149] and is usually designed for high aspect ratio reinforcements.

Recently, Chen et al. used the shear-lag model to confirm the load transfer mechanism of a CNT-Al nanocomposite by observing high strengthening efficiency and excellent congruence with predicted results. He supported his claims by examining pull outs of CNT surface fractures during the tensile test, which indicated interwall interactions with the matrix and highly effective load distribution, as shown in Figure 14a.[65] Boesl et al. did an *in situ* tensile test on a 1.0 vol% CNT-Al nanocomposite prepared by SPS to assess CNT strengthening behavior.[150] They reported a 40% increase in tensile strength as result of low fraction, long CNT, and minimum carbide reactions and importantly followed load-bearing strengthening by CNTs. The shear-lag model theoretical tensile result (90–110 MPa) for the Al–CNT nanocomposite agreed well with experimental values (95.5 MPa), which endorsed both the fiber strengthening mechanism and themodel. Figure 14b exhibits a CNT pull out from the Al matrix as a result of strong adhesion; hence, this behavior confirmed the stress transfer mechanism from matrix to CNTs as the cause of ruptured outer layers.

Similarly, Kurita et al. demonstrated the load-bearing contribution of MWCNTs in Al nanocomposites (0.6 vol% MWCNTs in Al matrix). They reported a UTS

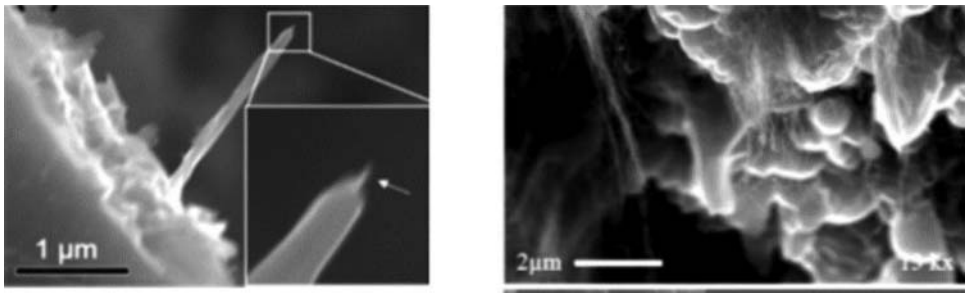

Figure 14. (a) Ruptured MWCNTs walls pulling out after CNT/Al composite tensile test; (b) SEM magnified image of a CNT pull out on a fractured surface. (© Elsevier Limited. Reprinted with permission from Chen and Boesl et al.[65,150] Permission to reuse must be obtained from the rightsholder.)

value consistent with the shear-lag model above this volume fraction. It most likely deviated from the model due to agglomerations which act like defects that cause a composite's mechanical properties to wane.[151] Shin et al. demonstrated the strengthening effect of graphene in an Al matrix and reasonably correlated experimental values with those predicted by the available theoretical models.[85] They also compared the strengthening efficiency of graphene with CNTs and strongly suggested that composite strength performance was associated with effective load transfer at the interface. Furthermore, they opined that stress transfer was more favorable to reinforcement, which has a larger specific surface area per volume and a capable interface with the matrix. They reported a tensile strength increment of 71.8% increment, which proved that graphene has greater ability to tolerate and transfer stress than CNTs because of the larger specific surface area per volume (12.8 times than of CNTs) granting a larger contact area (3.5 times), as does their 2D geometry. In addition, the shear-lag model supported their experimental results, further confirming the strengthening cause in the grapheme-Al nanocomposite.

Second, strengthening mechanism is dislocation interference (the Orowan looping mechanism). This process is frequently observed in nanoparticle size composites and is based on increased dislocation density.[152] Nanofillers are considered more effective than coarse fillers because their large inter-particle average distances cannot fulfill all requirements.[153] Moreover, experiments, molecular dynamics, and computer simulations have established that nanofillers offer excellent barriers to dislocation motion.[154] Generally, Orowan strengthening is the result of nano-reinforcement responses to dislocations. Nanofillers acts like an obstacle that impedes dislocation motion, thus preventing dislocation pile-ups (forest). This generates dislocation bowing and successive dislocation loops that pass through nanofillers to produce sufficient back-stress that drives back the dislocation motion. This is the mechanism known as Orowan looping that consequently improves the composite's strength. Some researchers conceive that the Orowan strengthening operates like grains in a matrix and consider it greater than reinforcement. However, to obstruct dislocation movement, the reinforcement must be present in the grains and not at grain boundaries.[155,156] Lahiri et al. observed the formation of dislocation forests in Al-9.5 CNT composites through a sandwich process and reported it as a major factor in strengthening increase (see Figures 15a,b). They attributed the dislocation forest and increased strength to the CNT content in the matrix.[157] Recently, Jiang et al. reported 90% and 81% increases in yield and compressive strengths, respectively, due to the effective constraint provided by graphene in Cu metal.

Third, related to dislocation generation via residual plastic strain due to large differences in texture, as reflected by an elastic and thermal expansion coefficient (CTE) mismatch between the metal matrix and nanofillers. A large coefficient difference in thermal expansion or the elastic modulus of nanofillers and metals is about 10:1, and are major causes of high dislocation pile-ups, also known as geometrically induced necessary dislocations (GNDs). This type of strengthening is also referred to as indirect strengthening and is created by residual strain gradients from contractions due to cooling after the elevated temperatures of processing. Nanofillers such as CNTs and graphene have thermal expansion coefficients of $\sim 10-^{6}\ K^{-1}$, whereas as Al's and Mg's are much larger at $23.6\times 10-^{6}\ K^{-1}$ and $27\times 10-^{6}\ K^{-1}$, respectively. Outcomes from this difference include: (i) the prismatic punching of dislocations at the interface and (ii) the work hardening the matrix.[158] The high aspect ratio of nanofiller forms high dislocation density and thereby increases strength. Notably, this type of strengthening requires coarse grains to better redistribute GNDs over the entire matrix and wherever the nanofiller has room enough to gather such dislocations. If not, GNDs are limited to nanostructured interfacial boundaries and allow inadequate strain hardening, as revealed by numerous TEM studies.[159–161] Surprisingly, recent reviews of CNT reinforced MMC literature failed to mention clear indications of thermal mismatch-induced strengthening

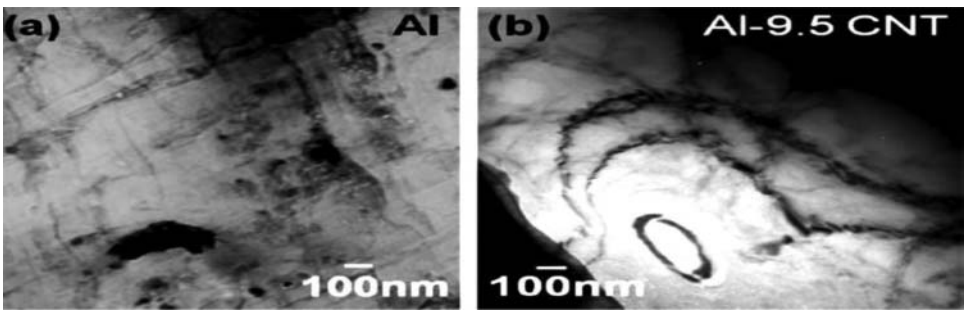

Figure 15. TEM images of (a) dislocation loops at sub boundaries; and (b) nanosized MLG particles in grain interiors forming dislocations. (© Elsevier Limited. Reprinted with permission from Lahiri et al.[157] Permission to reuse must be obtained from the rightsholder.)

applicability.[4,66,140,141] Nevertheless, this mechanism was predicted by some researchers for graphene-metal nanocomposites but never discussed in detail.[96,162,163] However, Liu et al. soundly posited that improved tensile properties of nanocomposite solders was likely due to the building of high dislocation density around graphene secondary to thermal mismatch strengthening.[164]

Last, crucial strengthening mechanism is grain boundary improvement or refinement, which plays a specific role in structural applications since microstructural developments are involved. It has been acknowledged by many researchers that grain refining is achieved by incorporating nanofillers in metals/alloys with a view to increase strength.[165,166] Strength is directly proportional to grain size, i.e., nanometer grain microstructures have greater strength than microcrystalline equivalents.[167–169] Generally, this type of mechanism follows the well-known Hall-Petch relationship, which is used to calculate the yield strength of polycrystalline metals. Stress concentration becomes higher as grain boundaries fail to increase as a consequence of finer grain size. In turn, this leads to dislocation forests at grain boundaries and more resistance to dislocation motion. Nam et al. demonstrated the relationship of yield strength to grain size by the addition of CNTs in an Al-Cu alloy. Figure 16 presents their findings of increased yield strength with decreasing grain size due to CNT effects.[146]

Xiong et al. opined that the key to graphene's strengthening mechanism in metals such as Fe, Mg, Ni, Cu, and Al was its enfolding of the metallic grains. They suggested this impeded dislocation activity at the grain's boundary and specifically targeted small grain formations during processing.[145] Moreover, they concluded that grain refinement was attained by plastic flow resistance as the result of dislocation density formation at the grain's boundaries. They further suggested an optimal grain size of 20–30 nm but no smaller; otherwise, atomic migration take place easily instead of flow stresses needed to hinder plastic deformation.[170,171]

Li et al. added CNTs to a Mg–6Zn matrix and predicted UTS values with the Kelly-Tyson equation with excellent results, showing that nanofillers significantly contributed to

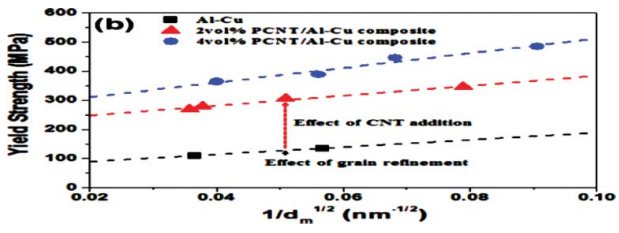

Figure 16. The Hall–Petch mechanism followed by Al–Cu and PCNT/Al–Cu composites (© Elsevier Limited. Reprinted with permission from Nam et al.[146] Permission to reuse must be obtained from the rightsholder.)

the refinement of grains in the Mg nanocomposite.[148,172] Borkar et al. synthesized 1–5 vol% graphene-Ni nanocomposites and achieved similar results. They attributed increased yield strength to the Hall-Petch strengthening mechanism and grain refinement.[121] Other mechanisms impact metal matrix strengthening but are not commonly appreciated. Some authors have associated increased precipitation hardening with the addition of CNTs along with dislocation generation due to their presence.[173,174]

5.2.1. Dislocation formation by C-nanofillers in metals: A case study

In recent years, a number of studies have established that dislocation propagation is disturbed by the creation of high-density interfaces by nano-reinforcement, and which powerfully challenge dislocation motion when shear force is applied. Essentially, this means that the more difficult the dislocation motion, the higher the strength of the composite. This can also be achieved by restricting dislocation motion in a constant slip plane via the difference in grain positioning and higher lattice disorder.[136] Piled up dislocations tend to segregate and escape through free openings at interfaces but nano-reinforcements do not allow them to shear their way through. Hence, the reinforcement successfully impedes gliding dislocations. Kim et al. demonstrated an extreme case of increased strength in a graphene-Cu-Ni nano-layered composite by using the nanopillar compression test.[113] They associated this behavior to graphene's ability to (i) block dislocation propagation at the interface caused Cu grain sizes (ranging from 125–143 nm) and (ii) layer spacing reiterations that ranged from 194–200 nm for plastic deformation to occur. They observed strength's dependence on layer spacing, which followed the familiar Hall-Petch relation, i.e., ($\sigma \alpha$ h-1/2), where (h) equals reiterate layer thickness. Increased dislocation density produces high shear flow stress that faces difficulty in overcoming available graphene layers at the interface. This strongly indicates the shifting of graphene's obstructive mechanism of plastic deformation to the next layer (Figure 17). Furthermore, they particularized role of graphene pinning and interactions with Ni at the atomic level. They achieved this by conducting molecular dynamic simulation studies that reflected graphene's stiffness and impermeable nature, as portrayed in Figure 18.

5.3. Strengthening mechanism contribution of C-nanofillers and effect on mechanical properties

As is known, C-nanofillers (CNTs and graphene) have the same molecular structure and properties but different morphology producing different results in terms of

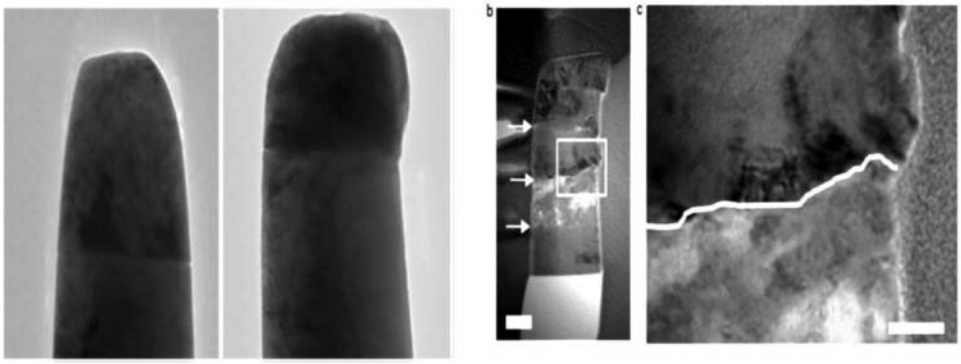

Figure 17. (a) Dislocation density blocking effect by graphene causing high shear flow stress; (b) TEM images showing dislocation motion obstruction by graphene before and after compression testing (© Nature Communications. Reproduced with permission from Kim et al.[154] Permission to reuse must be obtained from the rightsholder.)

enhanced properties. Rafiee et al. indicated that low-content graphene nanoplatelets exhibit more increase in tensile and toughness in epoxy than CNTs which can be attributed to the graphene unique 2D nature and better interaction with epoxy.[175] Similarly, strengthening the efficiency of CNTs and graphene predict their role in improvement in metal nanocomposites. Chen et al.[176] studied the effect of graphene nanoplatelets addition in Mg matrix via liquid and solid stirring techniques. They found a significant increase of 78% in hardness as compared to pure Mg. They also compared the hardness values achieved and strengthening the efficiency of GNPs with other reinforcement like CNTs, as seen in Figure 19. It can be clearly observed that GNPs has shown the pronounced effect on hardness and excellent strengthening efficiency to strengthen metal matrix as compared to other carbon and ceramic reinforcements. This confirms the GNPs superiority over other reinforcing agents due to its intrinsic properties, extremely large aspect ratio and unique morphology and low content usage as well. Enhancement in mechanical properties of MMNCs is usually governed by strengthening mechanism or models predicted by researchers followed by C-nanofiller.

In this contest, we have gathered data of CNTs and graphene reinforced MMNCs to highlight major mechanism operative and typical effect on mechanical properties. Tables 6 and 7 present a comprehensive mechanical properties data of the CNTs and graphene-reinforced metallic nanocomposites reported by various researchers over the last couple of years. The following conclusions can be drawn from these tables.

(i) Nearly all researchers have used powder metallurgy route to fabricate C-nanofillers nanocomposites due to its processing advantages.
(ii) C-nanofillers have proven themselves to be ideal reinforcements for enhancement in mechanical properties of nanocomposites as compared to their unreinforced counterparts.
(iii) Quantification or trend of the mechanical properties increase more than pure metal and alloys.
(iv) C-nanofillers contribute more to strengthen metals up to certain or small added fractions

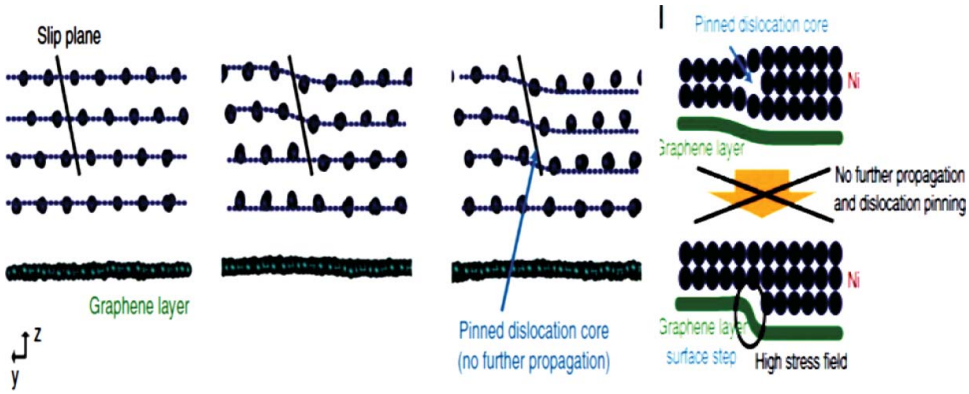

Figure 18. MD simulations representing single dislocation movement from start to middle followed by the pinning action that caused blocking at the Ni-graphene interface. Blue = Ni atoms, and green = grapheme; (d) Elaboration of dislocation propagation hindrance, revealing graphene's stiffness and bending characteristics. (© Nature Communications. Reproduced with permission from Kim et al.[154] Permission to reuse must be obtained from the rightsholder.)

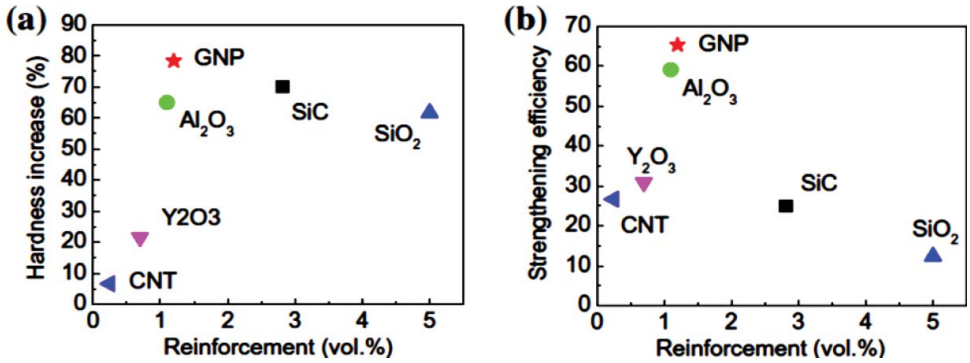

Figure 19. Comparison and effect of GNPs addition (a) Hardness and (b) difference in strengthening efficiency contribution with other nano-scale fillers in Mg-MMNCs (© Elsevier Limited. Reprinted with permission from Chen et al.[176] Permission to reuse must be obtained from the rightsholder.).

while high concentration leads to a decrease in properties possibly due to an agglomeration problem.

(v) C-nanofillers (CNTs and graphene) exhibited different strength enhancement contribution in metals. As clearly seen, graphene contributes more in strength improvement than do CNTs.

(vi) Most importantly, these tables reveal the possible strengthening mechanism followed by C-nanofillers as recorded by these researchers.

As depicted in these tables, C-nanofillers fully serve the purpose and properly utilize their reinforcing role in MMNCs. The development of C-nanofillers metallic nanocomposites still experience hindrances due to the

Table 6. Mechanical properties and strengthening mechanism contributions of different CNT-metal nanocomposites (summary of published literature for 2014 and 2015).

Researchers	Year	Matrix System	CNTs Content		Fabrication Methods	Strengthening Mechanism Contribution	Yield strength, MPa	Tensile strength, MPa	Fracture strain, %
			Vol%	Wt.%					
Borkar et al.[237]	2014	Ni	0	—	PM + SPS method	GR	350	—	30
			5.0	—	Ultrasonication + SPS Process		690	—	8.0
Ogawa et al.[264]	2015	Al	0	—	Ball milling + SPS +	GR + LT + TS + OS	239.3	378.3	—
			3	—	Hot Extrusion		287.5	427.1	—
Han et al.[265]	2015	AZ31 (Mg Alloy)	0	—	Ultrasonication + Hot	GR	220	301	12
			0.1	—	Extrusion + Melting		270	322	8.0
Nai et al.[113]	2014	Mg	—	0	PM + Microwave sintering	GR + CS	126 ± 1	171 ± 2	7.9 ± 0.3
			—	0.3			119 ± 4	163 ± 7	5.7 ± 0.2
			—	0.3Ni+CNT			206 ± 2	237 ± 1	6.4 ± 0.3
Chen et al.[65]	2015	Al	0	—	Solution ball milling + SPS process	LT	—	157	—
			0.51	—			—	180	20
			0.88	—			—	192	20
Shi et al.[266]	2014	Mg–6Zn	—	0	Ball milling + Ultrasonic melt process	GR + LT	35	155	7.0
			—	0.5			92	192	7.6
Boesl et al.[150]	2014	Al	—	0	Ultrasonication + SPS process	LT	68.1	—	—
			—	1.0			95.5	—	—
Chen et al.[81]	2015	Al	—	0	PM + SPS + Hot Extrusion	LT	90.3 ± 0.5	100.6 ± 0.6	38.3 ± 2.8
			—	0.6			114.1 ± 2.0	122.5 ± 2.3	25.4 ± 2.7
Li et al.[143,148,172]	2014	Mg–6Zn	0	—	Ultrasonication + melting mixing + Hot extrusion	LT + OS + GR	157 ± 5.5	271 ± 6.6	22 ± 3.4
			1.0	—			209 ± 6.6	321 ± 7.1	17 ± 4.5
Rashad et al.[99]	2015	AZ31 (Mg Alloy)	—	0	Semi powder metallurgy	TS + ES + OS + LT	195 ± 5	285 ± 2.9	14.5 ± 1.5
			—	0.3			210 ± 2.8	310 ± 5.4	13.3 ± 3.0
Park et al.[267]	2015	Al		0,	Wet ball milling +sonication+ HEBM+ melt blending+ casting	LT	56 ± 0.6	92 ± 0.3	21 ± 0.7
				0.1			71 ±3.5	103 ± 2.2	10 ± 1.2
				0.2			90 ± 2.7	114 ±1.6	9 ± 1.6
				0.3			102 ± 4.4	119 ± 4.5	2 ± 0.4
				0.4			111 ± 4.0	117 ± 5.5	1 ± 0.7

Table 7. Mechanical properties and strengthening mechanism contributions of different Graphene-metal nanocomposites (summary of published literature for 2014 and 2015).

Researchers	Published Year	Matrix System	Graphene Content Vol%	Graphene Content Wt.%	Fabrication Methods	Strengthening Mechanism Contribution	Yield Strength, MPa	Tensile Strength, MPa	Fracture Strain, %
Yan et al.[104]	2014	Al alloy	—	0	Ultrasonication + Ball milling+ heat isostatic pressing + Hot Extrusion	OS + GR + LT	214	373	12
			—	0.15			262	400	15
				0.5			319	467	18
Kim et al.[163]	2014	Cu	0	—	Ultrasonication + Ball milling+ high-ratio differential speed rolling	OS	314.2 ± 4.5	384.2 ± 8.2	25.1 ± 3.5
			0.5	—			323.4 ± 5.2	401.3 ± 5.2	21.1 ± 2.4
			1	—			360.5 ± 2.1	425.5 ± 3.3	16.4 ± 3.6
Chu et al.[110]	2014	Cu	0	—	ball milling + hot-pressing	GR	140	—	—
			5.0				170	—	—
			8.0	—			310	—	—
			12				190	—	—
Rashad et al.[250]	2014	Mg–1%Al–1%Sn–0.18%	—	0	Semi powder metallurgy	TS + ES + LT	161 ± 04	236 ±5.1	16.7± 03
			—	0.18			208 ± 5.3	269 ± 03	10.9 ±3.4
Rashad et al.[147]	2014	Mg–1%Cu	—	0	Semi powder metallurgy	TS + ES + OS + LT	104 ± 4.0	164 ± 5.0	6.2 ± 1.8
			—	0.18			160 ± 6.0	240 ± 2.0	10.4 ± 2.1
			—	0.36			184 ±3.0	252 ±3.0	12.2 ± 1.3
			—	0.54			226 ±5.0	260 ±5.0	4.8 ±2.5
Rashad et al.[105]	2015	Mg–0.5–1.5 Al	—	0	Semi powder metallurgy	TS + ES + OS + LT+ GS	162 ± 5.0	195 ± 4.0	3.7 ± 2.5
			—	0.5Al-0.18			173 ± 4.0	230 ± 5.1	10.7 ± 3
			—	1.0Al–0.18			190 ±5.3	254 ±3.0	15.5 ± 3.4
			—	1.5Al–0.18			209 ±3.9	268 ±4.5	12.7±2
Rashad et al.[99]	2015	AZ31 (Mg Alloy)	—	0	Semi powder metallurgy	TS + ES + OS + LT	195 ± 5.0	285 ± 2.9	14.5 ± 1.5
			—	0.3			173 ± 6.0	275 ± 5.7	21.7 ± 2.8
Li et al.[248]	2015	Al	—	0	Cryomilling + Hot Extrusion	LT + GR	125	147	17.3
			—	0.5			136	173	19.9
			—	1.0			194	248	8.3
			—	1.5			160	200	5.0
			—	2.0			130	175	2.0
Mei-Xia Li et al.[117]	2015	Cu	—	0	Ultrasonication + SPS process	LT + GR	128	214	38
			—	0.6			225	316	29
Chao Zhao[249]	2015	Ni	—	0	Molecular level mixing +SPS process	LT	193	485	34.2
			—	0.9			512	741	14.6
			—	1.5			826	948	12.1
							773	835	7.5
			—	2.4					
Hwang et al.[118]	2013	Cu	0	—	Molecular level mixing + SPS Process	OS + LT	160	255	—
			1.0	—			230	300	—
			2.5	—			284	335	—
Shin et al.[85]	2015	Al	0	—	PM process + Hot rolling	LT	262	—	13
			0.3	—			340	—	5.5
			0.5	—			400	—	5.0
			0.7	—	440	—	3.0		
Tang et al.[254]	2014	Ni/Cu	0	—	Ultrasonication +SPS process	LT	138	230	—
			0.5	—			195	271	12.5
			1.0	—	268	320	19		
Borkar et al.[121]	2015	Ni	0	—	Ball Milling + SPS process	GR + LT	160 ±5	—	—
			1.0	—			370 ±3	—	—
			2.2				390 ± 3.5	—	—
			5.0	—			350 ±6	—	—

(1) Load transfer strengthening = LT; (2) strengthening by dislocation interference (Orowan strengthening) = OS; (3) strengthening due to thermal, elastic moduli, and geometric mismatch between nanofiller and metal matrix = TS, ES, GS; (4) grain improvement strengthening = GR; (5) nanofiller dispersion strengthening = NS; (6) solution strengthening of carbon atoms = SS; (7) reaction carbide transition layer strengthening = CS; (8) nanofiller cluster strengthening = NCS; (9) precipitation hardening strengthening = PS.

unclear origins of strengthening. Therefore, it is very important to recognize relevant strengthening mechanisms of C-nanofillers which is a critical issue. Proper understanding can lead to design composites by utilizing the full potential of these C-nanofillers for required engineering applications. As discussed in the above section and based on the tables' data, C-nanofillers normally follow strengthening mechanisms, namely: (i) direct strengthening (load transfer strengthening) and (ii) indirect strengthening (grain refinement, dislocation-based strengthening). It can be clearly seen that almost every researcher has reported the synergistic effect of strengthening mechanisms. Among them, load transfer strengthening is dominantly followed by C-nanofillers and has evident effects on mechanical properties.[65] Here the following question arises: Do both CNTs and graphene equally follow this mechanism? As Tables 6 and 7 clearly demonstrate the variation of mechanical properties enhancement revealed by CNTs and graphene reinforced metallic nanocomposites, respectively. Therefore, it is important to highlight that particular difference which defines the importance of load transfer capability. Strengthening of MMNCs majorly relies on adopted processing techniques, dispersion, interface quality, and nanofiller intrinsic characteristics like size, shape, content, aspect ratio, properties, and geometry. There is no doubt that uniform dispersion of C-nanofillers is the ultimate key to efficiently transfer load to reinforcement. It is well known that strength surge is proportional to an increase of C-nanofillers content via increased load efficiency.[159] But higher content dispersion of both nanofillers is still challenging and resulted in agglomerations at the high content lead to the load transfer efficiency reduction from a matrix to reinforcement. Similarly, strong interfacial contact of C-nanofillers is crucial and necessary for effective load transfer, although mechanical properties of the C-nanofillers promise to provide needful strength but overall it is governed by the adopted processing route. During processing, the size of the nanofillers normally reduced and reached certain critical length (lc) of C-nanofillers which affects load bearing capacity. Shin et al.[177] calculated the critical length using the formula and found lc values for MWCNT and FLG equal to 1 and 0.381 μm. Nanofiller length should be higher that this critical length to experience maximum stress transfer otherwise nanofiller was unable to carry load stress and composite fails by the matrix tensile failure. They also declared that graphene contains unique geometry having 2D sheet form provided two faces for interaction and ideal for stress exchange with the matrix. Similarly, graphene possesses a higher specific surface area per volume which is 2.6 times that of CNTs, a major difference in stress transferring mechanism resulting in more strength enhancement as compared to CNTs. In another study, they also proved the graphene superiority in increasing compressive elastic modulus and yield stress of Ti and Al nanocomposites as compared to CNTs MMNCs shown in Figure 20. This figure clearly explains that graphene has a striking improvement in properties at low fraction addition as compared to CNTs' incorporation in Ti and Al matrices.

Another aspect of graphene is that it normally rests at intergranular regions or grain boundaries and because of 2D sheet nature, it covers more grains area than CNTs.[178] This resulted in crack movement delay and provides high resistance to crack propagation during subsequent MMNCs rupturing as seen in tensile testing.[179] Moreover, the large specific area of graphene needed higher energy to pull from the matrix than CNTs, as evident in many tensile fractures of MMNCs.[178,180] This discussion evidently provides the importance of graphene characteristic and load transfer mechanism resulting in higher strength as compared to CNTs.

As seen in Table 6 and Table 7, mechanical properties were also dictated by indirect strengthening mechanism

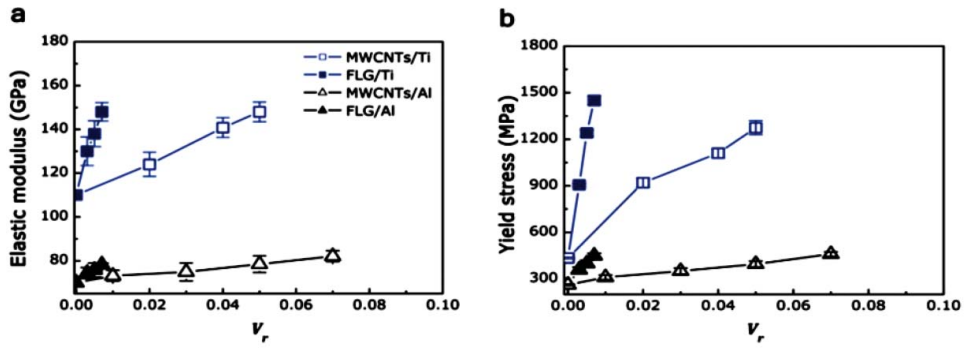

Figure 20. Performance comparison of CNTS and graphene in Al and Ti matrices over the range of volume fraction in terms of (a) elastic modulus and (b) compressive yield stress of the composites. (© Scientific Reports. Reproduced with permission from Shin et al.[177] Permission to reuse must be obtained from the rightsholder.)

(dislocation strengthening) of the C-nanofillers in different metals. This type of strengthening is related to the grain refinement (pinning effect), CTE mismatch, and dislocation density generation (prismatic punching effect). It is worth mentioning that these types of mechanisms functioning and extent of strength improvement is very much dependent on C-nanofillers size, aspect ratio, and dispersion, i.e., within the grains or at grain boundaries. During processing, C-nanofillers experience size reduction with a change in aspect ratio defines the mechanism to start play role in strength improvement. For instance, C-nanofillers with reduce size and aspect ratio may behaves like a dispersed particles led to dispersion strengthening and inappropriate for load transfer strengthening.[165] Therefore, indirect strengthening is also more pronounced in such type of nanocomposites. Generally, C-nanofillers increase hardness proportional to the strength of the MMNCs following this mechanism due to resultant reduction in grain size by pinning phenomena and dislocations density formation.[163] These also very important mechanisms of C-nanofillers in metals and can be effective to a large or small extent simultaneously linked to the volume fraction and nature of C-nanofillers property difference with matrices such as thermal or modulus mismatch which significantly help in dislocation hindrance and formation. Higher volume fractions of C-nanofillers led to lessen inter-distance between particles creating interference for dislocation motion.[148] Thus, a higher flow stress is needed to create pile up of dislocation at grain boundaries, eventually making it difficult to pass through grain boundaries.[181] Comparatively, CNTs are more capable for grain refinement than GNPs because their tubular structure well matched to settle within grains. Presence of CNTs majorly at grain boundaries generate high stresses to restrict grain coarsening resulting grain pinning and refinement.[155] Whereas graphene in the form of a sheet has flexibility and wrapping nature may not produce pinning effect such as CNTs. Similarly, dislocation density caused by strain produced due to thermal mismatch was shown by both C-nanofillers in most cases. Lastly, Orowan strengthening is also followed by these C-nanofillers but is much dependent on particle fragments' size during processing, particles dispersion state, and within grains, i.e., matrix grain size higher than nanofillers.[163] Overall, graphene sheets are believed to have provided more dislocation interference via planar morphology and higher aspect ratio. Figure 21 clearly demonstrates the contribution of C-nanofillers in terms of strengthening mechanism reported by researchers in the last few years (Tables 6 and 7). It can be observed that C-nanofillers mainly follow load transfer mechanism, then grain refinement by pinning effect, and then other

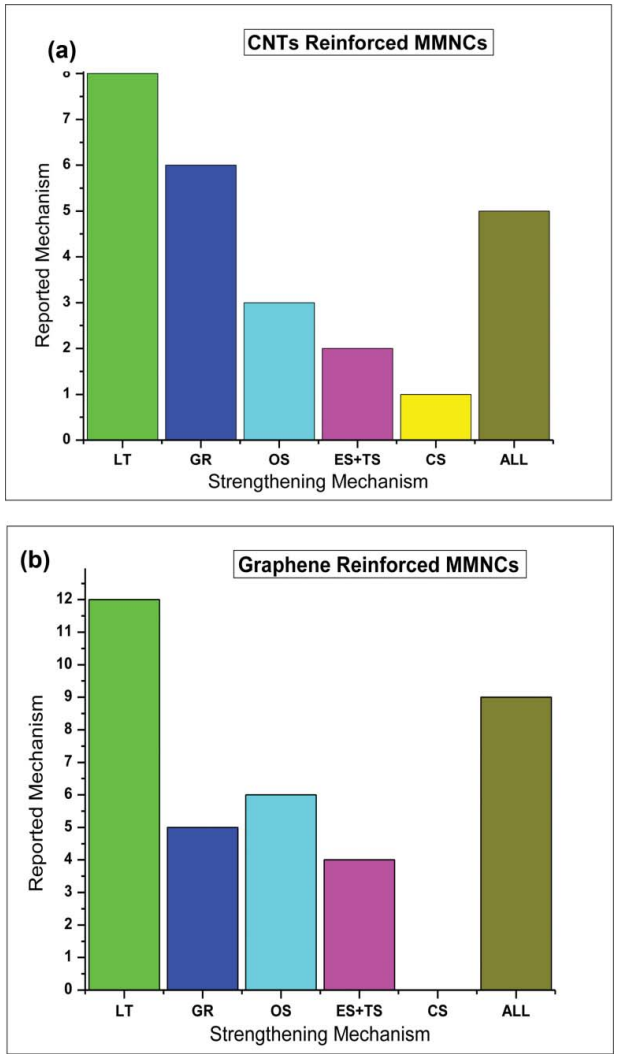

Figure 21. Strengthening mechanism contribution by (a) CNTs-reinforced MMNCs and (b) graphene-reinforced MMNCs.

mechanisms come in decreasing manner. Noticeably, CNTs have shown more grain refining ability than graphene as discussed above. Similarly, almost all researchers reported that C-nanofillers take part in strengthening by combined effects of strengthening, as evident in Figures 21a and 21b. As far as major strengthening contribution difference is concerned, we can easily witness mechanical properties in Tables 1 and 2 that graphene-reinforced MMNCs have shown more enhancement than CNTs-reinforced MMNCs which can be attributed to the graphene characteristics, morphology, and load bearing ability.

6. Tribological aspects of carbon-nanofillers (CNTs and Graphene) metal nanocomposites

Currently, structural and mechanical components used in automobiles and aerospace sectors are seeking innovative materials to provide improved mechanical integrity

with less material loss during operating conditions.[182] An effective way to control the wear and friction (tribology) behavior of the two sliding, rolling, or rotating contact interfaces is the use of suitable lubricants in order to reduce surface damage, saving fuel, and parts durability.[183] Solid lubricants (SL),[184] a good alternative to liquid lubricant is usually employed as ceramic or carbonaceous particulates and fibers reinforcements in metal matrices known as self-lubricating MMCs.[8] Over the last few years, MMCs have shown great promise to maintain high mechanical characteristics and superior tribological behavior under severe loading and impact conditions without distortion, deformation, fracture, and surface damages. Mechanical and tribo aspects of MMCs are attractive for many automotive and aerospace applications over the wide range offer increased component lifetime, increased energy efficiency reliability, durability, and better performance of mechanical component systems.[19] Solid lubricants formed a low shear strength lubricous layer between contact surfaces which is beneficial to the enhancement of the anti-friction, anti-wear properties, and high seizure resistance.[185] Solid lubricants play a dual role in metallic matrices such as: (i) to withstand stress effectively to enhance strength; and (ii) to protect matrix surface against destructive action of ploughing process during sliding leading to high tribological performance simultaneously.[158]

Previously, various hard and thermally stable micro-sized SL, such as SiC, B_4C, Al_2O_3, Ni_3Al, Pb, and graphite, have been tested for mechanical and tribo performances.[186] Although these SL have shown an acceptable increase in hardness, strength, and wear resistance they escorted some drawbacks like low ductility, low machinability, and susceptible crack formation for premature failure which led to an abrupt increase in wear rate and friction coefficient.[5] These issues can be related to the micron size, agglomeration, and weak bonding which led them to easy detachment from the matrix surfaces during sliding conditions and took part in the damaging surface by wear mechanism. In recent years, graphite, an allotrope of carbon, is extensively used as ideal SL in aluminum alloys to replace steel and cast iron parts like bushes, bearings, and pistons due to low cost, high thermal conductive nature, and excellent self-lubricating properties.[187–189] Formation of a graphitic lubricative film during surface interaction reduced shear and frictional stress, decreased the plastic deformation, and obstructed direct metal-to-metal contact, resulting in low damage accumulation, and, hence, enhanced anti-wear and anti-frictional properties to an insignificant extent.[190] Its lubrication effect and lubrication mechanism were extensively studied and well understood. More recently, Omrani et al. documented graphite lubrication effect and mechanism comprehensively.[19]

6.1. Effectiveness of carbon-nanofiller addition as nanosolid lubricants (nanoSL) in metals

In recent years, usage of macro-sized graphite addition in MMCs increased distinctly in many real-time applications because of excellent tribological performance.[191,192] But, on the other hand, MMCs' tribo properties are limited to some extent of the graphite content additionally necessary to maintain lubricative film and then decreased due to the soft nature, chemical inertness, surface lipophobicity, micron size, and agglomeration problem which resulted in a reduction of MMCs' mechanical strength markedly.[193,194] An effective way to cope with this limitation is to use nano-sized graphite instead of micron sized which would bring an increase in mechanical strength and improved tribo properties of nanocomposites rather than micro composites. It has been seen that adding nano-sized solid lubricants showed clean, smooth, fine grooves, and small deformations as compared to deteriorating, worn, and delaminating surfaces of pure metals and micro composites.[195] A detailed study conducted by Rajkumar et al.[196] using nano graphite (35 nm) (5–20 vol %) reinforced copper nanocomposite by PM processing. He compared graphite nano- and microparticles in addition to content effect on mechanical, physical properties, and tribological performance with respect to tribo parameters like normal load and sliding speed variations. Their findings revealed that copper nanocomposite up to 15 vol % exhibited better hardness, density, electrical conductivity, as well as low wear rate and COF than micro-composites' counterpart. Such performance of nanographite fraction (15 vol%) can be attributed to the reduced inter particle distances resulting blockade dislocations effectively and also due to well-developed continuous lubrication film on the surface which lowers deformation rate and wear debris lead to tribo properties enhancement. In contrast, beyond 15 vol % nanographite addition decrease in properties observed which is mainly due to particles agglomerations resulted in porosity, defects which severely effects on mechanical response, and, likewise, unable to sustain lubricious film by non-continuous graphite feeding to surface outcomes with deformation, fracture, and worn surface. Furthermore, previous studies revealed the importance of using different nanosized reinforcements over micro size in terms of mechanical and tribology improvement has already been discussed in detail.

The shift of research drive from macro- to nanosized particle has been accelerated significantly nowadays. In this regard, in order to accommodate graphite addition

deficiencies, such as low mechanical strength, and practice the nanosized advantage, novel carbon-nano solid lubricant (CNTs and graphene) is thought to be promising.[197] Owing to the nanoparticles unique structure, higher specific surface areas, high surface energy, easy shear capability with smooth surface, and extreme mechanical strength inspire researchers to use them as effective nano-solid lubricant (nanoSL) candidate as compared with microsized SL for fabricating metal matrix self-lubricating nanocomposites (MMNCs) for many tribological applications where anti-friction and anti-wear are of paramount importance.[198,199] After successful tribo performance of nanocarbons SL in polymer[200] and ceramics,[201] contact damage resistance would also be enhanced in MMNCs by incorporating nano-carbon SL which form nanometer-thick, hard, strong, and lubricating surface layer on metallic grains.[202] Zhai et al. found notably enhanced wear resistance and reduced COF at a low content of graphene nanoplatelets-reinforced Ni_3Al matrix composites due to the formation of an anti-wear protective layer on the sliding contact surfaces.[181] Lin et al. observed that specified CNTs content is needed to form a continuous lubricating film of carbon provides sufficient surface lubrication. According to him, 15 vol % CNTs content serve the purpose and more than this content cause CNTs agglomeration, surface brittleness, decrease hardness, and subsequently high friction and wear rates.[203] Similarly, CNTs also act as lubricious rollers during sliding contact of worn surfaces between nanocomposites and hard debris, hence reduce frictional shear and wear rates.[204] Xu et al.[205] briefly describe and compare the CNTs or graphene to graphite their respective lubrication effects and mechanisms, as shown in Figure 22.

An ideal condition of finely distributed three solid lubricants are presented in Figures 22a, 22d, and 22g. It can be deduced from the above scenario that these three lubricants are providing lubrication film on the surface during subsequent sliding condition. But the extent to maintain this film varies with respect to each other depending upon their respective lubricative nature. During repeated contact stresses and friction forces, graphite sheets easily squeeze out to the matrix surface, bared, sheared, and spread out to form a lubricative rich film.

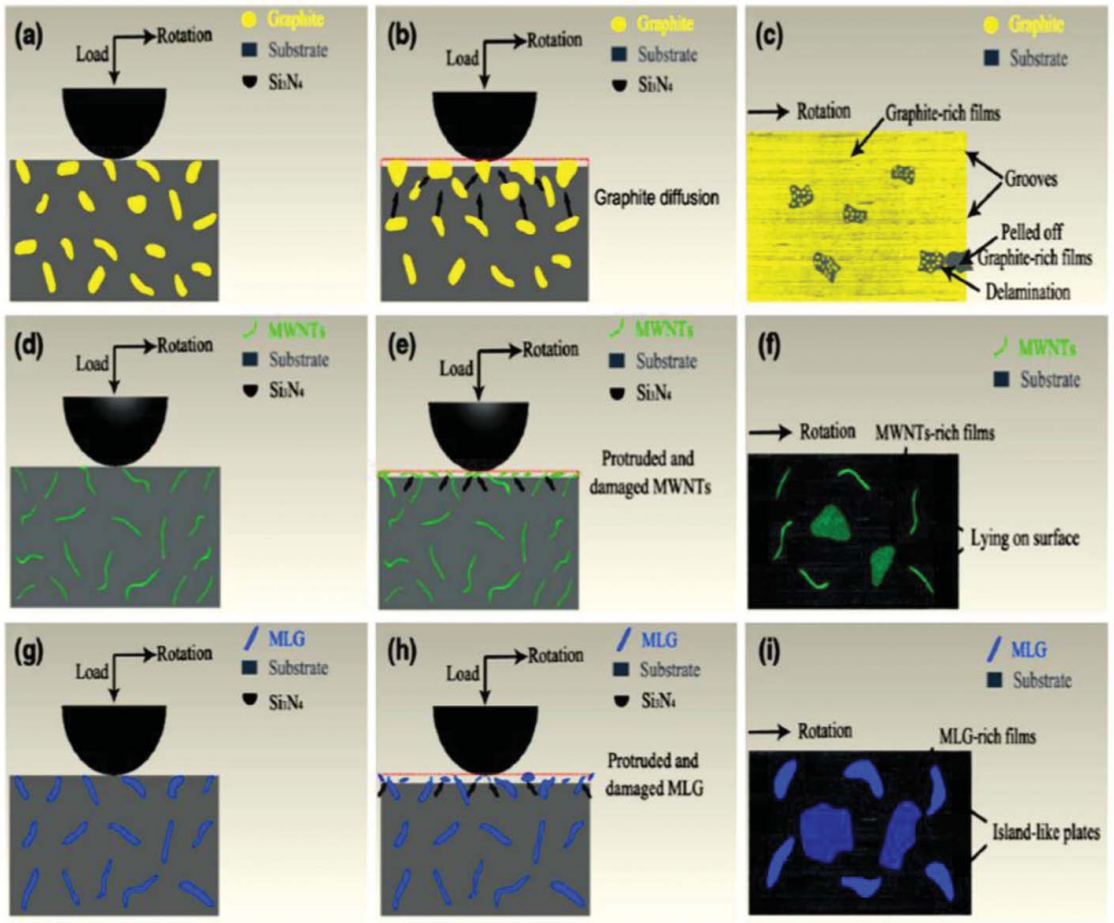

Figure 22. Different lubrication mechanism of the Graphite, MWCNTs, and graphene in NiAl matrix. (© Springer Link. Reprinted with permission from Xue et al.[205] Permission to reuse must be obtained from the rightsholder.)

However, due to soft nature, graphite easily detached and leave behind severe delamination lead to high friction and wear rates (see Figures 22b and 22c). On the other hand, CNTs and graphene presented compact rich fill on the worn surface due to stiff nature, high strength, and inherent lubricative property. After successive sliding cycles, they protruded off from the matrix and spread out on the worn surface getting smoother by filling the debris vacant places, as seen in Figures 22e, 22f, 22h, and 22i. This led to the reduction of friction and wear properties of the composites having smooth surfaces and low damage caused. Therefore, it is acceptable that CNTs and graphene nano-SL provide smoother and well-worn surfaces with continuous adherent film as compared to rough and loose films of graphitic-embedded composites.

6.2. Tribological properties of MMNCs using carbon-nanosolid lubricants (CNTs and Graphene)

Excellent potential as a solid lubricant of C-nanofillers is evident in Figure 22. As recognized, C-nanofillers effectively utilize their excellent mechanical properties like elastic modulus and tensile strength to play a significant role in enhancing mechanical properties (hardness, yield, and tensile/compressive strength) of metallic nanocomposites and directly linked to their tribological performance.[206] A decrease in mechanical properties of the composites may lead to a decrease in wear resistance. C-nanofillers commonly followed strengthening mechanisms (grain size refinement (Hall-Petch effect), Orowan looping, and dislocation generation or residual stresses formation from thermal mismatch) and helps in the formation of unique microstructural, i.e., nanometer grain size which ultimately increased hardness. Hardness is the important mechanical property used by many researchers to correlate the tribo behavior of C-nano-SL-reinforced MMNCs.[207] Usually, it has been realized that hardness is inversely proportional to the wear resistance of metallic nanocomposites reported in many previous works.[208] A typical Archard's equation is normally used to estimate the wear resistance degree due to evolved MMNCs hardness:[209]

$$V = K.\ \frac{L\ .\ P}{H}, \tag{4}$$

where V stands for worn volume, K is the friction coefficient, L equals to sliding distance, P is the applied load, and H is for hardness.

Tribology of metallic nanocomposites is defined by its degree of wear resistance and reduction of COF. C-nanofillers play the dual role such as to enhance mechanical properties (via reinforcement or load bearing) steered an increase in wear resistance and tribological properties (via graphitic structure nano-solid lubricant, nanoSL) provide necessary lubrication during wear, which led to reduce COF simultaneously.[210] This C-nanofillers' behavior attributed to stress concentration resistance at the worn surface, improving the matrix toughness, hinder the dislocation movement and restricted plastic deformation.[197,211–213] All these aspects contribute to increasing mechanical response and ultimate reduction of wear loss in MMNCs. Lubrication character and nature of C nanoSL works the same as of graphite, e.g., act as a spacer, avoid direct contact with surfaces, and continuous supply of film on the sliding interfaces resulting an increase wear resistance and decrease COF.[5] Many researchers reported different wear mechanisms for MMNCs active during sliding, impact, and relative motion of two mating surfaces are adhesive wear, abrasive wear, fatigue wear, micro cutting, delamination, and corrosive/oxidative wear depending upon the matrix compositions, reinforcement nature, size, and shape along with environmental, processing, and operational conditions.[197,205,214–217]

Most recently, Lee et al.[218] presented the classical wear maps of the unreinforced and reinforced metal composites to investigate the effect of solid lubricant addition in a metallic matrix. This map is based on the wear tracks, cross sections, and wear rates of the sintered composites at different speed and loads combinations. It has been divided into two regions, such as mild wear and severe wear along with seizure in the end. As seen in Figure 23, wear phenomena commences with removal of oxide layer and appearance of SL on the worn surface experience mild abrasive wear which is dominant at lower speed and loads. With increasing load, it shifts to the next region of both abrasive and adhesion wear because of continuous formation of an oxide layer and SL withdrawal by acting shear forces results in three body abrasion and crack formation via delamination behavior which is very much prominent in Figure 23 in the case of composites. As recognized, an addition of SL-delayed crack nucleation and propagation effectively so the region of severe wear is shorter in composites as compared to unreinforced metals. This behavior shown by composites has reduced wear rate due to delayed delamination and can be attributed to the improved properties such as hardness and strength due to SL addition.

It has been seen that unreinforced metals normally accompanied adhesive wear due to soft nature, low yield stress, large plastic deformations via increased surface temperature results in severe delamination, and micro

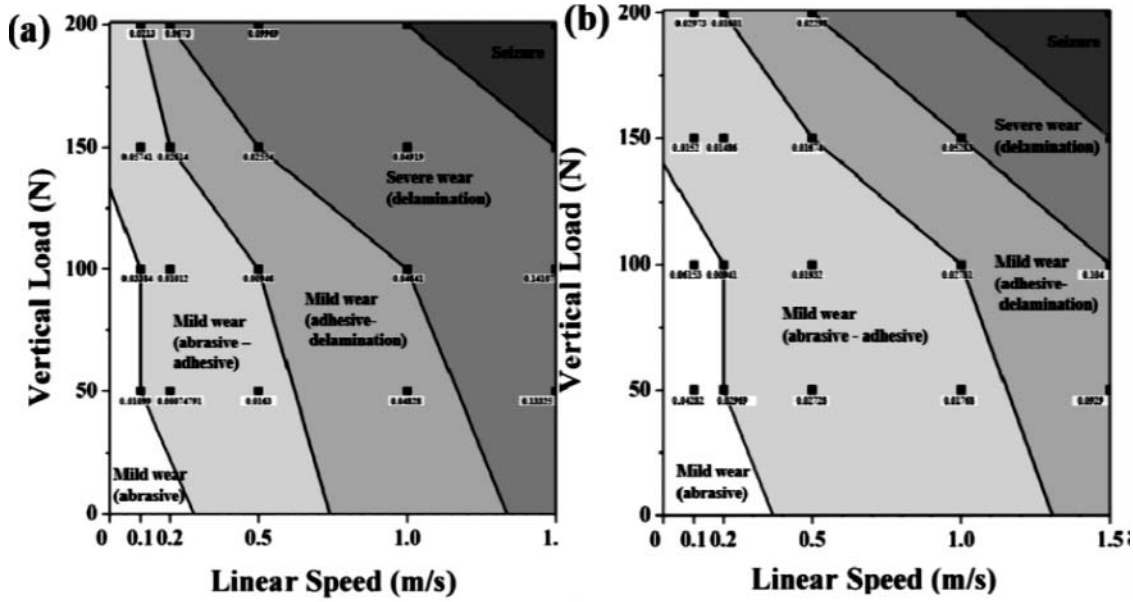

Figure 23. Wear maps of unreinforced and reinforced metallic composites. (© Elsevier Limited. Reprinted with permission from Lee et al.[218] Permission to reuse must be obtained from the rightsholder.)

ploughing that are not observed in C-nanoSL-reinforced MMNCs.[183] Worth noting, adding C-nanoSL is believed to be related to the shift of wear mechanism. This change brought a change from adhesive wear (unreinforced metal) to abrasive wear (nanoscale reinforced metals) and thus is a controlling factor in resultant low friction coefficient and wear rates. The role of nanoSL begins to start when low adhesive, harder metallic surface oxide layer flaked off due to successive wear process in sliding conditions of contact surfaces. Embedded nanoSL drew out at the clean metallic contact surface, thus cover the worn surface with a lubricious film and slowly worn off during sliding contact and hence stop further surface delamination and ultimately increase wear resistance.[4] The percentage improvement in the wear resistance of composites with respect to an alloy could be calculated from the measured wear rate values using the following equation [195]:

$$\mathrm{IWR_{ca}}(\%) = \left(\frac{W_a - W_c}{W_a}\right) \times 100, \tag{5}$$

where $\mathrm{IWR_{ca}}$ is the percentage improvement in the wear resistance of the composite with respect to an alloy, W_a is the wear rate of an alloy, and W_c is the wear rate of the composite. Several controlling influential factors such as: (i) materials or reinforcement's variables such as contents, size, shape, dispersion/distribution in metal matrix, interfacial quality, and type of processing technique[219–221] and (ii) mechanical

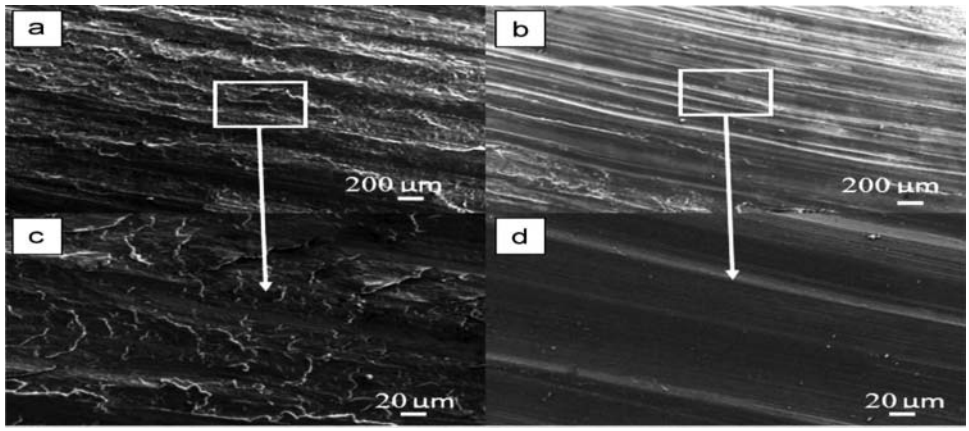

Figure 24. SEM images of the worn surfaces of the (a) unreinforced milled Al (b) 5wt% CNTs reinforced Al composite with respective magnified images (c, d). (© Elsevier Limited. Reprinted with permission from Bastwros et al.[226] Permission to reuse must be obtained from the rightsholder.)

or test variables (normal load, sliding speed, time, and distance) greatly contribute in dictating the tribo performance of the metallic composites have been reported in detail.[222,223] Similarly, the tribological performance of the nanoSL (CNTs and graphene) are also much affected and dependent on these parameters.[224] Full utilization of nanoSL incorporation can be possible by intelligent selection and optimization of these parameters to produce tailor-made MMNCs with much-improved tribo and mechanical behavior for the specific application. Among these factors, nanoscale fraction, dispersion, interfacial bonding, and processing technique are interlinked to each other and extremely important for desire improvement. Bustamante et al. claimed the increased in hardness and wear resistance of the CNTs reinforced aluminum composites prepared by the PM method is due to the high volume fraction and uniform dispersion.[225] The same behavior is also

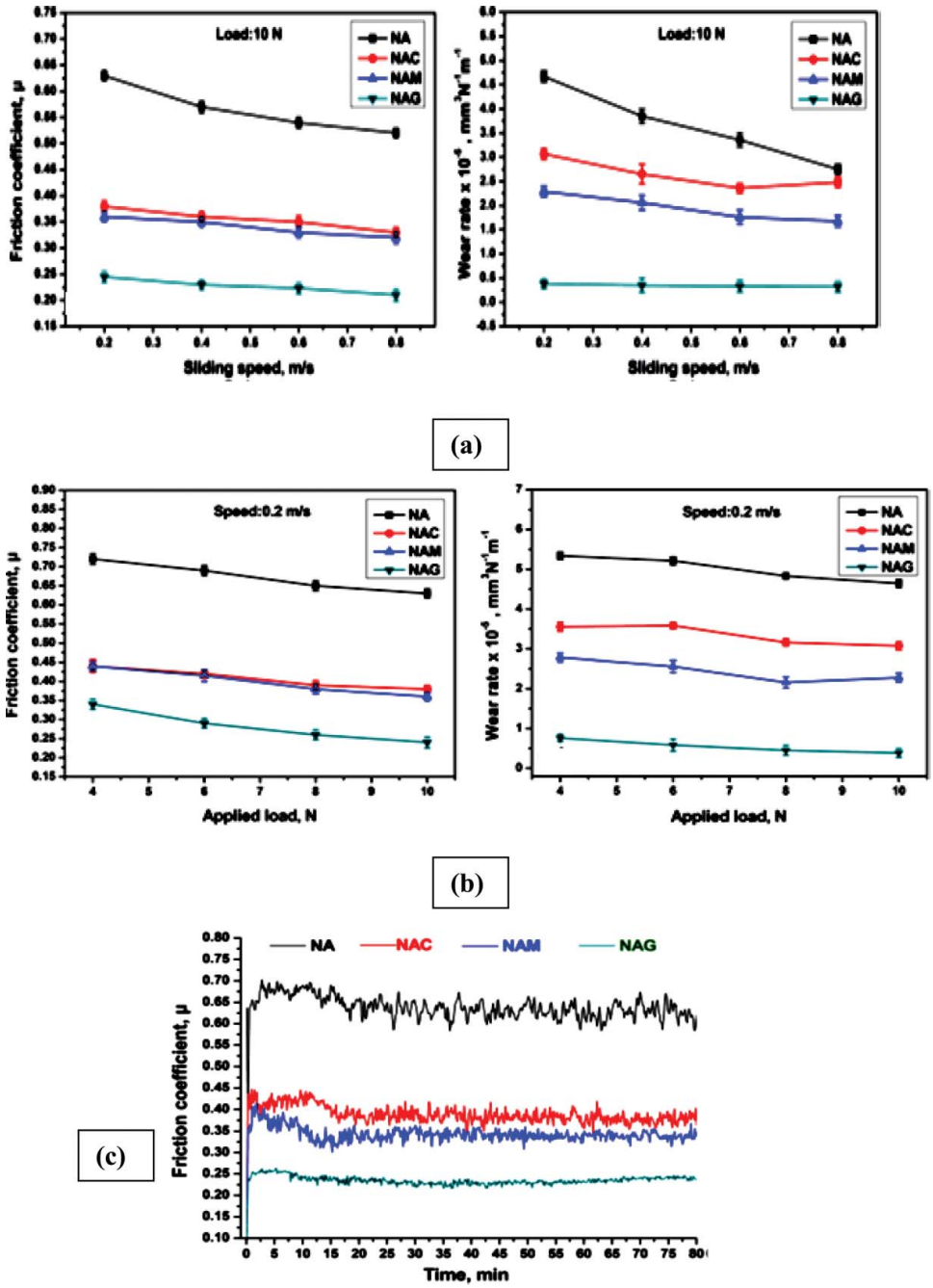

Figure 25. Effect of graphite (NAC), MWCNTs (NAM), and graphene (NAG) in NiAl-based alloy (NA) on friction coefficients and wear rates with respect to applied load (10N), constant sliding speed of 0.2 ms^{-1} and time (min). (© Springer Link. Reprinted with permission from Xue et al.[205] Permission to reuse must be obtained from the rightsholder.)

reported by Bastwros et al.[226] and reported that presence of CNTs in Al matrix formed a smooth surface with fine scratches and less material tearing as compared to unreinforced Al which has been severely delaminated and a rougher surface, as seen in Figure 24.

It has been seen that tribo properties of MMNCs have been inadequately studied for a few years. By far, some initial investigations reported promising results of nanoSL addition in reducing wear rate and friction coefficient of MMNCs. These results confirmed the successful nanoSL lubricating ability to protect metal surface wear and friction conditions. The nanoSL (CNTs and graphene) were mostly studied by adding into the metal matrices like nickel, copper, and aluminum due to their

Table 8. Data of CNTs-reinforced metallic nanocomposites (CNTs-MMNCs) tribological properties.

Researcher	Year	Matrix System	CNTs Fraction	Wear Rate	Mass Loss	COF	Test and Parameters	Mechanical Properties	Dispersion and Consolidation Techniques
Mindivan et al.[236]	2014	Mg–6 Al	0 (wt. %)	18.4 (10^{4}mm^3/N.m)	—	0.47	Reciprocating wear tester, load = 1 N, sliding speed = 0.0128 m/s.	Hardness = 38 (Hv)	Ball milling + Cold pressing + Hot extrusion
			0.5	13.4	—	0.42		41	
			1	14.6	—	0.4		35	
			2	12.09	—	0.39		33	
			4	12.13	—	0.38		30	
Carvalho et al.[268]	2016	AlSi	0 (wt. %)	—	0.0019(g)	—	Pin-on-plate, Load = 10 N, sliding distance = 148 m	Tensile strength = 170 Yield Strength = 152 Tensile strain, 13	Low energy ball milling + Hot Pressing
			2	—	0.00175	—		Tensile strength = 209, Yield Strength = 192, Tensile strain, 07	
Yildirim et al.[186]	2016	7075 Al	0 (wt. %)	3 (10^{-7}mm^3/N.m)	50 (mg)	—	Pin-on-disk, Load = 30N, sliding speed = 1 m/s, Sliding Distance = 2500 m	Hardness = 54 (Hv)	Powder metallurgy technique
			0.5	1	15	—		64.78	
			1	1.5	25	—		83.7	
			2	8	105	—		62.11	
			3	11	210	—		68.6	
			4	12	225	—		65.5	
Kumar et al.[213]	2016	Al	0 (wt %)	115(wear depth, μrm)	—	—	Ball on Plate, Speed = 20 rpm, Load = 15 N	Hardness = 170 (MPa)	Powder metallurgy route
			1	52	—	—		220	
			2	35	—	—		225	
			3	85	—	—		200	
Manikandan et al.[217]	2016	Al	0 (wt %)	42 (mm^3/kgm)	—	0.11	Pin-on-disk, load = 0.5 kg (max), Speed = 0.5 m/s, distance = 300m	Hardness = 19.66 (Hv)	Ball Milling + Conventional Sintering
			0.5	44	—	0.105		25.6	
			1	46	—	0.1		27.45	
			1.5	49	—	0.098		30.6	
			2	51	—	0.095		23.05	
Carvalho et al.[212]	2015	AlSi	0 (wt. %)	—	0.002 (g)	—	Pin-on-plate, Load = 10 N, sliding distance = 148 m	Hardness = 59 (Hv)	Low energy ball milling + Hot Pressing
			2	—	0.00175	—		71	
			4	—	0.00125	—		73	
			6	—	0.00625	—		80	
Jayaraman et al.[269]	2016	AZ31 Mg	0 (wt. %)	—	12 (mg)	—	Pin-on-disk, Load = 15.7 N, 25.5 N, and 35.32 N, sliding speed = 1.04 m/s	Hardness = 62 (Hv)	High Energy Ball Milling + Conventional Sintering + Hot Extrusion
			0.33	—	9.5	—		61	
			0.66	—	10	—		64	
			1	—	2	—		66	
			—	—	0.02	0.27		65	
			—	—	0.042	0.275		60	

immense real-world consumption and applications. Recently, Xu et al. conducted comparative studies to assess the best lubricating ability of graphite, CNTs, and graphene nanoparticles in the NiAl-based alloy. Tribological results acknowledge nanoSL lubrication ability which is far more superior to un-reinforced and graphitic added alloy. Similarly, they also reported that nanoSL produced less delaminated surfaces than graphitic-reinforced metal showing their potential to act as ideal anti-friction and anti-wear lubricants for metal matrices.[205]

It can be clearly seen in Figures 25a and 25b that friction coefficients and wear rates of NAC, NAM, and NAG continuously decreasing with the increase in sliding speed under constant load and applied load under constant sliding speed when compared to NA confirmed the excellent lubricating effect of solid lubricants. In addition, nanoSL, such as MWNTs and graphene-reinforced NA, exhibited better lubrication effect exposed on the worn surfaces forming less delaminating or damage surfaces than graphite. Overall, we can say that NAM contains graphene has shown the best lubrication effect to reduce friction coefficient as a function of time (Figure 25c) by forming effective continuous solid lubricant-rich film exposed and smeared on the worn surface during the sliding process decrease the direct contacting as compared to NAM and NAC.

Table 9. Data of graphene-reinforced metallic nanocomposites (Graphene-MMNCs) tribological properties.

Researcher	Year	Matrix System	GNPs Fraction	Wear Rate	Mass Loss	COF	Test and Parameters	Mechanical Properties	Dispersion and Consolidation Techniques
Xue et al.[270]	2013	Ni_3_Al	0 (wt. %)	231.4 × 10^{-6}(mm^3/N.m)	—	0.71	ball-on-disk, Load = 13 N(max), sliding speed of 0.20 m/s	Hardness = 4.20 (GPa)	Ball Milling + SPS technique
			1	8.9	—	0.33		8.05	
Ghazaly et al.[271]	2013	2124Al	0	0.175 × 10^{-4} (mm^3/N.m)	2 (mg)		Pin-on-disk, Load = 100 N, sliding speed = 300 rpm, sliding distance = 1.0 km	Hardness = 175 (Hv)	Turbula Mixing + High Energy Ball Milling+ Conventional Sintering
			0.5	0.313	7			230	
			3	0.088	3			270	
			5	0.35	12			205	
Zhai et al.[181]	2015	Ni_3-Al	0 (wt. %)	4.2×10^{-5}(mm^3/N.m)	—	0.5	Pin-on-disk, load = 11.65 N, Speed = 1.0 m/s (max)	Hardness = 4.3 (GPa)	Ball Milling + SPS Technique
			0.5	—	—	—		4.9	
			1	1	—	0.2		6.5	
			1.5	—	—	—		6.3	
			2	—	—	—		5.4	
Khorshid et al.[272]	2015	Al	0 (wt. %)	—	0.015 (g)	0.25	Pin-on-disk, Load = 15 N (max), sliding speed = 150rpm (max), sliding distance = 1.13km	Hardness = 111 (Hv)	Ball Milling + Hot compaction
			0.1	—	0.014	0.25		98	
			1	—	0.02	0.24		97	
Algul et al.[273]	2015	Ni	100 (mg/L)	10.17×10^{-4} (mm^3/N.m)	—	0.5		Hardness = 427 ± 8	Pulse electrode position technique
			250	9.25	—	0.2		451 ± 9	
			500	8.56	—	0.15		492 ± 9	
Alamet al.[216]	2016	Al	0 (wt. %)	85 (wear depth, μrm)	—		Ball on Plate, Load = 15 N	Hardness = 169.7 MPa	Ultrasonication + Powder Metallurgy Technique
			1	61	—	—		452	
			2	43	—	—		375	
			3	37	—	—		370	
			5	120	—	—		200	
Kumar et al.[274]	2016	6061 Al	0 (wt. %)	—	0.04 (g)	0.48	Pin-on-Disc, Load = 9 kgf (Max), speed = 500 rpm	Hardness = 60 (Hv)	Sonication + Powder Metallurgy Technique
			0.2	—	0.028	0.29		62	
			0.4	—	0.02	0.27		65	
			0.6	—	0.042	0.275		60	

A supportive literature is available that displays the decrease in wear rate with an increase in volume fraction of reinforcements which can be attributed to the availability of a large amount of lubrication film to reduce contact surface interaction,[190] whereas, this behavior exhibited by composites up to a certain level of a fraction to achieve improved wear performance.[227]. As mentioned earlier, dispersing CNTs and graphene at large volume fractions along with poor wetting with metal matrices is a challenging task due to their re-agglomeration ability so as to decrease their surface energy. This leads to weakly bonded agglomerated and clustered nanoparticles remnants in final composites act as voids or porosities. These agglomerated nanoparticles could be easily torn off during sliding conditions resulting in a severe decrease in the wear resistance of the composite. There is another thought that these agglomerations could have positive effects on tribological properties as in the case of CNTs. Due to shear forces during sliding, the condition might disaggregate those agglomerates of CNTs and results in individual CNTs on the worn sliding contact surface that could possibly increase friction resistance. Therefore, improved dispersion, distribution, agglomeration prevention, and quality interface with metal matrices is a prerequisite for high tribo behavior. A lot of effort has been devoted to addressing these factors convincingly by adopting various techniques in order to study their effects on mechanical properties of MMNCs reported in Section 5 but tribological properties evaluation of these composites are still needed. In this regard, we have gathered data (see Tables 8 and 9) from researcher's efforts in the last few years to assess the extent of the tribological effect of CNTs and graphene addition in different metal matrices. These tables contain information of the C-nanofillers dispersion techniques along with consolidation techniques effect, extent of C-nanofillers content addition effect on tribological as well as mechanical properties, and, importantly, info related to tribo testing parameters used by these investigators so far. These tables evidently show that C-nanofillers were widely assessed for tribo performance and has produced significant results contributed by their intrinsic superior properties and lubricative nature. Likewise, it can be clearly seen that dispersion has a pronounced effect on tribo performances of these C-nanofillers which have been catered by researchers mostly by using powder metallurgy route like ball milling technique with a combination of secondary consolidation methods. These tables also demonstrate that hardness is the main mechanical property presented by mostly researchers linked with tribological properties. Therefore, it can be established that C-nanofillers have a great potential for high tribological performance. Proper utilization of C-nanofillers potential by addressing present challenges by processing optimization steps and new techniques can surely be helpful in producing quality MMNCs with much higher mechanical and tribological properties for real-time engineering applications.

7. Conclusion

In conclusion, this critical article puts forward the claim that C-nanofillers (CNTs and graphene) have excellent potential of metal reinforcement and enhanced tribo capabilities due to exceptional strength, inflexibility, and graphitic lubricant nature that produce remarkable improvements in mechanical and tribological properties in MMNCs. The interest in using C-nanofillers to reinforce metals increases for various reasons as made evident by the literature. However, practical applications still remain in the early stages. Correlative issues such as (i) the dispersion and wetting of C-nanofillers with metals and (ii) poor interface development must still be addressed so this class of materials is fully utilized for commercial applications. These issues are of ultimate concern as they delineate definitive nanocomposite properties and remain as challenges to quality nanocomposite fabrication. With new advancements in processing methods and approaches, these matters of concern will eventually be controlled. This article highlighted these issues with an emphasis on reliable processing for the uniform dispersion of C-nanofillers and metal-interface interactions.

- This study clearly unveils the importance and key role of C-nanofillers dispersion dependence on overall final MMNCs properties. Undoubtedly, enhanced mechanical and tribological properties can only be achieved after controlling C-nanofillers dispersion in metallic matrices.
- Until now, powder metallurgy methods remain the most promising technique due to ease of use with the ability to adjust parameters to more appropriately address challenges. P/M has also proven to be the most effective approach to the pre-dispersion of C-nanofillers in solvents via controlled sonication. Even so, many crucial concerns have not been fully explored and a significant need to carefully optimize all processing steps remains. Similarly, consolidation techniques attached to P/M methodology also demand fine-tuning to achieve better mechanical properties.
- While many methods have been devised to combat the difficulty of C-nanofiller dispersion in metals, numerous process variables have not been studied or optimized. Moreover, C-nanofiller agglomeration (clustering) and structural changes subsequent to

dispersion prove unfavorable for the attainment of desired product properties. Overall, organized investigations are needed to balance the surface treatment of C-nanofillers with processing conditions in the fabrication of metal nanocomposites to avoid unwanted outcomes.

- Mechanical properties usually correlate with effective stress transfer from the matrix to the C-nanofiller and can only be accomplished with strong interfacial contact. Efforts are needed to create a better interface for a more effective load transfer to optimize final product properties. In addition, fundamental studies on stress transfer mechanisms and bond strength measurement between C-nanofillers and the metal matrix are needed.
- Very few studies have been conducted on modeling and the prediction of mechanical properties by various strengthening mechanisms. Although different models are used as important tools to predict nanocomposite strength, the relation between experimental results and predicted values needs amplification to build confidence in results. Such efforts can open abundant opportunities for the use of metallic nanocomposites in a wide range of applications.
- Tribological potential of C-nanofillers is still not much exploited. At present, results assure the excellent performance of C-nanofillers as solid lubricants compared to existing counterparts. Therefore, we believe that monitoring existing challenges and benefitting the mechanical and tribological characteristics of C-nanofillers could produce future MMNCs with more versatile and demanding properties for various engineering applications.

References

1. R. Casati, and M. Vedani, Metal matrix composites reinforced by nano-particles—a review. *Metals* **4**(1), 65–83 (2014).
2. N. Chawla, and Y.-L. Shen, Mechanical behavior of particle reinforced metal matrix composites. *Adv. Eng. Mater.* **3**(6), 357–370 (2001).
3. N. Chawla, and K. Chawla, Metal-matrix composites in ground transportation. *JOM* **58**(11), 67–70 (2006).
4. A.D. Moghadam, et al. Mechanical and tribological properties of self-lubricating metal matrix nanocomposites reinforced by carbon nanotubes (CNTs) and graphene–A review. *Compos. Part B Eng.* **77**, 402–420 (2015).
5. R. Tyagi, *Processing Techniques and Tribological Behavior of Composite Materials*, IGI Global (2015).
6. Y. Dong, R. Umer, and A. Lau, *Fillers and Reinforcements for Advanced Nanocomposites*, (2015); p. 587.
7. S.C. Tjong, *Carbon Nanotube Reinforced Composites: Metal and Ceramic Matrices*, John Wiley & Sons (2009).
8. A.D. Moghadam, et al. Functional metal matrix composites: self-lubricating, self-healing, and nanocomposites-an outlook. *JOM* **66**(6), 872–881 (2014).
9. S.C. Tjong, Novel nanoparticle−reinforced metal matrix composites with enhanced mechanical properties. *Adv. Eng. Mater.* **9**(8), 639–652 (2007).
10. Z. Ma, et al. Nanometric Si 3 N 4 particulate-reinforced aluminum composite. *Mater. Sci. Eng. A* **219**(1), 229–231 (1996).
11. S. Sajjadi, H. Ezatpour, and H. Beygi, Microstructure and mechanical properties of Al–Al 2 O 3 micro and nano composites fabricated by stir casting. *Mater. Sci. Eng. A.* **528**(29), 8765–8771 (2011).
12. Y.-C. Kang, and S.L.-I. Chan, Tensile properties of nanometric Al 2 O 3 particulate-reinforced aluminum matrix composites. *Mater. Chem. Phys.* **85**(2), 438–443 (204).
13. M. Mashhadi, H. Khaksari, and S. Safi, Pressureless sintering behavior and mechanical properties of ZrB 2–SiC composites: effect of SiC content and particle size. *J. Mater. Res. Technol.* **4**(4), 416–422 (2015).
14. J.S. Moya, S. Lopez-Esteban, and C. Pecharroman, The challenge of ceramic/metal microcomposites and nanocomposites. *Progr. Mater. Sci.* **52**(7), 1017–1090 (2007).
15. D. Jun, et al. Dry sliding friction and wear properties of Al 2 O 3 and carbon short fibres reinforced Al–12Si alloy hybrid composites, Wear. **257**(9), 930–940 (2004).
16. N. Hosseini, et al. Tribological properties of Al6061–Al 2 O 3 nanocomposite prepared by milling and hot pressing. *Mater. Des.* **31**(10), 4777–4785 (2010).
17. N. Hosseini, et al. A comparative study on the wear properties of coarse-grained Al6061 alloy and nanostructured Al6061–Al 2 O 3 composites. *Tribol. Int.* **54**, 58–67 (2012).
18. A. Agarwal, S.R. Bakshi, and D. Lahiri, *Carbon Nanotubes: Reinforced Metal Matrix Composites*, CRC Press (2010).
19. E. Omrani, et al. Influences of graphite reinforcement on the tribological properties of self-lubricating aluminum matrix composites for green tribology, sustainability, and energy efficiency—a review. *Int. J. Adv. Manuf. Technol.* **83**(1–4), 325–346 (2016).
20. S. Iijima, and T. Ichihashi, "Single-shell carbon nanotubes of 1-nm diameter," *Nature*, vol. 364, p. 737, 1993.
21. K. Novoselov, and A. Geim, The rise of graphene. *Nat. Mater.* **6**, 183–191 (2007).
22. G. Mittal, et al. A review on carbon nanotubes and graphene as fillers in reinforced polymer nanocomposites. *J. Industr. Eng. Chem.* **21**, 11–25 (2015).
23. W. Yihong, S. Zexiang, and Y. Ting, *Two-Dimensional Carbon: Fundamental Properties, Synthesis, Characterization, and Applications*, CRC Press (2014).
24. S.G. Advani, *Processing and Properties of Nanocomposites*, World Scientific (2007).
25. M. M. J. Treacy, T. W. Ebbesen, and J. M. Gibson, "Exceptionally high Young's modulus observed for individual carbon nanotubes," *Nature*, vol. 381, pp. 678–680, 1996.
26. C. Lee, et al. Measurement of the elastic properties and intrinsic strength of monolayer graphene. *Science* **321** (5887), 385–388 (2008).

27. J. H. Warner, F. Schaffel, M. Rummeli, and A. Bachmatiuk, *Graphene: Fundamentals and emergent applications*: Newnes, 2012.
28. R.S. Ruoff, and D.C. Lorents, Mechanical and thermal properties of carbon nanotubes. *Carbon* **33**(7), 925–930 (1995).
29. F. D'Souza, and K.M. Kadish, *Handbook Of Carbon Nano Materlals*. 2011.
30. S.H. Chae, and Y.H. Lee, Carbon nanotubes and graphene towards soft electronics. *Nano Converg.* **1**(1), 1(2014).
31. T. Dürkop, et al. Extraordinary mobility in semiconducting carbon nanotubes. *Nano Lett.* **4**(1), 35–39 (2004).
32. A.S. Mayorov, et al. Micrometer-scale ballistic transport in encapsulated graphene at room temperature. *Nano Lett.* **11**(6), 2396–2399 (2011).
33. K.I. Bolotin, et al. Ultrahigh electron mobility in suspended graphene. *Solid State Commun.* **146**(9), 351–355 (2008).
34. A. Javey, et al. Ten-to 50–nm-long quasi-ballistic carbon nanotube devices obtained without complex lithography. *Proc. of the National Academy of Sciences of the United States of America* **101**(37), 13408–13410 (2004).
35. J. Yu, et al. Graphene-on-diamond devices with increased current-carrying capacity: carbon sp2–on-sp3 technology. *Nano Lett.* **12**(3), 1603–1608 (2012).
36. E. Pop, et al. Thermal conductance of an individual single-wall carbon nanotube above room temperature. *Nano Lett.* **6**(1), 96–100 (2006).
37. A.A. Balandin, et al. Superior thermal conductivity of single-layer graphene. *Nano Lett.* **8**(3), 902–907 (2008).
38. B. V. Ramnath, C. Parswajinan, C. Elanchezhian, S. V. Pragadeesh, P. R. Ramkishore, and V. Sabarish, "A Review on CNT Reinforced Aluminium and Magnesium Matrix Composites," *Applied Mechanics and Materials*, vol. 591, pp. 120–123, 2014.
39. H. Kim, A.A. Abdala, and C.W. Macosko, Graphene/polymer nanocomposites. *Macromolecules* **43**(16), 6515–6530 (2010).
40. J.N. Coleman, U. Khan, and Y.K. Gun'ko, Mechanical reinforcement of polymers using carbon nanotubes. *Adv. Mater.* **18**(6), 689–706 (2006).
41. J.H. Lee, et al. Cryomilling application of graphene to improve material properties of graphene/chitosan nanocomposites. *Compos. Part B Eng.* **45**(1), 682–687 (2013).
42. A. Shukla, et al. Processing of copper–carbon nanotube composites by vacuum hot pressing technique. *Mater. Sci. Eng. A* **560**, 365–371 (2013).
43. P. D. Pastuszak and A. Muc, "Application of composite materials in modern constructions," *Key Engineering Materials*, vol. 542, pp. 119–129, 2013.
44. R. Moriche, S. Prolongo, M. Sánchez, A. Jiménez-Suárez, M. Sayagués, and A. Ureña, "Morphological changes on graphene nanoplatelets induced during dispersion into an epoxy resin by different methods," *Composites Part B: Engineering*, vol. 72, pp. 199–205, 2015.
45. W. Qin, et al. Mechanical and electrical properties of carbon fiber composites with incorporation of graphene nanoplatelets at the fiber–matrix interphase. *Compos. Part B Eng.* 2015. **69**, 335–341.
46. O.-K. Park, et al. Synthesis and properties of iodo functionalized graphene oxide/polyimide nanocomposites. *Compos. Part B Eng.*, 365–371 (2014).
47. F. Qiu, et al. Functionalized graphene sheets filled isotactic polypropylene nanocomposites. *Compos. Part B Eng.* **71**, 175–183 (2015).
48. T. Hertel, R.E. Walkup, and P. Avouris, Deformation of carbon nanotubes by surface van der Waals forces. *Phys. Rev. B.* **58**(20), 13870 (1998).
49. L. Jiang, et al. A cohesive law for carbon nanotube/polymer interfaces based on the van der Waals force. *J. Mech. Phys. Solids* **54**(11), 2436–2452 (2006).
50. S. Nuriel, et al. Direct measurement of multiwall nanotube surface tension. *Chem. Phys. Lett.* **404**(4), 263–266 (2005).
51. K.P. So, et al. Improving the wettability of aluminum on carbon nanotubes. *Acta Materialia* **59**(9), 3313–3320 (2011).
52. A.A. Sahraei, et al. Enhanced hardness and electrical properties of copper nanocomposites reinforced by functionalized MWCNTs. *J. Compos. Mater.* **48**(28), 3485–3497 (2014).
53. K. Chu, et al. Improvement of interface and mechanical properties in carbon nanotube reinforced Cu–Cr matrix composites. *Mater. Des.* **45**, 407–411 (2013).
54. M. Jafari, et al. Mechanical properties of nanostructured Al2024–MWCNT composite prepared by optimized mechanical milling and hot pressing methods. *Adv. Powder Technol.* **23**(2), 205–210 (2012).
55. H. Li, et al. Mechanical properties and interfacial analysis of aluminum matrix composites reinforced by carbon nanotubes with diverse structures. *Sci. Mater.Eng. A* **577**, 120–124 (2013).
56. H. Choi, J. Shin, and D. Bae, The effect of milling conditions on microstructures and mechanical properties of Al/MWCNT composites. *Compos. Part A Appl. Sci. Manufact.* **43**(7), 1061–1072 (2012).
57. R. Patakfalvi, et al. Anchoring of silver nanoparticles on graphite and isomorphous lattices. *J. Phys. Chem. C* **111**(14), 5331–5336 (2007).
58. M. Shirai, M., K. Igeta, and M. Arai, Formation of platinum nanosheets between graphite layers. *Chem. Commun.* (7), 623–624 (2000).
59. S.K. Shaikhutdinov, and F. Cadete Santos Aires, Evolution of the rhodium colloid supported on graphite studied by atomic force microscopy in the tapping mode. *Langmuir* **14**(13), 3501–3505 (1998).
60. P.-C. Ma, et al. Dispersion and functionalization of carbon nanotubes for polymer-based nanocomposites: a review. *Compos. Part A Appl. Sci. Manufact.* **41**(10), 1345–1367 (2010).
61. K.S. Munir, et al. Effect of dispersion method on the deterioration, interfacial interactions and re-agglomeration of carbon nanotubes in titanium metal matrix composites. *Mater. Des.*, **88**, 138–148 (2015).
62. S. Cho, et al. Multiwalled carbon nanotubes as a contributing reinforcement phase for the improvement of thermal conductivity in copper matrix composites. *Scripta Materialia* **63**(4), 375–378 (2010).
63. J. Torralba, C. Da Costa, and F. Velasco, P/M aluminum matrix composites: an overview. *J. Mater. Process. Technol.* **133**(1), 203–206 (2003).
64. J. Fogagnolo, et al. Effect of mechanical alloying on the morphology, microstructure and properties of aluminium matrix composite powders. *Mater. Sci. Eng. A* **342**(1), 131–143 (2003).

65. B. Chen, et al. Load transfer strengthening in carbon nanotubes reinforced metal matrix composites via in-situ tensile tests. *Compos. Sci. Technol.* **113**, 1–8 (2015).
66. K.S. Munir, P. Kingshott, and C. Wen, Carbon nanotube reinforced titanium metal matrix composites prepared by powder metallurgy—a review. *Crit. Rev. Solid State Mater. Sci.* **40**(1), 38–55 (2015).
67. S. Saravanan, K. Sivaprasad, and S. Kumaresh Babu, Dispersion and thermal analysis of Carbon nanotube reinforced AA 4032 Alloy produced by high energy ball milling. *Exper. Techniq.* **37**(4), 14–18 (2013).
68. C. He, et al. An approach to obtaining homogeneously dispersed carbon nanotubes in Al Powders for preparing reinforced Al−matrix composites. *Adv. Mater.* **19**(8), 1128–1132 (2007).
69. R. Pérez-Bustamante, et al. Characterization of Al 2024-CNTs composites produced by mechanical alloying. *Powder Technol.* **212**(3), 390–396 (2011).
70. Kuzumaki, T., et al. Processing of carbon nanotube reinforced aluminum composite. *J. Mater. Res.* **13**(09), 2445–2449 (1998).
71. A.M. Esawi, et al. Fabrication and properties of dispersed carbon nanotube–aluminum composites. *Mater. Sci. Eng. A* **508**(1), 167–173 (2009).
72. F. Ostovan, et al. Effects of CNTs content and milling time on mechanical behavior of MWCNT-reinforced aluminum nanocomposites. *Mater. Chem. Phys.* **166**, 160–166 (2015).
73. O. Carvalho, et al. Optimization of AlSi–CNTs functionally graded material composites for engine piston rings. *Mater. Des.* **80**, 163–173 (2015).
74. J. Texter, Graphene dispersions. *Curr. Opin. Coll. Interf. Sci.* **19**(2), 163–174 (2014).
75. K.S. Munir, and C. Wen, Deterioration of the strong sp2 carbon network in carbon nanotubes during the mechanical dispersion processing-a review. *Crit. Rev. Solid State Mater. Sci.* 1–20 (2016).
76. P. Vichchulada, et al. Sonication power for length control of single-walled carbon nanotubes in aqueous suspensions used for 2-dimensional network formation. *J. Phys. Chem. C* **114**(29), 12490–12495 (2010).
77. H. Yoon, et al. Controlling exfoliation in order to minimize damage during dispersion of long SWCNTs for advanced composites. *Sci. Rep.* **4** (2014).
78. S. Simões, et al. Influence of dispersion/mixture time on mechanical properties of Al–CNTs nanocomposites. *Compos. Struct.* **126**, 114–122 (2015).
79. I. Ahmad, B. Yazdani, and Y. Zhu, Recent advances on carbon nanotubes and graphene reinforced ceramics nanocomposites. *Nanomaterials* **5**(1), 90–114 (2015).
80. Z. Sun, et al. Quantitative evaluation of surfactant-stabilized single-walled carbon nanotubes: dispersion quality and its correlation with zeta potential. *J. Phys. Chem. C* **112**(29), 10692–10699 (2008).
81. B. Chen, S. Li, H. Imai, L. Jia, J. Umeda, M. Takahashi, et al., "An Approach for Homogeneous Carbon Nanotube Dispersion in Al Matrix Composites," *Materials & Design*, vol. 72, pp. 1 -8, 201
82. S.I. Cha, et al. Strengthening and toughening of carbon nanotube reinforced alumina nanocomposite fabricated by molecular level mixing process. *Scripta Materialia* **53**(7), 793–797 (2005).
83. B. J. Rael, Y. Fu, T. A. Khraishi, and Y.-B. Jiang, "Optimizing powder metallurgy methods: Effects of carbon nanotube dispersal mechanisms on mechanical properties of aluminium/carbon nanotube composites," *Journal of Composite Materials*, vol. 50, pp. 2375–2388, 2016.
84. L. Jiang, et al. The use of flake powder metallurgy to produce carbon nanotube (CNT)/aluminum composites with a homogenous CNT distribution. *Carbon* **50**(5), 1993–1998 (2012).
85. S. Shin, et al. Strengthening behavior of few-layered graphene/aluminum composites. *Carbon* **82**, 143–151 (2015).
86. H. Choi, et al. Preparation by mechanical alloying of Al powders with single-, double-, and multi-walled carbon nanotubes for carbon/metal nanocomposites. *Compos. Sci. Technol.* **74**, 91–98 (2013).
87. F. Rikhtegar, S. Shabestari, and H. Saghafian, The homogenizing of carbon nanotube dispersion in aluminium matrix nanocomposite using flake powder metallurgy and ball milling methods. *Powder Technol.* **280**, 26–34 (2015).
88. N. Al-Aqeeli, et al. Structure of mechanically milled CNT-reinforced Al-alloy nanocomposites. *Mater. Manufact. Process.* **28**(9), 984–990 (2013).
89. Y.J. Noh, et al. Ultra-high dispersion of graphene in polymer composite via solvent free fabrication and functionalization. *Sci. Rep.* **5** (2015).
90. K. Hu, et al. Graphene-polymer nanocomposites for structural and functional applications. *Progr. Polym. Sci.* **39**(11), 1934–1972 (2014).
91. F. Latief, et al. Fabrication of exfoliated graphite nanoplatelets-reinforced aluminum composites and evaluating their mechanical properties and corrosion behavior. *J. Analyt. Appl. Pyrolysis* **92**(2), 485–492 (2011).
92. M. Bastwros, et al. Effect of ball milling on graphene reinforced Al6061 composite fabricated by semi-solid sintering. *Compos. Part B Eng.* **60**, 111–118 (2014).
93. Y. Cui, et al. Effect of ball milling on the defeat of few-layer graphene and properties of copper matrix composites. *Acta Metallurgica Sinica (Engl. Lett.)* **27**(5), 937–943 (2014).
94. A.F. Boostani, et al. Enhanced tensile properties of aluminium matrix composites reinforced with graphene encapsulated SiC nanoparticles. *Compos. Part A: Appl. Sci. Manufact.* **68**, 155–163 (2015).
95. A. Das, and S.P. Harimkar, Effect of graphene nanoplate and silicon carbide nanoparticle reinforcement on mechanical and tribological properties of spark plasma sintered magnesium matrix composites. *J. Mater. Sci. Technol.* **30**(11), 1059–1070 (2014).
96. M. Rashad, et al. Effect of Graphene Nanoplatelets addition on mechanical properties of pure aluminum using a semi-powder method. *Progr. Nat. Sci. Mater. Int.* **24**(2), 101–108 (014).
97. M. Rashad, et al. Development of magnesium-graphene nanoplatelets composite. *J. Compos. Mater.* **49**(3), 285–293 (2015).
98. M. Rashad, M., et al., Effect of graphene nanoplatelets (GNPs) addition on strength and ductility of magnesium-titanium alloys. *Journal of Magnesium and alloys*, 2013. **1**(3), 242–248.

99. M. Rashad, et al. Use of high energy ball milling to study the role of graphene nanoplatelets and carbon nanotubes reinforced magnesium alloy. *J. All. Compd.* **646**, 223–232 (2015).
100. Q. Zhang, et al. The road for nanomaterials industry: a review of carbon nanotube production, post−treatment, and bulk applications for composites and energy storage. *Small* **9**(8), 1237–1265 (2013).
101. M.A. Rafiee, et al. Fracture and fatigue in graphene nanocomposites. *Small* **6**(2), 179–183 (2010).
102. Z. Xu, and C. Gao, In situ polymerization approach to graphene-reinforced nylon-6 composites. *Macromolecules* **43**(16), 6716–6723 (2010).
103. H. Li, et al. Alumina powder assisted carbon nanotubes reinforced Mg matrix composites. *Mater. Des.* **60**, 637–642 (2014).
104. S. Yan, et al. Investigating aluminum alloy reinforced by graphene nanoflakes. *Mater. Sci. Eng. A* **612**, 440–444 (2014).
105. M. Rashad, M., et al., Improved strength and ductility of magnesium with addition of aluminum and graphene nanoplatelets (Al+ GNPs) using semi powder metallurgy method. *J. Industr. Eng. Chem.* **23**, 243–250 (2015).
106. M. Li, et al. Highly enhanced mechanical properties in Cu matrix composites reinforced with graphene decorated metallic nanoparticles. *J. Mater. Sci.* **49**(10), 3725–3731 (2014).
107. A. Desai, and M. Haque, Mechanics of the interface for carbon nanotube–polymer composites. *Thin-walled Struct.* **43**(11), 1787–1803 (2005).
108. P. Karapappas, et al. Enhanced fracture properties of carbon reinforced composites by the addition of multi-wall carbon nanotubes. *J. Compos. Mater.* (2009).
109. D.C. Davis, et al. Improvements in mechanical properties of a carbon fiber epoxy composite using nanotube science and technology. *Compos. Struct.* **92**(11), 2653–2662 (2010).
110. K. Chu, and C. Jia, Enhanced strength in bulk graphene–copper composites. *Physica Status Solidi* **211**(1), 184–190 (2014).
111. C. He, et al. Mechanical properties and microstructures of carbon nanotube-reinforced Al matrix composite fabricated by in situ chemical vapor deposition. *J. Alloys Cmpd.* **487**(1), 258–262 (2009).
112. A. Maqbool, et al. Mechanical characterization of copper coated carbon nanotubes reinforced aluminum matrix composites. *Mater. Character.* **86**, 39–48 (2013).
113. M.H. Nai, J. Wei, and M. Gupta, Interface tailoring to enhance mechanical properties of carbon nanotube reinforced magnesium composites. *Mater. Des.* **60**, 490–495 (2014).
114. C. Zhao, and J. Wang, Fabrication and tensile properties of graphene/copper composites prepared by electroless plating for structrual applications. *Physica Status Solidi* **211**(12), 2878–2885 (2014).
115. D. Lin, C.R. Liu, and G.J. Cheng, Single-layer graphene oxide reinforced metal matrix composites by laser sintering: Microstructure and mechanical property enhancement. *Acta Materialia* **80**, 183–193 (2014).
116. Y. Peng, et al. Ultrasound-assisted fabrication of dispersed two-dimensional copper/reduced graphene oxide nanosheets nanocomposites. *Compos. Part B Eng.* **58**, 473–477 (2014).
117. M. X. Li, J. Xie, Y. D. Li, and H. H. Xu, "Reduced graphene oxide dispersed in copper matrix composites: Facile preparation and enhanced mechanical properties," *physica status solidi (a)*, vol. 212, pp. 2154–2161, 2015.
118. J. Hwang, et al. Enhanced mechanical properties of graphene/copper nanocomposites using a molecular−level mixing process. *Adv. Mater.* **25**(46), 6724–6729 (2013).
119. S. Khorasani, S. Heshmati-Manesh, and H. Abdizadeh, Improvement of mechanical properties in aluminum/CNTs nanocomposites by addition of mechanically activated graphite. *Compos. Part A: Appl. Sci. Manufact.* **68**, 177–183 (2015).
120. W.-W. Liu, et al. Synthesis and characterization of graphene and carbon nanotubes: A review on the past and recent developments. *J. Industr. Eng. Chem.* **20**(4), 1171–1185 (2014).
121. T. Borkar, J. Hwang, J. Tiley, S. Hong, and R. Banerjee, "Excellent Strength-Ductility Combination in Nickel-Graphene Nanoplatelet (GNP/Ni) Nanocomposites," *Journal of Alloys and Compounds*, vol. 646, pp. 135–144, 2015.
122. M. Bastwros, et al. Fabrication of graphene reinforced aluminum composite by semi-solid processing. in *ASME 2013 International Mechanical Engineering Congress and Exposition*, American Society of Mechanical Engineers (2013).
123. T. Laha, et al. Tensile properties of carbon nanotube reinforced aluminum nanocomposite fabricated by plasma spray forming. *Compos. Part A: Appl. Sci. Manufact.* **40**(5), 589–594 (2009).
124. R. Pérez-Bustamante, et al. Microstructural characterization of Al-MWCNT composites produced by mechanical milling and hot extrusion. *J. Alloys Compnd.* **495**(2), 399–402 (2010).
125. R. Perez-Bustamante, et al. Novel Al-matrix nanocomposites reinforced with multi-walled carbon nanotubes. *J. Alloys Compnd.* **450**(1), 323–326 (2008).
126. A.M. Esawi, and M.A. El Borady, Carbon nanotube-reinforced aluminium strips. *Compos. Sci. Technol.* **68**(2), 486–492 (2008).
127. H. Kwon, et al. Investigation of carbon nanotube reinforced aluminum matrix composite materials. *Compos. Sci. Technol.* **70**(3), 546–550 (2010).
128. K. Morsi, et al. Spark plasma extrusion (SPE) of ball-milled aluminum and carbon nanotube reinforced aluminum composite powders. *Compos. Part A: Appl. Sci. Manufact.* **41**(2), 322–326 (2010).
129. H. Kwon, et al. Combination of hot extrusion and spark plasma sintering for producing carbon nanotube reinforced aluminum matrix composites. *Carbon* **47**(3), 570–577 (2009).
130. J. Lipecka, et al. Evaluation of thermal stability of ultrafine grained aluminium matrix composites reinforced with carbon nanotubes. *Compos. Sci. Technol.* **71**(16), 1881–1885 (2011).
131. R. George, et al. Strengthening in carbon nanotube/aluminium (CNT/Al) composites. *Scripta Materialia* **53**(10), 1159–1163 (2005).
132. D. Lahiri, et al. Insight into reactions and interface between boron nitride nanotube and aluminum. *J. Mater. Res.* **27**(21), 2760–2770 (2012).
133. E. Dujardin, et al. Wetting of single shell carbon nanotubes. *Adv. Mater.* **10**(17), 1472–1475 (1998).

134. R. Deaquino-Lara, et al. Structural characterization of aluminium alloy 7075–graphite composites fabricated by mechanical alloying and hot extrusion. *Mater. Des.* **53**, 1104–1111 (2014).
135. W. Zhou, et al. Interface and interfacial reactions in multi-walled carbon nanotube-reinforced aluminum matrix composites. *Carbon* **96**, 919–928 (2016).
136. S. Cho, et al. Effective load transfer by a chromium carbide nanostructure in a multi-walled carbon nanotube/copper matrix composite. *Nanotechnology* **23**(31), 315705 (2012).
137. S. Bartolucci, et al. Properties of aluminum-graphene nanocomposites. in *AIP Conference Proceedings*. American Institute of Physics, (2012).
138. S.F. Bartolucci, et al. Graphene–aluminum nanocomposites. *Mater. Sci. Eng. A* **528**(27), 7933–7937 (2011).
139. M.K. Shin, et al. Synergistic toughening of composite fibres by self-alignment of reduced graphene oxide and carbon nanotubes. *Nat. Commun.* **3**, 650 (2012).
140. S.R. Bakshi, and A. Agarwal, An analysis of the factors affecting strengthening in carbon nanotube reinforced aluminum composites. *Carbon* **49**(2), 533–544 (2011).
141. S. Bakshi, D. Lahiri, and A. Agarwal, Carbon nanotube reinforced metal matrix composites-a review. *Int. Mater. Rev.* **55**(1), 41–64 (2010).
142. G. Wu, G., et al., Effects of particle/matrix interface and strengthening mechanisms on the mechanical properties of metal matrix composites. *Compos. Interf.* **21**(5), 415–429 (2014).
143. C. Li, et al. Distribution and integrity of carbon nanotubes in carbon nanotube/magnesium composites. *J. Alloys Compnd.* **612**, 330–336 (2014).
144. L. Wang, et al. Microstructure and properties of carbon nanosheet/copper composites processed by particle-assisted shear exfoliation. *RSC Adv.* **5**(25), 19321–19328 (2015).
145. D.-B. Xiong, et al. Graphene-and-copper artificial nacre fabricated by a preform impregnation process: bioinspired strategy for strengthening-toughening of metal matrix composite. *ACS Nano* **9**(7), 6934–6943 (2015).
146. D.H. Nam, et al. Synergistic strengthening by load transfer mechanism and grain refinement of CNT/Al–Cu composites. *Carbon* **50**(7), 2417–2423 (2012).
147. M. Rashad, F. S. Pan, M. Asif, and A. Ullah, "Improved mechanical properties of magnesium -graphene composites with copper -graphene hybrids," *Materials Science and Technology*, vol. 31, pp. 1452–1461, 2015.
148. C. Li, et al. Microstructure and strengthening mechanism of carbon nanotubes reinforced magnesium matrix composite. *Mater. Sci. Eng. A* **597**, 264–269 (2014).
149. H. Fukuda, and T.-W. Chou, An advanced shear-lag model applicable to discontinuous fiber composites. *J. Compos. Mater.* **15**(1), 79–91 (1981).
150. B. Boesl, et al. Direct observation of carbon nanotube induced strengthening in aluminum composite via in situ tensile tests. *Carbon* **69**, 79–85 (2014).
151. H. Kurita, H et al., Load-bearing contribution of multi-walled carbon nanotubes on tensile response of aluminum. *Compos. Part A: Appl. Sci. Manufact.* **68**, 133–139 (2015).
152. M.-K. Yeh, N.-H. Tai, and J.-H. Liu, Mechanical behavior of phenolic-based composites reinforced with multi-walled carbon nanotubes. *Carbon* **44**(1), 1–9 (2006).
153. Z. Zhang, and D. Chen, Consideration of Orowan strengthening effect in particulate-reinforced metal matrix nanocomposites: a model for predicting their yield strength. *Scripta Materialia* **54**(7), 1321–1326 (2006).
154. Y. Kim, et al. Strengthening effect of single-atomic-layer graphene in metal–graphene nanolayered composites. *Nat. Commun.* **4** (2013).
155. H. Choi, J. Shin, and D. Bae, Grain size effect on the strengthening behavior of aluminum-based composites containing multi-walled carbon nanotubes. *Compos. Sci. Technol.* **71**(15), 1699–1705 (2011).
156. H. Choi, et al. Reinforcement with carbon nanotubes in aluminum matrix composites. *Scripta Materialia* **59**(3), 360–363 (2008).
157. Lahiri, D., et al. Dual strengthening mechanisms induced by carbon nanotubes in roll bonded aluminum composites. *Mater. Sci. Eng. A* 2009. **523**(1), 263–270.
158. S.C. Tjong, Recent progress in the development and properties of novel metal matrix nanocomposites reinforced with carbon nanotubes and graphene nanosheets. *Mater. Sci. Eng. R: Rep.* **74**(10), 281–350 (2013).
159. S. Dong, et al. Size dependent strengthening mechanisms in carbon nanotube reinforced metal matrix composites. *Compos. Part A: Appl. Sci. Manufact.* **68**, 356–364 (2015).
160. Qu, S., et al. A study of particle size effect and interface fracture in aluminum alloy composite via an extended conventional theory of mechanism-based strain-gradient plasticity. *Compos. Sci. Technol.* **65**(7), 1244–1253 (2005).
161. R. Vogt, et al. The absence of thermal expansion mismatch strengthening in nanostructured metal–matrix composites. *Scripta Materialia* **61**(11), 1052–1055 (2009).
162. R. Pérez-Bustamante, et al. Microstructural and hardness behavior of graphene-nanoplatelets/aluminum composites synthesized by mechanical alloying. *J. Alloys Compnd.* **615**, S578–S582 (2014).
163. W. Kim, T. Lee, and S. Han, Multi-layer graphene/copper composites: Preparation using high-ratio differential speed rolling, microstructure and mechanical properties. *Carbon* **69**, 55–65 (2014).
164. X. Liu, et al. Effect of graphene nanosheets reinforcement on the performance of Sn· Ag· Cu lead-free solder. *Mater. Sci. Eng. A* **562**, 25–32 (2013).
165. K. Kim, et al. Grain refinement assisted strengthening of carbon nanotube reinforced copper matrix nanocomposites. *Appl. Phys. Lett.* **92**(12), 121901 (2008).
166. C. Deng, et al. Processing and properties of carbon nanotubes reinforced aluminum composites. *Mater. Sci. Eng. A* **444**(1), 138–145 (2007).
167. E. Ma, et al. Strain hardening and large tensile elongation in ultrahigh-strength nano-twinned copper. *Appl. Phys. Lett.* **85**(21), 4932–4934 (2004).
168. Y. Wang, et al. High tensile ductility in a nanostructured metal. *Nature* **419**(6910), 912–915 (2002).
169. X. Li, et al. Competing grain-boundary-and dislocation-mediated mechanisms in plastic strain recovery in nanocrystalline aluminum. *Proc. of the National Academy of Sciences* **06**(38), 16108–16113 (2009).
170. H. Choi, et al. Tensile behavior of bulk nanocrystalline aluminum synthesized by hot extrusion of ball-milled powders. *Scripta Materialia* **59**(10), 1123–1126 (2008).

171. K. Padmanabhan, et al. Inverse Hall–Petch effect and grain boundary sliding controlled flow in nanocrystalline materials. *Mater. Sci. Eng. A* **452**, 462–468 (2007).
172. C. Li, et al. Effect of solidification on microstructures and mechanical properties of carbon nanotubes reinforced magnesium matrix composite. *Mater. Des.* **58**, 204–208 (2014).
173. D.H. Nam, et al. Effect of CNTs on precipitation hardening behavior of CNT/Al–Cu composites. *Carbon* **50**(13), 4809–4814 (2012).
174. H. Choi, et al. Strengthening in nanostructured 2024 aluminum alloy and its composites containing carbon nanotubes. *Compos. Part A: Appl. Sci. Manufact.* **42**(10), 1438–1444 (2011).
175. M.A. Rafiee, et al. Enhanced mechanical properties of nanocomposites at low graphene content. *ACS Nano* **3** (12), 3884–3890 (2009).
176. L.-Y. Chen, et al. Novel nanoprocessing route for bulk graphene nanoplatelets reinforced metal matrix nanocomposites. *Scripta Materialia* **67**(1), 29–32 (2012).
177. S. Shin, et al. Strengthening behavior of carbon/metal nanocomposites. *Sci. Rep.* **5** (2015).
178. D. Lahiri, et al. Graphene-induced strengthening in spark plasma sintered tantalum carbide–nanotube composite. *Scripta Materialia* **68**(5), 285–288 (2013).
179. B. Chen, et al. Inter-wall bridging induced peeling of multi-walled carbon nanotubes during tensile failure in aluminum matrix composites. *Micron* **69**, 1–5 (2015).
180. R. Atif, et al. Use of morphological features of carbonaceous materials for improved mechanical properties of epoxy nanocomposites. *RSC Adv.* **6**(2), 1351–1359 (2016).
181. W. Zhai, et al. Grain refinement: a mechanism for graphene nanoplatelets to reduce friction and wear of Ni 3 Al matrix self-lubricating composites. *Wear* **310**(1), 33–40 (2014).
182. J.M. Mistry, and P.P. Gohil, An overview of diversified reinforcement on aluminum metal matrix composites: Tribological aspects. *Proc. of the Institution of Mechanical Engineers, Part J: Journal of Engineering Tribology*, 350650116658572 (2016).
183. P.L. Menezes, et al. *Tribology for Scientists and Engineers*, 2Springer (2013).
184. F.J. Clauss, *Solid Lubricants and Self-lubricating Solids*, Elsevier (2012).
185. J.P. Davim, *Ecotribology: Research Developments*, Springer (2015).
186. M. Yildirim, D. Özyürek, and M. Gürü, "Investigation of Microstructure and Wear Behaviours of Al Matrix Composites Reinforced By Carbon Nanotube," *Fullerenes, Nanotubes and Carbon Nanostructures*, vol. 24, pp. 467–473, 2016.
187. R. Deaquino-Lara, et al. Tribological characterization of Al7075–graphite composites fabricated by mechanical alloying and hot extrusion. *Mater. Des.* **67**, 224–231 (2015).
188. A. Zeren, Effect of the graphite content on the tribological properties of hybrid Al/SiC/Gr composites processed by powder metallurgy. *Industr. Lubr. Tribol.* **67**(3), 262–268 (2015).
189. P. Ravindran, et al. Tribological behaviour of powder metallurgy-processed aluminium hybrid composites with the addition of graphite solid lubricant. *Ceram. Int.* **39** (2), 1169–1182 (2013).
190. P.L. Menezes, et al. Self-lubricating behavior of graphite-reinforced composites, in *Tribology for Scientists and Engineers*, Springer (2013); 341–389.
191. E. Omrani, et al. Effect of graphite particles on improving tribological properties Al-16Si-5Ni-5Graphite self-lubricating composite under fully flooded and starved lubrication conditions for transportation applications. *Int. J. Adv. Manuf. Technol.* 1–11 (2016).
192. P.C. Roshini, et al. Ultrasonic-assisted synthesis of graphite-reinforced Al matrix nanocomposites. *J. Mater. Eng. Perform.* **24**(6), 2234–2239 (2015).
193. A. Baradeswaran, and A.E. Perumal, Wear and mechanical characteristics of Al 7075/graphite composites. *Compos. Part B Eng.* 2014. **56**, 472–476.
194. L. Jinfeng, et al. Effect of graphite particle reinforcement on dry sliding wear of SiC/Gr/Al composites. *Rare Metal Mater. Eng.* **38**(11), 1894–1898 (2009).
195. P.K. Rohatgi, et al. Tribology of metal matrix composites, in *Tribology for Scientists and Engineers*, Springer (2013); 233–268.
196. K. Rajkumar, and S. Aravindan, Tribological behavior of microwave processed copper–nanographite composites. *Tribol. Int.* **57**, 282–296 (2013).
197. L. Reinert, S. Suárez, and A. Rosenkranz, Tribo-mechanisms of carbon nanotubes: friction and wear behavior of CNT-reinforced nickel matrix composites and CNT-coated bulk nickel. *Lubricants* **4**(2), 11 (2016).
198. S.-m. Zhou, et al. Fabrication and tribological properties of carbon nanotubes reinforced Al composites prepared by pressureless infiltration technique. *Compos. Part A: Appl. Sci. Manufact.* **38**(2), 301–306 (2007).
199. A. Al-Qutub, et al. Wear and friction behavior of Al6061 alloy reinforced with carbon nanotubes. *Wear* **297**(1), 752–761 (2013).
200. X.-J. Shen, et al. Significantly modified tribological performance of epoxy nanocomposites at very low graphene oxide content. *Polymer* **54**(3), 1234–1242 (2013).
201. B. Yazdani, et al. Tribological performance of graphene/carbon nanotube hybrid reinforced Al2O3 composites. *Sci. Rep.* **5** (2015).
202. D. Berman, et al. Extraordinary macroscale wear resistance of one atom thick graphene layer. *Adv. Funct. Mater.* **24**(42), 6640–6646 (2014).
203. C. Lin, et al. Manufacturing and tribological properties of copper matrix/carbon nanotubes composites. *Wear* **270** (5), 382–394 (2011).
204. I. Ahmad, A. Kennedy, and Y. Zhu, Wear resistant properties of multi-walled carbon nanotubes reinforced Al 2 O 3 nanocomposites. *Wear* **269**(1), 71–78 (2010).
205. Z. Xu, et al. Comparison of tribological properties of NiAl matrix composites containing graphite, carbon nanotubes, or graphene. *J. Mater. Eng. Perform.* **24**(5), 1926–1936 (2015).
206. X. Zhang, et al. Fabrication and tribological properties of copper matrix composite with short carbon fiber/reduced graphene oxide filler. *Tribol. Int.* **103**, 406–411 (2016).
207. K.T. Kim, S.I. Cha, and S.H. Hong, Hardness and wear resistance of carbon nanotube reinforced Cu matrix nanocomposites. *Mater. Sci. Eng. A* **449**, 46–50 (2007).

208. A. Maiti, et al. Carbon nanotube-reinforced Al alloy-based nanocomposites via spark plasma sintering. *J. Compos. Mater.* **49**(16), 1937–1946 (2015).
209. B. Prasad, T. Dan, and P. Rohatgi, Pressure-induced improvement in interfacial bonding between graphite and the aluminium matrix in graphitic-aluminium particle composites. *J. Mater. Sci. Lett.* **6**(9), 1076–1078 (1987).
210. R. Maurya, et al. Effect of carbonaceous reinforcements on the mechanical and tribological properties of friction stir processed Al6061 alloy. *Mater. Des.* **98**, 155–166 (2016).
211. A.D. Moghadam, et al. Effect of in-situ processing parameters on the mechanical and tribological properties of self-lubricating hybrid aluminum nanocomposites. *Tribol. Lett.* **62**(2), 1–10 (2016).
212. O. Carvalho, et al. Improvement on sliding wear behavior of Al/c iron tribopair by CNT's reinforcement of an Al alloy. *Tribol. Trans.* **58**(4), 643–653 (2015).
213. L. Kumar, S.N. Alam, and S.K. Sahoo, Mechanical properties, wear behavior and crystallographic texture of Al–multiwalled carbon nanotube composites developed by powder metallurgy route. *J. Compos. Mater.*, 0021998316658946 (2016).
214. T.R. Prabhu, Investigations of the effects of particle properties on the wear resistance of the particle reinforced composites using a novel wear model. *Int. J. Computat. Mater. Sci. Eng.* **5**(02), 1650013 (2016).
215. Y. Song, et al. Microscopic mechanical properties of titanium composites containing multi-layer graphene nanofillers. *Mater. Des.* **109**, 256–263 (2016).
216. S.N. Alam, and L. Kumar, Mechanical properties of aluminium based metal matrix composites reinforced with graphite nanoplatelets. *Mater. Sci. Eng. A* **667**, 16–32 (2016).
217. P. Manikandan, et al. Micro/nanostructure and tribological characteristics of pressureless sintered carbon nanotubes reinforced aluminium matrix composites. *J. Nanomater.* (2016).
218. E.S. Lee, et al. Effects of Al-Si/SiC p powder on the sinterability and wear properties of Al-Zn-Mg powder. *J. Alloys Cmpnd.* **689**, 145–152 (2016).
219. A.A. Adebisi, et al. Effect of variable particle size reinforcement on mechanical and wear properties of 6061Al–SiCp composite. *Compos. Interf.* **23**(6), 533–547 (2016).
220. M. Moazami-Goudarzi, and F. Akhlaghi, Wear behavior of Al 5252 alloy reinforced with micrometric and nanometric SiC particles. *Tribol. Int.* **102**, 28–37 (2016).
221. A. Pramanik, Effects of reinforcement on wear resistance of aluminum matrix composites. *Trans. Nonferr. Met. Soc. China* **26**(2), 348–358 (2016).
222. J. Singh, Fabrication characteristics and tribological behavior of Al/SiC/Gr hybrid aluminum matrix composites: A review. *Friction*, 1–17 (2016).
223. V. Kumar, R.K. Gautam, and R. Tyagi, Tribological behavior of Al-based self-lubricating composites. *Compos. Interf.* **23**(6), 481–492 (2016).
224. G. Hatipoglu, et al. The effect of sliding speed on the wear behavior of pulse electro Co-deposited Ni/MWCNT nanocomposite coatings. *Tribol. Int.* **98**, 59–73 (2016).
225. R. Perez-Bustamante, et al. Wear behavior in Al 2024–CNTs composites synthesized by mechanical alloying. *Wear* **292**, 169–175 (2012).
226. M.M. Bastwros, A.M. Esawi, and A. Wifi, Friction and wear behavior of Al–CNT composites. *Wear* **307**(1), 164–173 (2013).
227. H. Choi, S. Lee, and D. Bae, Wear characteristic of aluminum-based composites containing multi-walled carbon nanotubes. *Wear* **270**(1), 12–18 (2010).
228. B.Z. Jang, and A. Zhamu, Processing of nanographene platelets (NGPs) and NGP nanocomposites: a review. *J. Mater. Sci.* **43**(15), 5092–5101 (2008).
229. X. Huang, Fabrication and properties of carbon fibers. *Materials* **2**(4), 2369–2403 (2009).
230. Y. Huang, et al. Carbon materials reinforced aluminum composites: a review. *Acta Metallurgica Sinica (Engl. Lett.)* **27**(5), 775–786 (2014).
231. D.B. Miracle, et al. *ASM Handbook*, vol. 21. ASM International Materials Park, OH (2001).
232. C.R. Bradbury, et al. Hardness of multi wall carbon nanotubes reinforced aluminium matrix composites. *J. Alloys Cmpnd.* **585**, 362–367 (2014).
233. R. Pérez-Bustamante, et al. Effect of milling time and CNT concentration on hardness of CNT/Al 2024 composites produced by mechanical alloying. *Mater. Character.* **75**, 13–19 (2013).
234. S. Singhal, S., et al., Fabrication and characterization of Al-matrix composites reinforced with amino-functionalized carbon nanotubes. *Compos. Sci. Technol.* **72**(1), 103–111 (2011).
235. P. Koppad, et al. Microstructure and microhardness of carbon nanotube reinforced copper nanocomposites. *Mater. Sci. Technol.* **29**(5), 605–609 (2013).
236. H. Mindivan, et al. Fabrication and characterization of carbon nanotube reinforced magnesium matrix composites. *Appl. Surf. Sci.* **318**, 234–243 (2014).
237. T. Borkar, et al. Strength versus ductility in carbon nanotube reinforced nickel matrix nanocomposites. *J. Mater. Res.* **29**(06), 761–769 (2014).
238. M.R. Basariya, V. Srivastava, and N. Mukhopadhyay, Microstructural characteristics and mechanical properties of carbon nanotube reinforced aluminum alloy composites produced by ball milling. *Mater. Des.* **64**, 542–549 (2014).
239. S. Yoo, S. Han, and W. Kim, Strength and strain hardening of aluminum matrix composites with randomly dispersed nanometer-length fragmented carbon nanotubes. *Scripta Materialia* **68**(9), 711–714 (2013).
240. J. Liao, and M.-J. Tan, Mixing of carbon nanotubes (CNTs) and aluminum powder for powder metallurgy use. *Powder Technol.* **208**(1), 42–48 (2011).
241. J.-z. Liao, M.-J. Tan, and I. Sridhar, Spark plasma sintered multi-wall carbon nanotube reinforced aluminum matrix composites. *Mater. Des.* **31**, S96–S100 (2010).
242. S. Simões, et al. Improved dispersion of carbon nanotubes in aluminum nanocomposites. *Compos. Struct.* **108**, 992–1000 (2014).
243. M.K. Mani, et al. Fabrication of carbon nanotube reinforced iron based magnetic alloy composites by spark plasma sintering. *J. Alloys Cmpnd.* **601**, 146–153 (2014).
244. J. Suh, and D. Bae, Mechanical properties of Fe-based composites reinforced with multi-walled carbon nanotubes. *Mater. Sci. Eng. A* **582**, 321–325 (2013).

245. K.T. Kim, et al. Microstructures and tensile behavior of carbon nanotube reinforced Cu matrix nanocomposites. *Mater. Sci. Eng. A* **430**(1), 27–33 (2006).
246. Z. Xue, et al. Microstructures and tensile behavior of carbon nanotubes reinforced Cu matrix composites with molecular-level dispersion. *Mater. Des.* **34**, 298–301 (2012).
247. M. Lal, et al. An alternative improved method for the homogeneous dispersion of CNTs in Cu matrix for the fabrication of Cu/CNTs composites. *Appl. Nanosci.* **3**(1), 29–35 (2013).
248. J. Li, et al. Microstructure and tensile properties of bulk nanostructured aluminum/graphene composites prepared via cryomilling. *Mater. Sci. Eng. A* **626**, 400–405 (2015).
249. C. Zhao, Enhanced strength in reduced graphene oxide/nickel composites prepared by molecular-level mixing for structural applications. *Appl. Phys. A* **118**(2), 409–416 (2015).
250. M. Rashad, et al. Powder metallurgy of Mg–1% Al–1% Sn alloy reinforced with low content of graphene nanoplatelets (GNPs). *J. Industr. Eng. Chem.* **20**(6), 4250–4255 (2014).
251. J. Dutkiewicz, et al. Microstructure and properties of bulk copper matrix composites strengthened with various kinds of graphene nanoplatelets. *Mater. Sci. Eng. A* **628**, 124–134 (2015).
252. P. Zhao, and S. Ji, Refinements of shear-lag model and its applications. *Tectonophysics* **279**(1), 37–53 (1997).
253. X.-L. Gao, and K. Li, A shear-lag model for carbon nanotube-reinforced polymer composites. *Int. J. Solids Struct.* **42**(5), 1649–1667 (2005).
254. Y. Tang, et al. Enhancement of the mechanical properties of graphene–copper composites with graphene–nickel hybrids. *Mater. Sci. Eng. A* **599**, 247–254 (2014).
255. N. Hansen, Hall–Petch relation and boundary strengthening. *Scripta Materialia* **51**(8), 801–806 (2004).
256. T. Nieh, and J. Wadsworth, Hall-Petch relation in nanocrystalline solids. *Scripta Metallurgica et Materialia* **25** (4), 955–958 (1991).
257. E. Orowan, Problems of plastic gliding. *Proc. Phys. Soc.* **52**(1), 8 (1940).
258. J.N. Coleman, et al. High performance nanotube-reinforced plastics: understanding the mechanism of strength increase. *Adv. Funct. Mater.* **14**(8), 791–798 (2004).
259. R. Arsenault, and N. Shi, Dislocation generation due to differences between the coefficients of thermal expansion. *Mater. Sci. Eng.* **81**, 175–187 (1986).
260. R.E. Smallman, and A. Ngan, *Physical Metallurgy and Advanced Materials*, Butterworth-Heinemann (2011).
261. A. Sanaty-Zadeh, Comparison between current models for the strength of particulate-reinforced metal matrix nanocomposites with emphasis on consideration of Hall–Petch effect. *Mater. Sci. Eng. A* **531**, 112–118 (2012).
262. M. Kassner, Taylor hardening in five-power-law creep of metals and Class M alloys. *Acta Materialia* **52**(1), 1–9 (2004).
263. N. Fleck, M. Ashby, and J. Hutchinson, The role of geometrically necessary dislocations in giving material strengthening. *Scripta Materialia* **48**(2), 179–183 (2003).
264. F. Ogawa, and C. Masuda, Microstructure evolution during fabrication and microstructure–property relationships in vapour-grown carbon nanofibre-reinforced aluminium matrix composites fabricated via powder metallurgy. *Compos. Part A: Appl. Sci. Manufact.* (2015).
265. G. Han, et al. Synthesis of CNT-reinforced AZ31 magnesium alloy composites with uniformly distributed CNTs. *Mater. Sci. Eng. A* **628**, 350–357 (2015).
266. H. Shi, et al. A novel method to fabricate cNT/Mg–6Zn composites with high strengthening efficiency. *Acta Metallurgica Sinica (Engl. Lett.)* **27**(5), 909–917 (2014).
267. J.G. Park, D.H. Keum, and Y.H. Lee, Strengthening mechanisms in carbon nanotube-reinforced aluminum composites. *Carbon* **95**, 690–698 (2015).
268. O. Carvalho, et al. Mechanisms governing the tensile, fatigue, and wear behavior of carbon nanotube reinforced aluminum alloy. *Mech. Adv. Mater. Struct.* **23**(8), 917–925 (2016).
269. J. Jayaraman, J., R. Kuppusamy, and H. Rao, Investigation on wear properties of AZ31–MWCNT nanocomposites fabricated through mechanical alloying and powder metallurgy. *Sci. Eng. Compos, Mater.* **23**(1), 61–66 (2016).
270. B. Xue, Q. Zhu, X. Shi, W. Zhai, K. Yang, and Y. Huang, "Microstructure and Functional Mechanism of Friction Layer in Ni3Al Matrix Composites with Graphene Nanoplatelets," *Journal of Materials Engineering and Performance*, pp. 1–8, 2016.
271. A. Ghazaly, B. Seif, and H. Salem, Mechanical and tribological properties of AA2124−Graphene self lubricating nanocomposite. *Light Met.*, 411–415 (2013).
272. M. Tabandeh-Khorshid, E. Omrani, P. L. Menezes, and P. K. Rohatgi, "Tribological performance of self-lubricating aluminum matrix nanocomposites: role of graphene nanoplatelets," *Engineering Science and Technology, an International Journal*, vol. 19, pp. 463–469, 2016.
273. H. Algul, M. Tokur, S. Ozcan, M. Uysal, T. Cetinkaya, H. Akbulut, et al., "The effect of graphene content and sliding speed on the wear mechanism of nickel -graphene nanocomposites," *Applied Surface Science*, vol. 359, pp. 340–348, 2015.
274. H. Algul, M. Tokur, S. Ozcan, M. Uysal, T. Cetinkaya, H. Akbulut, et al., "The effect of graphene content and sliding speed on the wear mechanism of nickel -graphene nanocomposites," *Applied Surface Science*, vol. 359, pp. 340–348, 2015.